


Damage and Vulnerability Analysis of Debris Slide Impacts to Buildings through Analytical Methods

AARON ORR
March, 2019

SUPERVISORS:
Dr O. C. (Olga) Mavrouli
Dr C. J. (Cees) van Westen



Damage and Vulnerability Analysis of Debris Slide Impacts to Buildings through Analytical Methods

AARON ORR

Enschede, The Netherlands, March, 2019

Thesis submitted to the Faculty of Geo-Information Science and Earth Observation of the University of Twente in partial fulfilment of the requirements for the degree of Master of Science in Geo-information Science and Earth Observation.

Specialisation: Applied Earth Sciences

SUPERVISORS:

Dr O. C. (Olga) Mavrouli

Dr C. J. (Cees) van Westen

THESIS ASSESSMENT BOARD:

Prof Dr N. (Norman) Kerle (Chair)

Dr H. (Harry) Seijmonsbergen (External Examiner, University of Amsterdam)

DISCLAIMER

This document describes work undertaken as part of a programme of study at the Faculty of Geo-Information Science and Earth Observation of the University of Twente. All views and opinions expressed therein remain the sole responsibility of the author and do not necessarily represent those of the Faculty.

ABSTRACT

Landslides, historically, result in thousands of deaths, billions of dollars in damages and economic loss worldwide. To comprehend the degree of risk for buildings subject to landslide impacts, the vulnerability of buildings subject to landslide impacts is a topic receiving attention, and essential to present holistically. However, the current methods of researching the vulnerability of buildings subject to landslide impacts, often present uncertainties in connecting the driving forces with resulting damage; furthermore, the data available on landslide impacts to buildings of a common structural typology are scarce.

This research aims to develop a holistic analysis of the vulnerability of buildings subject to landslide impacts through analytical methods and back analysis of buildings damaged from landslides. The research focuses on a common structural typology of the Commonwealth of Dominica; Dominica is the study area of several disaster risk reduction programs, such as the Caribbean Handbook on Risk Information Management (CHARIM) project led by a faculty of ITC, University of Twente, due to the frequent damage induced during the Atlantic hurricane seasons.

Fieldwork for data collection of building affected by landslides primarily focuses on building dimensions, damaged structural and non-structural members, and landslide intensity-indicators. Collectively, ten buildings affected by debris slides, debris flows, flooding, and high wind speeds in Dominica were surveyed. One of the ten buildings was analysed with analytical simulations of the building's response to simulated landslide impacts and is presented in this thesis. The analytical simulations begin with using the software numerical software RAMMS, with deriving landslide parameters, such as total landslide volume, for structural response analysis with the software Blender; additionally the add-ons Bullet Constraint Builder and Impulse. A parametric analysis was performed in Blender to calibrate the run-out kinematics and impact dynamics, then the analysis of a building's response to simulated landslide impacts was performed. Last, supplemental simulations were performed to observe the simulated damage to a common structural typology of Dominica from single impacts with a controlled velocity.

The presented research was validated through back-analysis using collected data of in-situ structural typologies, deposited landslide types, landslide induced damage; as well as, literature values of mortar engineering properties. However, the simulated damage from the analysis was always more extensive than the observed damage during data collection. It was determined the modelled particle size of the landslide and assigned breaking thresholds of the mortar walls, in particular of the mortar, have the most significant effect in the simulation performed while researching the vulnerability of buildings subject to landslide impacts.

Keywords: landslide, damage, building, model, vulnerability, analytical methods, numerical simulations, structural response

ACKNOWLEDGEMENTS

To my loving parents, I can't express the gratitude I have for the opportunities y'all have blessed me with. There were times I thought I would fail, and y'all supported me through them, reminding me to be patient, and learn at my own pace. I want to thank y'all, for being so patient with me throughout my academic journey. Now on to the next chapter....

Thank you, I love you

To my advisor, Olga, you have been a fantastic mentor throughout my research, and time at ITC. Thank you for always being welcoming and keeping me motivated. You made me rethink the quality of work I'm capable of producing and inspired me to work harder than I ever have on an academic project. You were, also, very patient with me and my revisions, for which, I am grateful.

Thank you

To Cees, you have been an influential mentor in my academics, and I enjoyed getting to spend time with you in Dominica. Thank you for all your guidance and reviews.

To Kai Kostack and Oliver Walter, thank you for your contributions to my research, your guidance with the Bullet Constraint Builder was essential for me to reach my goal.

To Jacob, I don't know how it ended up this way, but somehow you being so far away has always motivated me to do my best where I'm at, so I can return, and celebrate with you. You've motivated and encouraged me so many times, when I didn't know where I was going, helping me weigh the options. I'm excited to watch your journey to med-school and motivate you along the way.

To my loyal friends who have stuck with me through this academic journey, I look forward to reuniting and building a future together. Chris, you've been my friend for the longest, and in a heartbeat came to visit me after I had just started college in Alaska. Thank you for staying so close over the years. Fletcher and Madison, y'all were quick to follow Chris up to Alaska, and those memories are immeasurable. Y'all are two of the biggest inspirations for how I want to work in the future, thank y'all for staying close. Sean and Trever, how did we end up almost dying in -40°C , coming from Texas? It's because y'all support me and are willing to travel for me. Y'all always have my back, thank y'all for staying close. Frank and Cassie, y'all came all the way out here to hang out, even though I had to work on my thesis, and y'all motivated me to stay focused; also, Frank thank you for offering to review my work, the support was motivating, thank y'all for staying close.

Last, but not least, I want to reflect on my efforts throughout my academics. My will took me to Alaska to study engineering, build trails in the mountains, and make life-long friendships. Then, I left for the Netherlands and started all over. In a sense school is all I've ever done, so, what's next?

TABLE OF CONTENTS

1.	INTRODUCTION.....	1
1.1.	Background	1
1.2.	Area of Study.....	2
1.3.	Problem Statement.....	5
1.4.	Literature Review: Physical Vulnerability of Buildings.....	7
1.5.	Objectives and Research Questions.....	10
1.6.	Thesis Outline.....	11
2.	METHODOLOGY	12
2.1.	Development of Fieldwork	13
2.2.	Collection of Data & Empirical Damage Assessments	13
2.3.	Analytical Modelling & Simulations.....	15
3.	DATA COLLECTION.....	22
3.1.	Site Selection & Developing A Landslide Assessment.....	22
3.2.	Structural Data Collection & Damage Empirical Assesment	24
4.	ANALYTICAL SIMULATION OF BUILDING RESPONSE TO LANDSLIDE IMPACTS	29
4.1.	Landslide Modelling and Flow Simulations using RAMMS	29
4.2.	Alternative Landslide for Continuing Analysis of Building Response to Landslide Impacts	34
5.	DISCUSSION & CONCLUSIONS	52
5.1.	Effect of Input-Data Quality	52
5.2.	Limitations of the Preformed Simulations.....	54
5.3.	Conclusions on Analysis of Buildings Subject to Simulated Landslide Impacts	54

LIST OF FIGURES

- Figure 1.1: Map of landslide-induced deaths 2004 – 2010
- Figure 1.2: Shaded relief map of Dominica and the study area
- Figure 1.3: Outcrop along the west coast of Dominica
- Figure 1.4: Geological map of Dominica
- Figure 1.5: Dominica landslide susceptibility maps
- Figure 2.1: Flow scheme of the fieldwork development stage
- Figure 2.2: Flow scheme of the empirical assessment and data collection stage
- Figure 2.3: An example of how to sketch a floor plan
- Figure 2.4: Flow scheme of the analysis and development of vulnerability curves
- Figure 2.5a – 2.5c: Preview of modelling a landslide in Blender
- Figure 2.6: Example of how structural frames are modelled in Blender
- Figure 2.7: Visual representation of simulated building constraints
- Figure 3.1: Post-Hurricane Maria landslide inventory
- Figure 3.2: Towns where data was collected of buildings damaged by landslides
- Figure 3.3: Single-story concrete block building affected by a debris slide
- Figure 3.4: Single-story building, raised on a reinforced concrete frame, affected by debris flows
- Figure 3.5: Location plan of Sites 8, 9, and Building 1
- Figure 3.6: In-situ landslide-induced damage to Building 1
- Figure 3.7: In-situ landslide-induced damage to Building 1 cont.
- Figure 3.8: Map of Pichelin, buildings visited, surveyed, and landslides from inventory
- Figure 3.9: Location plan of Sites 4, 5, and Building 2
- Figure 3.10: Side profile of Building 2
- Figure 3.11: Inside of Building 2
- Figure 3.12: Affected façade of Building 2
- Figure 3.13: Damage of Building 2
- Figure 3.14: Map of NE Elms Hall, buildings visited, surveyed, and landslides from inventory
- Figure 4.1: Two-meter landslide modelled in RAMMS for Building 2
- Figure 4.2: Simulated max flow height of 2.0m landslide
- Figure 4.3: Simulated max flow height of 2.0m landslide after adjusting obstacle boundary
- Figure 4.4: Landslide modelled 3.5m in RAMMS for Building 2
- Figure 4.5: Simulated max flow height of 3.5m landslide
- Figure 4.6: Simulated max flow velocity of 3.5m landslide
- Figure 4.7: Landslide modelled in Blender
- Figures 4.8a – 4.8d: Effect of simulated hillslope’s surface response
- Figure 4.9: Effect of landslide barriers
- Figure 4.10: Results of landslide barriers
- Figure 4.11: Effect of simulated landslide particle size
- Figure 4.12: Simulated max flow height of alternative landslide using RAMMS
- Figure 4.13: Simulated max flow velocities of alternative landslide using RAMMS
- Figures 4.14a & 4.14b: Effect of alternative landslide properties simulated in Blender
- Figures 4.15a & 4.15b: Effect of hillslope surface response with alternative landslide
- Figures 4.16a – 4.16d: Effect of increasing the distance from the building to the hillslope
- Figure 4.17: Modelled Building 2 and landslide
- Figures 4.18a – 4.18d: Surface response of 5.0 for 5.0m & 6.0m distances to the hillslope

Figures 4.19a – 4.19d: Surface response of 3.0 for 5.0m & 6.0m distances to the hillslope
Figures 4.20a – 4.20d: Surface response of 0.0 for 5.0m & 6.0m distances to the hillslope
Figure 4.21: Simulation results with Bullet Constraint Builder
Figure 4.22: Visualisation of simulated damage
Figure 4.23: Damage using wall discretisation (2.0m)
Figure 4.24: Visualisation of simulated damage with unaffected wall discretisation
Figure 4.25: Effect of simulation run-time
Figure 4.26: Visualisation of simulated damage with increased run-time
Figure 4.27: Damage using wall discretisation (10.0m) for unaffected walls
Figure 4.28: Damage using full slab for unaffected walls
Figure 4.29: Damage removing unaffected walls
Figure 4.30: Damage using 2.0m discretisation for impacted wall
Figure 4.31: Visualisation of simulated damage using 2.0m discretisation for impacted wall
Figure 4.32: Damage using optimal parameters from parametric analysis
Figure 4.33: Damage using optimal parameters and concrete blocks for affected wall
Figure 4.34: Simulation results increasing the mortar breaking thresholds
Figure 4.35: Plan view of simulated damage
Figure 4.36: Visualisation of simulated damage
Figure 4.37: Different simulated damage using same mortar breaking thresholds
Figure 4.38: Bullet Constraint Builder's force visualiser
Figure 4.39: Constraint numbers
Figure 4.40: Simulated vertical pressure gradient on building
Figure 4.41: Simulated lateral pressure on building
Figure 4.42a – 4.42e: Vulnerability curves
Figure 5.1: RAMMS analysis of Building 1
Figure 5.2: Simulated flow direction in RAMMS for Building 2
Figure 5.2: Alternative ways to model a landslide in Blender
Figure 5.3: Kinematic effect of alternative models
Figure 5.4: Effect of modelled landslide boundaries

LIST OF TABLES

- Table 2.1: Stages 1 & 2 of Research Methodology
- Table 2.2: Stages 3 & 4 of Research Methodology
- Table 2.3: Blender Landslide Properties
- Table 3.1: Observed Damage of Building 1
- Table 3.2: Observed Damage of Building 2
- Table 4.1: RAMMS Release Properties
- Table 4.2: Simulated Soil Size & Landslide Properties
- Table 4.3: Simulated Soil Size & Landslide Properties cont.
- Table 4.4: Simulated Soil Size & Landslide Properties Adjusted
- Table 4.5: Simulated Soil Size & Landslide Properties Adjusted cont.
- Table 4.6: Alternative RAMMS Release Properties
- Table 4.7: Simulated RAMMS Landslide Properties
- Table 4.8: Simulated Blender Landslide Properties
- Table 4.9: Bullet Constraint Builder Pre-processing settings
- Table 4.10: Mortar Breaking Thresholds
- Table 4.11: Ceiling (Slab) Simulated Dimensions
- Table 4.12: Beam & Column Simulated Dimensions
- Table 4.13: Unadjusted Parameters during Mortar Calibration
- Table 4.14: Initial Mortar Breaking Thresholds

1. INTRODUCTION

1.1. Background

Mountainous regions are desirable places to live; however, demographic expansion and touristic development into landslide susceptible terrain, historically, results in substantial damage to vulnerable infrastructure, injuries and fatalities. Landslides annually result in thousands of deaths, and there is an increasing trend in the number of fatality-inducing landslides worldwide (Petley, 2018). Froude & Petley (2018) researched events from 2004 – 2016 in an analysis of a global dataset and recorded 55,997 deaths from 4,862 landslides worldwide. Figure 1.1 presents events 2004 – 2010; India, China, and the Philippines rank the highest in the number of landslide events, with 393, 353, and 226 landslides respectively. Landslides result in an average of 25 – 50 people killed a year in the U.S. (USGS.gov, 2019), and in Europe, between 1995 – 2014, 476 landslides resulted in 1,370 reported deaths (García-Davalillo et al., 2016). Furthermore, García-Davalillo et al. (2016) reported that natural events triggered the majority of landslides 2008 – 2014. There are several types of landslide triggering agents, movement types, and compositions; a landslide’s movement type and composition describe a landslide’s classification. Human-induced landslide triggering agents include; slope re-profiling, groundwater flow perturbation, fast pore pressure changes, surface water overland flow modifications, land-use changes, land degradation, inappropriate artificial structures, vibrations, explosives, and ageing or deterioration of infrastructure (Jaboyedoff et al. 2016). Natural landslide triggering agents, such as heavy rainfall, snowmelt, and seismic events, often result in multiple hazards such as flooding and ground movement; subsequently, the media then portrays damage during these events comprehensively as hurricane or earthquake-induced.

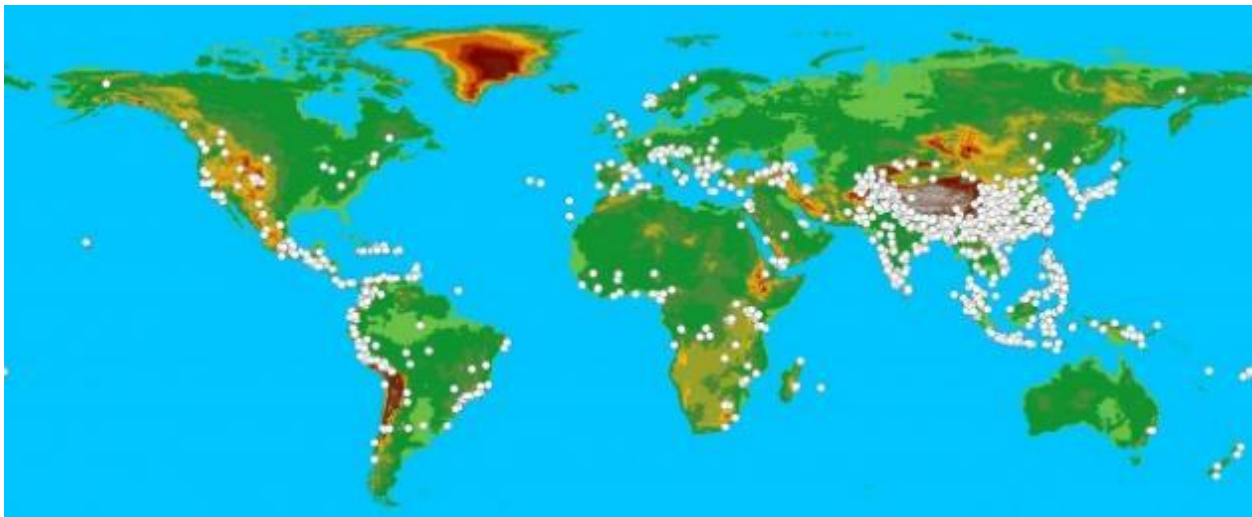


Figure 1.1: Locations of documented landslide-induced deaths 2004 – 2010 (Petley, 2012)

The worldwide annual economic loss from landslide-induced damage is in the billions of dollars. García-Davalillo et al. (2016) approximated Europe’s annual average economic loss, due to landslides, is 4.7 billion Euros (\$5.3 billion U.S). In 1983 a single landslide event in Thistle, Utah resulted in \$200 – 400 million of economic loss (Burt, 2014). In 2014, a landslide in Nepal resulted in 21 houses damaged, 156 deaths or lost, and a total migrated population of 1,011 (Amatya, 2014). More recently, in Naga City, Philippines, 2018, a massive landslide affected over 8,600 people, totally damaged 77 homes, and the reported costs of assistance

were approximately ₱80.4 million (\$1.5 million U.S) (Ontanillas, 2018). Additionally, in Sausalito, California on February 14, 2019, a mudslide destroyed a neighbourhood and displaced 15 people (Garces, 2019).

The Caribbean islands are another region with frequent, natural, and human-induced landslides. Erosion of the volcanic deposits creates weak regolith layered with clay, which then fails during extreme weather or human-induced triggering agents. Hurricane Maria, 2017, resulted in thousands of landslides including more than 40,000 on the island of Puerto Rico (Bessette-Kirton et al., 2019). For the Caribbean Windward Islands, landslides result in an annual average cost between \$115,000 - \$121,000 (DeGraff et al., 1989). Furthermore, landslides on the Windward Islands often result in damage to roads, bridges, and agriculture which economically affects more people. The Windward Islands are susceptible to the majority of landslide movement types such as slides, flows, and falls; with extreme rainfall being the essential triggering agent. The primary human-induced triggering agents of the Windward Islands are road cuts and agricultural practices (DeGraff, 1999). Another island subject to frequent landslides is the Commonwealth of Dominica; the Good Hope landslide of 1986 resulted in the death of a child, loss of a health clinic, primary school, cropland, and a 90.0-meter segment of the road (van Westen, 2016)

Because natural hazards frequently affect the Caribbean Islands and the terrain is highly susceptible to flooding and landslides, mainly, extreme rainfall triggers the majority landslides, several projects are in process to aid the affected countries. A project funded by the World Bank, in 2014, is the Caribbean Handbook on Risk Information Management (CHARIM) project. The primary objective of the CHARIM project, led by a Faculty of ITC, University of Twente, “is to build capacity of government clients in the Caribbean region, and specifically in the countries of Belize, Dominica, St. Lucia, St. Vincent and the Grenadines, and Grenada, to generate landslide and flood hazards and risks information and apply this in disaster risk reduction use cases focusing on planning and infrastructure through the development of a handbook and, hazard maps, use cases and data management strategy” (CHARIM.net, 2019).

1.2. Area of Study

The selected country for analysing the physical vulnerability of buildings exposed to landslide impacts is the Caribbean island the Commonwealth of Dominica. Specifically, the towns Elms Hall, Kings, Hill, Castle Comfort, Loubiere, Pointe Michel, Pichelin, Soufriere, Berekua, Dubuc, and Fond St. Jean located in the parishes St. George, St. Patrick, St. Luke, and St. Mark (Figure 1.2); Chapter 3 and Appendix II of this thesis, about collection of data, describe the towns with greater detail. The Commonwealth of Dominica is located in the Caribbean Sea amongst the Lesser Antilles; the island is between Guadeloupe and Martinique. Dominica has an area of 750 km², a coastline of 148 km, a population of 72,000, and a population density of 96/km² concentrated around the coast (TheCommonwealth.org, 2019). Roseau is the capital of Dominica and access to the island is only available via low passenger aircraft at the Douglas-Charles, Canefield airports, and via seaports. Dominica’s economy is dependent on agriculture, tourism and exports; however, extreme weather frequently ravages their croplands. The primary crops of Dominica are coconuts, bananas, and citrus fruits; additionally, cocoa, coffee and vegetables (Momsen & Niddrie, 2018). Dominica uses timber and concrete blocks in traditional housing. Structural typologies include wood frame buildings, single-story concrete block buildings, two-story buildings with wood frames on top of a concrete block first story, and two-story concrete block buildings; each of the structural typologies ranges in vulnerability based on their construction (Cuny, 2019)



Figure 1.2: Shaded relief map of Dominica with parish boundaries (Central Intelligence Agency, 1990); the study area is outlined in red, and the airports are marked with an “X”

1.2.1. Climate

Dominica is a subtropical island, with meteorological stations at the airports. Douglas-Charles is on the north-east coast, and the Canefield airport is north of Roseau on the leeward side of the island (Figure 1.2). The Dominica Meteorological Service reports 30-year climatological averages from the Douglas-Charles and Canefield Airport meteorological data; however, meteorological data collected at the airports vary due to their locations on the island. Temperatures are relatively consistent at both locations, the annual average is 27°C (Dominica Meteorological Service, 2019), whereas, rainfall in the last 30 years varies significantly. Dominica’s rainy season is between June and November; Douglas-Charles Airport annual average rainfall total is 2,652.7mm with the wettest month in November, and Canefield Airport annual average rainfall is 1,759.8mm with the wettest month in September. According to the Dominica Meteorological Service 30-year climatological averages, the windward side of the Island is slightly cooler, more humid, and receives more annual rainfall.

1.2.2. Geology & Soils

Dominica is a volcanic island with ash, pyroclastic deposits, and lava flows dating to the Miocene. The oldest sediments are present on the east coast of Dominica, and younger Pleistocene deposits, composed of ignimbrite and ash, are primarily in the central and southern region (Roobol & Smith, 2004). Dominica is predominately composed of acid andesite and dacitic lava (DeGraff et al., 1989); additionally, basaltic lava flows, limestone and conglomerates (Figure 1.3). The many peaks of Dominica form from dacite and andesite deposits; whereas, conglomerates and raised limestone from the Pleistocene are present on Dominica's west coast (Figure 1.4). Dominica is a mountainous island 59% covered in dense forest (The Commonwealth, 2019.); nine active volcanoes make Dominica one of the highest concentrations of volcanoes in the world. The tropical clay soils of Dominica are highly porous, affecting runoff processes and groundwater flow (Rouse et al. 1986). Several types of vegetation grow from the fertile volcanic soil, such as pantropical vegetation, xerophytic vegetation, dry tropical forest, mesophytic vegetation, and tangled mossy forests of the upper slopes (Hodge, 1943).



Figure 1.3: Conglomerates on the west coast of Dominica (Avirtualdominica.com, 2018)

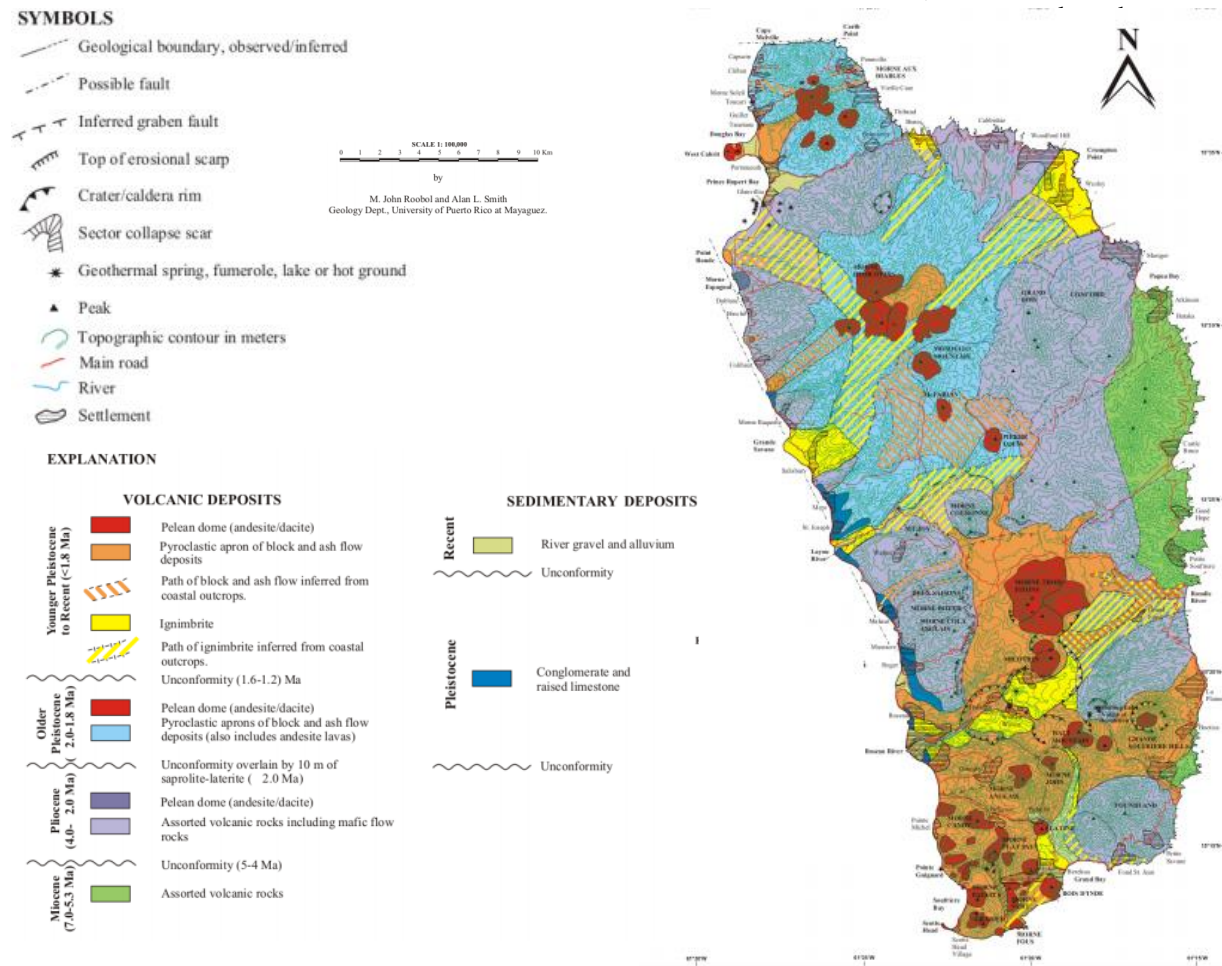


Figure 1.4: Geological map of Dominica; (Roobol & Smith, 2004)

1.2.3. Dominica's Natural Landslide Triggering Agent

For countries such as the Commonwealth of Dominica, debris slides and debris flows frequently coincide with hurricanes and prolonged rain events. In the Commonwealth of Dominica's history, Hurricane Maria is the strongest hurricane to make landfall (Pasch et al., 2018). Hurricane Maria, September 16 – 30, 2017, affected the Commonwealth of Dominica, Guadeloupe, and Martinique. Hurricane Maria first made landfall on Dominica with category five wind speeds, and according to the Post Disaster Needs Assessment of Dominica the identified recovery needs were \$1.37 billion (Government of the Commonwealth of Dominica, 2017). The disaster in the commonwealth Dominica is the

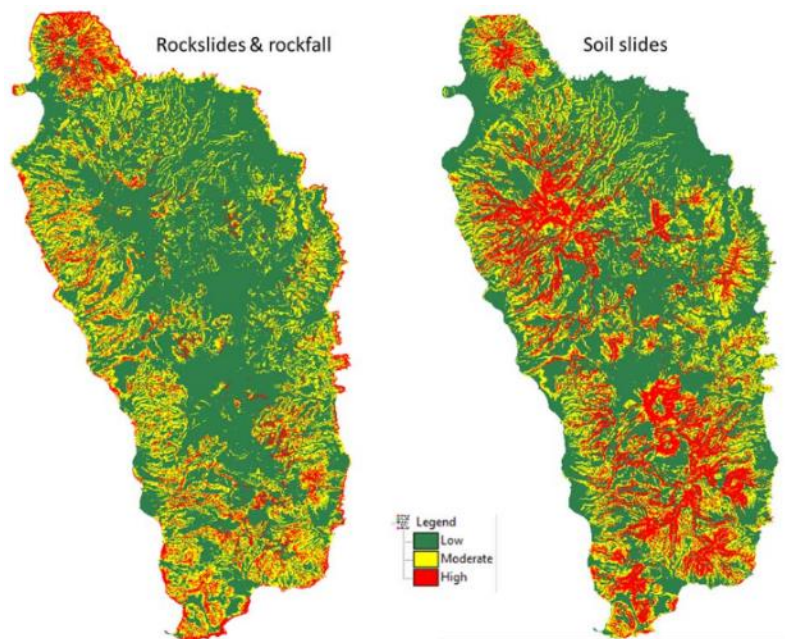


Figure 1.5: Dominica landslide susceptibility maps; rockfalls concentrated on the coast, and debris slides concentrated on the mountain slopes; (van Westen, 2016)

product of a multi-hazard environment including landslides; however, it is easy to over-simplify from the media as hurricane-induced. Coincidentally, data and reports on landslides are less abundant in comparison to hurricanes. According to Pasch et al. (2018) Douglas-Charles Airport, Hurricane Maria, reached maximum 10 minute 150 mph wind speeds, 22.8 inches of rainfall, and resulted in a total of 31 direct deaths with 34 missing; direct deaths including drowning in storm surges, rough seas, rip currents, freshwater floods, lightning strikes and wind-related deaths. Excluded from these hazards are landslides, which account for a significant amount of economic loss. Historically, landslides in the Commonwealth of Dominica have been a frequent hazard; from 1925 to 1986 five landslide events resulted in 25 people dying (DeGraff et al., 1989). Van Westen et al. (2015) used UNOSAT satellite-detection for landslides in the Commonwealth of Dominica and totalled 700 landslides after Tropical Storm Erica in the south-eastern part of Dominica; furthermore, van Westen (2016), compiled landslide inventories made in 1987, 1990, 2007, 2009, 2010, 2011, and 2013 for a national scale landslide susceptibility assessment. Figure 1.5 presents susceptibility maps, developed by van Westen (2016), of the Commonwealth of Dominica, for rockfalls, rockslides, and soil slides. Additionally, van Westen et al. (2017) attribute Hurricane Maria with triggering a total of 9,960 landslides, collectively 10.3 km² and 1.37% of the island.

1.3. Problem Statement

Landslides are a worldwide phenomenon; however, planning, mitigation, and resilience vary per region. It is particularly demanding for economically-struggling communities and regions with frequent events. Given the high landslide risk and numerous events in the Caribbean, it has been under the focus of the World Bank and

research institutes. Zafra (2015) and van Westen (2016) both researched landslide susceptibility in the Commonwealth of Dominica. Yifru (2015) assessed the road corridors of the Commonwealth of Dominica for landslide hazards, and reported only one year in the Commonwealth of Dominica, between 2009 and 2013, passed without a landslide event on the roads. Additionally; UNITAR-UNOSAT (2017), post-Hurricane Maria, mapped potentially damaged buildings and calculated the related density in the Commonwealth of Dominica's parishes using OpenStreetMap pre-building footprints and satellite imagery. Due to the frequency of events, it is important to understand the risk of buildings to landslide impacts better, and a holistic approach to researching vulnerability. However, vulnerability is an element dependent variable requiring extensive research for different elements at risk. Physical vulnerability is the product of a building's intrinsic properties and the landslide type. For example, in the landslide inventory, produced by van Westen et al. (2017), the landslide types are debris slides, debris flows, rock falls, and sediment streams. Each landslide type varies in composition, geometry, intensity and magnitude; also, Dominica's buildings vary in construction materials, and structural typologies, resulting in contrasting degrees of vulnerability.

A country often reassesses the vulnerability of affected infrastructure typologies after events of significant magnitude to improve risk assessments based on new experiences. A fundamental way to assess vulnerability is by empirically back analysing past events. Empirical landslide and damage assessments provide data about landslide attributes such as composition and geometry; as well as, the types of structures and damage inflicted. A report from an empirical assessment usually provides qualitative data about the degree of damage, or quantitative data in terms of economic loss. Additionally, empirical assessments provide rapid data collection with large samples; however, collision data is often absent or vague. A building's intrinsic properties, such as construction material strengths, are an essential component of vulnerability analysis. Alternative ways of analytically assessing vulnerability are experimental tests and numerical procedures. However, experimental vulnerability tests, on common building typologies are limited, and numerical procedures often decouple run-out analysis and impact analysis deriving vulnerability directly from damage. Furthermore, analytical methods are abundant in seismic engineering, dynamic impact studies for protection measures, and hazard mitigation, in comparison to damage of common buildings to landslide impacts.

Landslide vulnerability and damage assessment, both human-influenced and natural hazards, need further researching with quality input data for analytical methods to provide quantitative information. Assessing the robustness of buildings subject to adverse loading, in particular, with numerical methods is beneficial due to the flexibility of simulating scenarios which have not taken place. Furthermore, advances in three-dimensional modelling software, and collapse simulations make supplement vulnerability research advantageous when integrated into structural, and hazard, analysis due to the flexibility to create simulations and adjust attributes in the scenarios. Several, theoretical, methods are available for landslide vulnerability assessment; however, a comprehensive event analysis is uncommon.

Currently, there is, relatively, limited research and data of buildings of a common structural typology which reach vulnerability to landslide impacts holistically; analysing the landslide intensity, the impact dynamics, and the progression of damage over the course of a landslide event. This research aims to analyse the vulnerability of a common structural typology in the Commonwealth of Dominica, linking landslide intensity to impact dynamics to the degree of loss, utilising the three-dimensional creation suite Blender (Foundation, 2018). Blender in combination with an analytical constraint builder, Bullet Constraint Builder (Kostack & Walter, 2016), is capable of simulating a structure's dynamic behaviour for entire buildings, including non-structural elements, and progressive collapsing; whereas, traditionally, numerical methods analyse single facades or

structural frames. In the process, investigate thresholds for landslide characteristics that will result in varying degrees of damage to a common Dominican structural typology.

1.4. Literature Review: Physical Vulnerability of Buildings

This review uses the following equation for risk:

$$\text{Risk} = \text{Hazards} \times \text{Elements at Risk} \times \text{Vulnerability} \times \text{Cost} \quad (1)$$

The vulnerability variable is interpreted from the United Nations Disaster Relief Organization (UNDRO) Natural Disasters and Vulnerability Analysis Report as the degree of loss to an element at risk using a scale of 0 – 1, no damage to total loss respectively (Office of the United Nations Disaster Relief Co-ordinator, 1980).

Essentially there are two views of vulnerability; a technical or engineering sciences perspective and a social sciences perspective (Ciurean et al., 2013). Landslide physical vulnerability describes the relationship between landslide impact intensity and proportional damage. Furthermore, there are numerous approaches to research landslide vulnerability, many of which have epistemic uncertainties in proxies used for the hazard characterisation or aleatory uncertainties about parameters such as trajectory and impact angle (Guillard-Gonçalves et al., 2016). Concerning the physical vulnerability of buildings to landslide impacts, there are uncertainties related to the structural characteristics and the interaction of soil, rock, and debris with it.

1.4.1. Empirical Assessments

Researchers use historical data collection and in-situ back analysis for empirical assessments; historical data, such as landslide inventories, and insurance reports of landslide-induced damage, aid in the statistical approaches to landslide risk (Remondo et al., 2005). However, there is a high level of uncertainty in the degree of damage to the affected elements in historical data. In-situ empirical assessments express physical vulnerability in terms of the degree of loss; similar to the scale developed by UNDRO; however, make assumptions and idealisation of impact forces. Additionally, the extent of the study area affects the detail of an empirical assessment. Ciurean et al. (2013) aimed at developing tools for measuring vulnerability and documented how vulnerability is site-specific and scale-dependent (Ciurean et al., 2013). Furthermore, vulnerability assessments have problems with down and up-scaling due to generalisations and assumptions.

The advantage of assessing at a regional scale is rapidly acquiring data with empirical assessments (Palmisano et al., 2016). However, the empirical methods (Palmisano et al., 2016) used is limited to data on slow-moving landslide-induced damage; furthermore, do not make distinctions between structural typologies and qualitatively classifies the damage. Regardless of the number of uncertainties, empirical assessments provide the most data available for producing damage intensity ratios; usually relating low-intensity events with low damage ratios and high-intensity events with high damage. Additionally, (Fuchs et al., 2007) presented an empirical approach to vulnerability analysis resulting in an exponential relationship between intensity and vulnerability, and reported vulnerability derived from empirical assessments do not ensure a linear relationship between intensity and damage.

Agliardi et al. (2009) developed an empirical vulnerability function based on computed impact energy and the degree of loss for elements at risk, and a vulnerability analysis focused on rockfall at given probabilities of occurrence, magnitude, exposure, and economic value, to produce a vulnerability curve; a vulnerability curve is a function to relate the degree of loss to a hazard intensity. Furthermore, Agliardi et al. (2009) reported accurate 3D numerical modelling in rockfall analysis, can support risk assessments. There are inherent uncertainties with empirical methods; however, analytical methods aid in bridging the gaps.

1.4.2. Analytical Methods

Analytical methods in research for protection structures include protection from rockfall. Schellenberg et al. (2011) presented an analytical model, referred to as a blind prediction test, using falling weight impact tests. However, there are assumptions in Schellenberg's et al. (2011) analysis in terms of idealised impact magnitudes. Analytical methods, additionally, provide greater detail on the response of a building subject to landslide impacts in comparison to empirical methods. A similarity to empirical methods is the collection of data for analysis through historical data, in-situ assessments. However, analytical methods require more detailed building information and landslide characteristics; when deriving information analytically about hazards, and elements at risk, such as landslide intensity, magnitude, run-out distribution, types of damage or structural behaviour it is essential to choose an appropriate type of analytical method.

The use of analytical and numerical methods is popular in dynamic analysis of structures; three common numerical methods used for dynamic analysis are the Finite Element Method, the Discrete Element Method and the Applied Element Method. Jalayer et al. (2018) demonstrated how numerical modelling and in-situ back analysis of observed debris flow-induced damage could be modelled congruently in masonry buildings with the finite element method. The finite element method is capable of modelling complex non-linearities and solid elements making it useful for structural analysis. Another example using the finite element method for structural analysis, and vulnerability to damage by rockfall, researched by Mavrouli & Corominas (2010), uses the application of omitting impacted load-bearing columns and the redistribution of the respective load until reaching equilibrium. Varying combinations of column removal are modelled to simulate rockfall of varying diameter, energy, and trajectory. Mavrouli et al. (2010) further describe when a mass impacts a particular structure with residual kinetic energy, initial damage of critical structural elements can result in extensive damage and progressive collapse. However, the model, presented by Mavrouli et al. (2010), does not consider the spread or stacking of debris and possible successive collisions of debris. For large simulations the Finite Element Method is computationally taxing; a faster alternative is the Discrete Element Method.

Utilising discrete volume elements is a faster method than the finite element method, and preferred, for larger structures and 3D software. Discrete element models can simulate extensive damage to structures at a lower computational cost than models using the finite element method (Adam et al., 2018), and are used to simulate the displacement of structures (Gu et al., 2014). Gu et al. (2014) discussed the collision of fractured components with debris stacking could be visually simulated and integrated into a model with the discrete element method. A similar process of analytical modelling and damage simulation is in the subsequent research including the influence of debris inside and surrounding a structure after impact.

The proposed research analyses numerical-simulations of buildings impacted by landslides using the 3D animation suite Blender (The Blender Foundation, 2018); animation software which uses rigid body physics and contact detection techniques to simulate collisions are relatively similar to a discrete element model (Longshaw et al., 2009). Another benefit of computationally simulating structural behaviour is the flexibility in

adjusting the building and hazard attributes; however, analytical methods and computational modelling for future risk predictions are scarce. The software in this research uses bullet physics, similar to the discrete element method, for simulations which solve dynamic loading through an iterative process. In addition to Blender, the simulations use the Bullet Constraint Builder (Kostack & Walter, 2016), which applies a compressive, tensile, shear, and angular strengths to each constraint resulting in a unique breaking threshold based on realistic material properties. The combined methods of bullet physics, and the Bullet Constraint Builder's yield strengths are similar to an applied element method.

1.4.3. Vulnerability & Fragility Curves

Vulnerability curves are functions relating to the degree of loss, of a specific element, to a specific hazard intensity. Although numerical methods are useful for detailed analysis of hazards and elements at risk, vulnerability data needs to be transparent and transferable for future landslide risk assessments. A common approach is developing vulnerability curves from empirical analysis. Fuchs et al. (2007) use an economic approach in their empirical analysis, deriving quantitative vulnerability values from observed monetary loss. There is a limit to the transferability of Fuchs' et al. (2007) results due to insufficient data, and the extent of deposit heights in the analysis. Furthermore, a deposit height does not directly relate to a degree of damage, because the centre of mass and magnitude may vary. Also, when defining vulnerability as an indication of the degree of loss, research may incorporate several parameters, such as damage patterns in buildings, a monetary value in repairs, amount of property damage, or value of sections of a building into vulnerability functions (Papathoma-Köhle et al., 2012). However, as noted by Papathoma- Köhle et al. (2012) vulnerability curves require a significant amount of information about structural typologies and impact intensity which often isn't detailed well in post-event damage assessments. Traditionally, historical data and numerical simulations integrate into vulnerability curves using height, velocity, and impact pressure (Quan Luna et al., 2011); however, input data to derive vulnerability is scarce and vague about building states before damage.

Fragility curves are functions which express the probability of reaching a predefined damage state. Mavrouli et al. (2014) used a classification system, similar to UNDRO, based on frame typology, infill wall typology, and openings. Empirical assessments and numerical models are applicable for deriving intensity values with fragility curves; however, as in most cases, data is often insufficient. Whether assessing a single or multi-hazard event, for optimal validation the structural analysis must be incorporated with measured damage data and landslide intensity. However, analytical methods often decouple the impact analysis and damage results; resulting in assumption about the intensity and the development of damage. This research aims to supplement available data of vulnerability research of building responses to landslide impacts by producing vulnerability curves with analytical-numerical methods and back-analysis of building damaged by landslides in Dominica. The advantage of this research method is the flexibility with modelling the hazard and the elements at risk, essentially simulating a holistic vulnerability analysis from a landslide release to total induced damage of a building.

1.5. Objectives and Research Questions

General objectives: Analyse the vulnerability of a building, of a common structural typology, and landslide-induced damage through analytical-numerical methods and back analysis for the development of vulnerability curves.

Specific objective 1: Assess post-Hurricane Maria landslide datasets for selection of affected areas and develop a damage assessment checklist for fieldwork.

RQ 1a: What type of landslides overlap accessible neighbourhoods?

RQ 1b: Does satellite imagery aid in determining the hazard type and intensity?

RQ 1c: What are the standard construction materials and building typologies of the study area (single story, high-rise, or complex).

Specific objective 2: Collect data through fieldwork at the sites selected in specific objective 1 for impact analysis.

RQ 2a: What damage is due to landslides, and what damage is due to other hazards?

RQ 2b: Where is the landslide scarp, and what is the spatial extent of the run-out?

RQ 2c: What are the landslide compositions; are there intensity indicators?

Specific objective 3: Analyze landslide intensity through back analysis using a numerical run-out model RAMMS (RAMMS DEBRISFLOW v.1.7.20, 2018)

RQ 3a: Is the model appropriate for this type of analysis?

RQ 3b: Can the model be parametrised?

RQ 3c: How can the model be validated?

Specific objective 4: Simulate the interaction between landslide impacts and buildings, perform a parametric analysis, using the animation software Blender (Blender v.2.79, 2018); including the Blender add-on Version 3.30 of Bullet Constraint Builder (Kostack & Walter, 2016), and Version 1.0 Impulse (Craddock, 2016)

RQ 4a: What differences are present in the models in comparison to the observed data collected during fieldwork; which differences are more important?

RQ 4b: What modelling parameters need to be calibrated and how?

RQ 4c: What modelling parameters have the most significant influence in the Blender simulations?

Specific objective 5: Perform a damage analysis using a single impacting element with alternative modelled impact heights, total volume, and velocity to produce vulnerability curves

RQ 5a: What degrees of damage are induced altering the impacting intensities; height, volume, and velocity?

RQ 5b: What contrasts are there in using different intensity variables to produce vulnerability curves?

1.6. Thesis Outline

The following five chapters outline the thesis structure:

Chapter one: Introduction

This chapter includes a background to the topic of landslides, building vulnerability, and damage analysis. A literature review, examples of relevance the research general and specific objectives with research questions.

Chapter two: Methodology

This chapter presents the methodology of the research, including the development of fieldwork, the collection of data, analytical modelling, simulations, and flow schemes of the research stages.

Chapter three: Data Collection

This chapter is an overview of the selection of sites for surveying landslide-induced damage to buildings in Dominica. Also, it describes the collection of data at the selected sites.

Chapter four: Analytical Simulations of Building Response to Landslide Impacts

This chapter explains the process of analytical simulations. Starting with RAMMS, modelling landslides and analysing the modelled max flow values. Then, structural response analysis in Blender simulating landslide impacts to a building of a common structural typology. Last, a damage analysis using single impacts and constant velocities for the development of vulnerability curves.

Chapter five: Discussion & Conclusions

The final chapter is a discussion about the research and concluding remarks.

2. METHODOLOGY

The research methodology has four stages of completing the research objectives; the first stage begins with the preparation for fieldwork, and data collection, to determine where in the Commonwealth of Dominica landslides, triggered during Hurricane Maria, overlap accessible neighbourhoods. Furthermore, determine what types of landslides, the magnitude of the damage induced to the buildings, the common structural typologies and the construction materials. The second stage of the research presents how the empirical assessments and the collection of data at affected buildings proceed, including how damage, structural and landslide properties were documented. In the third stage of research, the analysis begins with using the numerical software RAMMS to model the landslide intensity, then, the animation software Blender to analyse modelled building responses to simulated landslide impacts. In the final stage of research the applicability of the software for analytical vulnerability assessments of buildings was determined, and, a damage analysis was performed simulating single impacts, of a constant velocity, to a building of a common structural typology. The simulated damage from the performed analysis using single impacts is then presented as vulnerability curves. Tables 2.1 & Figure 2.1 present the theoretical research method for the development of fieldwork and the collection of data.

Table 2.1: Stages 1 & 2 of Research Methodology

Stage	Activities and Products
Fieldwork Preparation	<ol style="list-style-type: none"> 1) Select sites with landslides overlapping neighbourhoods 2) Develop an assessment checklist for surveying
Data Collection & Empirical Damage Assessment	<ol style="list-style-type: none"> 3) Document hazard types, intensity indicators, structure types and construction materials; 4) Classify the total degree of landslide-induced damage to the building

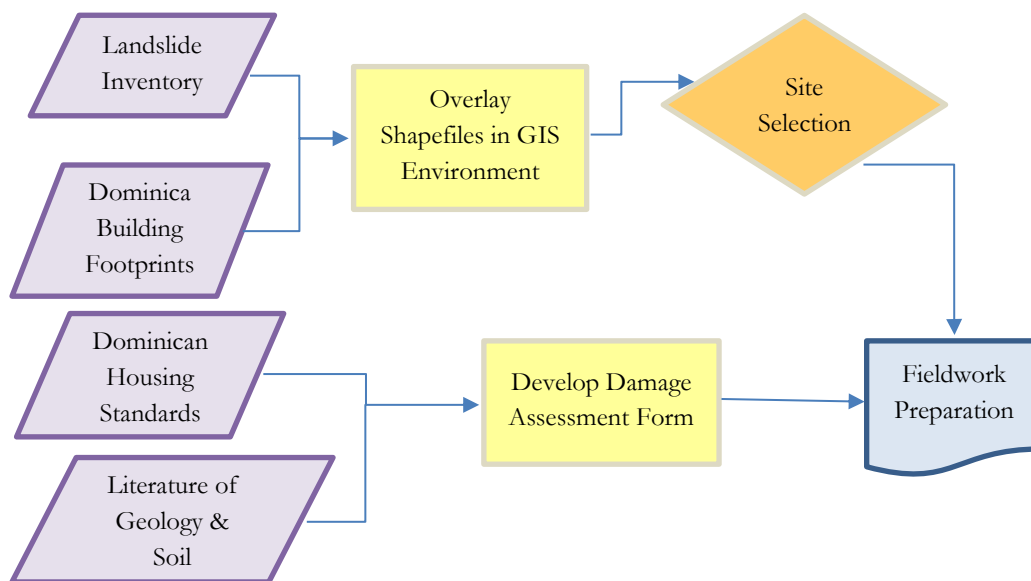


Figure 2.1: Flow scheme of the preparation for fieldwork.

2.1. Development of Fieldwork

The development of fieldwork corresponded to the research specific objective 1 and was divided into two steps to prepare for acquiring damage data during fieldwork. First the sites were selected by assessing the post-Hurricane Maria landslide inventory and the OpenStreetMap building footprints in the Commonwealth of Dominica; then, a surveying assessment was developed based on the identified landslide types, intensity indicators, and structural types identified in the study area from satellite imagery, and literature on the Commonwealth of Dominica's building standards.

2.1.1. Site Selection for Fieldwork & Development of Surveying Assessment;

- To select sites for data collection the following steps were performed:

Shapefiles of a landslide inventory produced by van Westen et al. (2017) and OpenStreetMap building footprints for the study area were acquired. The shapefiles were then overlapped in a GIS environment to assess which neighbourhoods were affected landslides. Additionally, unmanned aerial vehicle (UAV) imagery and DigitalGlobal Google Earth historical imagery were assessed for possible overlooked landslides and affected buildings omitted in the inventory. Maps were then produced for 23 sites selected, including the location of the affected buildings, landslide scarps, run-outs, and access to the site.

- To develop a surveying procedure, the following steps were performed:

First literature on the country's housing standards, geology, soils, and past events were reviewed; then, the landslide types identified during the selection of sites, and construction materials from the Guide to Dominica's Housing Standards (physicalplanning.gov.dm, 2018). Additionally, the input data required for analysis with RAMMS and Blender was reviewed, to acquire the necessary parameters during fieldwork. A systematic procedure to survey the landslides, the affected building typologies, and landslide-induced damage was developed and is presented in Appendix I. Finally, the maps developed during the site selection, and the surveying procedure was combined into the fieldwork preparation presented in the flow scheme of Figure 2.1.

2.2. Collection of Data & Empirical Damage Assessments

Fieldwork was comprised of empirical site assessments and data collection at landslide-affected buildings of a common structural typology; Figure 2.2 presents the theoretical flow scheme.

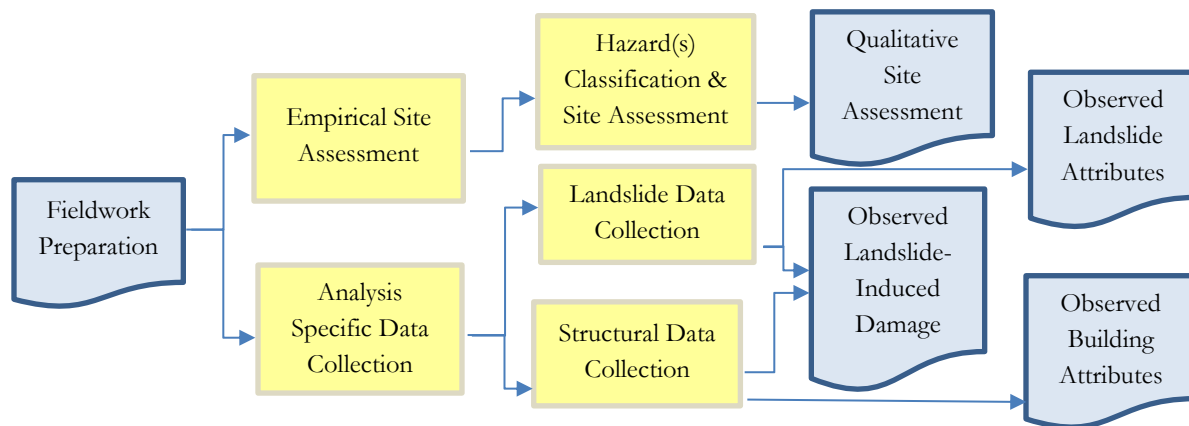


Figure 2.2: The flow scheme of the empirical assessment and the collection of data continues from Figure 2.1

2.2.1. Fieldwork & Site Assessments.

The collection of data corresponds to the research specific objective 2; during the collection of data the 23 sites selected during the preparation for fieldwork were visited, and empirical observation of buildings damaged by landslides was documented including details of the vegetation, structures, mitigation, and the easily identifiable landmarks. Then, damage to the structural frame and walls of the building from wind, flooding, debris slides, debris flows, rockfall, and impacts from vegetation were documented; specifically, damaged roofs from wind, water stains from flooding, or an accumulation zone from a landslide impact. Additionally, when possible the landslide scarp was documented for an input parameter with the software RAMMS.

After the damage inducing hazards were documented, the spatial extent of the building was sketched with the dimensions of the affected area, and the distances to neighbouring buildings. Additionally, the location of large auxiliaries, such as septic tanks or outdoor baths, the distance between the building and the fence, wall, protection or mitigation were documented and sketched. Next, the landslide-induced damage to the building was detailed by including the number of damaged floors, openings, structural members, infill walls, and rooms with debris inside.

The floor plans were sketched to aid in modelling the building in Blender for impact analysis, with dimensions of the structural frame, the infill wall dimensions, the construction materials, the locations of openings, and the door orientations. Figure 2.1 was a reference on how to draw floor plans with infill walls, door orientations, and the damaged façades were indicated on the sketches. The dimensions of windows and openings were documented; as well as, the position of staircases, and assumed relevant specifications. Additionally, photographs of each floor and damage façades were documented. Then, dimensions of the foundation and roof were documented, and the total number of damaged columns, beams, load-bearing walls, and damaged stairs or decorative structures per floor were documented

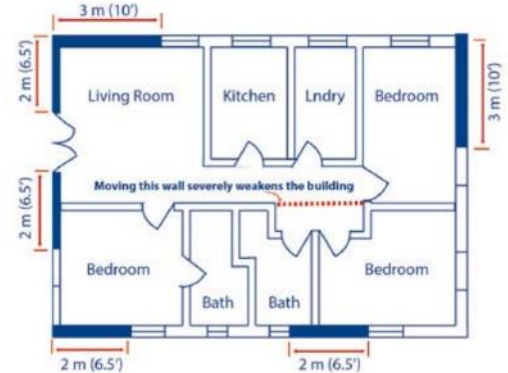


Figure 2.3: An example of how to sketch a floor plan (The Ministry of Planning and Economic Development, 2018)

The total degree of damage, including damage induced by hazards other than landslides, to the surveyed building was documented using the following classification scheme inspired by Palmisano et al. (2016):

- None
- Light: Non-structural damage only
- Minor: Significant non-structural damage; minor structural damage
- Moderate: Significant structural and non-structural damage
- Severe: Irreparable structural damage; will require demolition
- Collapse: Complete structural collapse

After surveying the landslide-affected building's structural typology, and damage, the landslide intensity indicators were documented, to aid in back analysis when modelling, including the debris height around the building, the composition of the accumulated landslide at the affected building, the building's orientation in the accumulated debris, and the building's location relative to hillslope.

2.3. Analytical Modelling & Simulations

The analytical methodology is divided into analytical simulations and development of vulnerability curves; the analytical modelling and simulations correspond to the research specific objectives 3 & 4. Table 2.2 & Figure 2.4 presents the theoretical flow scheme of the analysis, starting with the acquired outputs presented in Figure 2.2.

Table 2.2: Stages 3 & 4 of Research Methodology

Stage	Activities and Products
Analytical Modelling & Simulation	1) Hazard & structural modelling 3) Evaluate software applicability for landslide-induced damage 2) Event simulations & calibration
Development of Vulnerability Curves	3) Determine the intensity variables 4) Interpret results

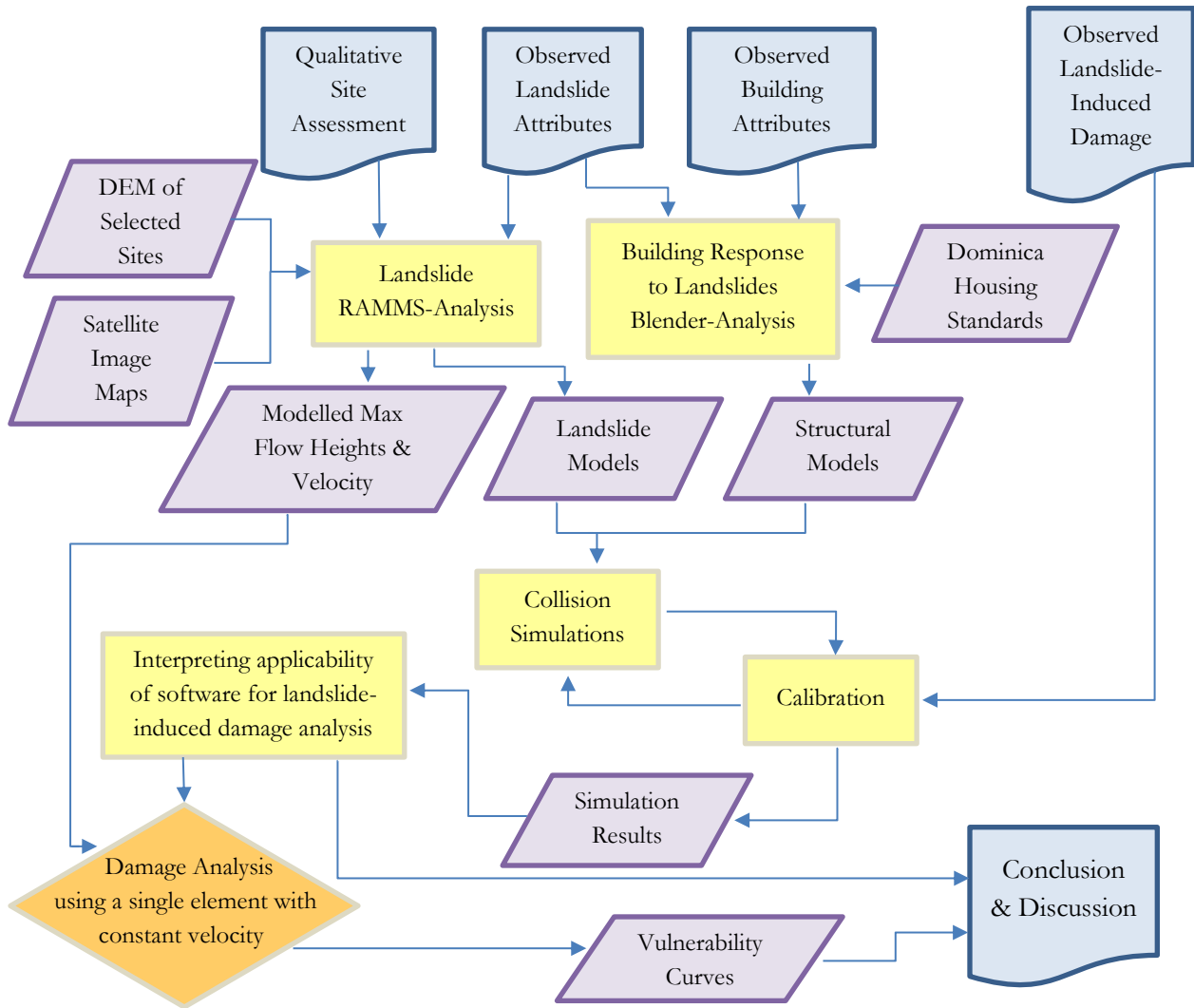


Figure 2.4: The flow scheme of the analysis and development of vulnerability curves continues from Figure 2.2

The software used for analysis were Rapid Mass Movement Simulation (RAMMS) (RAMMS DEBRISFLOW v1.7.20, 2018) and Blender v2.9 (Foundation, 2018); additionally, the Blender add-ons Bullet Constraint Builder v3.30 (Kostack & Walter, 2016) and Impulse v1.0 (Craddock, 2016). RAMMS was utilised for the numerical modelling of block-release landslides, of shallow depths and small volume, to simulate max flow heights and velocities in the study area. After modelling the landslide parameters in the RAMMS analysis, the Blender physics engine was utilised for simulating physical phenomena, such as landslide impacts to buildings, with rigid body physics. The rigid body physics with Blender is similar to discrete element modelling, in that the modelled elements interact based on their geometry, and there is no deformation to the element when simulated. The modelled elements are affected by gravity, simulated forces, and then, the modelled buildings were enhanced with real-world breaking thresholds at the connection of the modelled elements. Additionally, the structural typology of the model used in the core of this analysis, Building 2 from the collection of data, was analysed for simulated damage using the Blender add-on, Impulse, which allows the user to assign a constant velocity to modelled elements.

2.3.1. Max Flow Analysis Using RAMMS

The presented analysis using the software RAMMS corresponds to the research specific objective 3. A 5.0-meter digital elevation model (DEM) was acquired from the CHARIM GeoNode (CHARIM.net, 2019), and cropped to the survey extent in a GIS environment; additionally, maps were created from Google Earth historical imagery and cropped to the survey extent to increase processing speeds of the RAMMS analysis. After inputting the DEM and the map into RAMMS, the landslide release area and the landslide depth were determined from the map and data collected during fieldwork. The location of the landslide, specifically, was determined by observing the erosion from the event visible in Google Earth historical imagery, and the landslide depth was calibrated between depths observed during fieldwork. A block release was selected for the analysis because debris flow simulations in RAMMS require a hydrograph which has been unobtainable due to the site-specific events. However, debris flows were mostly observed during fieldwork, and the influence of water during the landslide event was significant due to the event occurring in response to Hurricane Maria. Furthermore, because engineering soil properties, such as internal friction angles, of the soils in the study area were not obtained, the dry coulomb type friction assigned in RAMMS was derived from literature values of a volcanic soil (Zhu, 2019).

The remaining parameters before starting the RAMMS simulations were curvature, erosion, and obstacles. Depending on the input data quality and real-world topography, enabling the curvature increases the friction in a simulation, and the effect was determined insignificant due to the spatial extent of the study area; therefore, curvature was disabled. Erosion in RAMMS models the net decrease in elevation, and aids in predicting the total volume of debris in max flow distributions. However, the erosion parameter requires data of erosion depths and rates, which have been unobtainable due to the site-specific areas; therefore, erosion was disabled. Last, an obstacle was added to the model by drawing a polygon around the affected buildings; the obstacle was used to divert flow in the RAMMS analysis, and acquire max flow heights, and velocities, against the obstacle. The RAMMS analysis produces distribution maps of max flow height, velocity, pressure, flow momentum, and shear stress, with a resolution equal to the DEM. The max flow height distribution, then, compared with the observed debris height during fieldwork and adjustments to the release depth were made to acquire relatively equal max flow heights at the affected building. The landslide properties, used to model flow heights with the greatest resemblance to the observed debris heights, were documented for modelling the landslide in Blender, as well as the simulated max flow heights and velocities for calibration of the simulations. The following parameters from the RAMMS results were documented:

- The planar distance from the building to the landslide
- The planar area of the landslide and the total volume
- The average slope angle of the landslide
- The simulated max height and velocity distributions against the modelled obstacle

2.3.2. Simulations of Landslide-Induced Damage to Buildings

The presented analysis corresponds to the research specific objective 4 and is the beginning of analysis using the software Blender. The analysis in Blender began with modelling the landslide and simulations to assess the run-out kinematics and accumulation zones. A parametric analysis was performed, and the optimal calibrations of the modelled soil-elements, the distance between the building and the hillslope, and the hillslope surface response were determined. The surface response parameter does not correspond to internal friction angles of the simulated landslide; it is a Blender specific parameter used to determine the degree of loss to a simulated element's velocity when colliding with another element. Additionally, the surface response parameter has an effect on modelled objects sliding against each other, such as the soil-elements of the landslide directly in contact with the failure plane. After the parametric analysis of the modelled landslide, the modelled building was enhanced with the Bullet Constraint Building to connect the simulated building elements with real-world breaking thresholds. Next, the modelled building was subject to simulated landslide impacts and the damage was analysed. Then an attempt was made to calibrate the mortar wall breaking thresholds; however, final values were not validated. The impact dynamics with the modelled building, from the simulated landslide, were visualised to analyse the simulated landslide-induced forces on the building. After analysing the simulated forces, the applicability of the software for landslide-induced damage analysis was evaluated. Last, a decision was made to analyse impact forces on the building using a single element with a constant velocity for the development of vulnerability curves.

2.3.2.1. Modelling of the Landslide & Simulation of the Run-out

Before analysis of the building's response to landslide impacts, a parametric analysis of the landslide simulation was performed. The landslide properties described in the previous RAMMS analysis were used to model the landslide in the animation software Blender. The hillslope was modelled as an angled plane using the average slope angle of the landslide modelled in the previous RAMMS analysis. The ground surface was modelled, initially; however, during the analysis of the building's response to simulated landslide impacts, a new ground surface was simulated to include the foundation of the buildings. The initial model of the building, for the parametric analysis of the landslide, was a single element with the dimensions of the measured building. The building was modelled in this way to simulate the landslide with the maximum number of computational calculations used on the run-out kinematics; the initial priority of the landslide was to simulate the distribution of the landslide with the highest accuracy.

The modelled landslide, hillslope, building, and ground were then assigned passive rigid body types to interact with other elements in the simulation but remain static. The landslide design starts as a rectangular volume with an equivalent planar area, depth, and volume as the landslide properties from the previous RAMMS analysis (Figure 2.5a). Then, the modelled landslide was discretised into smaller soil-elements of equal cubic geometry to model the landslide composition. Table 2.3 & Figure 2.5a present the initial modelling of the landslide; the soil-elements were given a minimum of 1.0 cm space between each other because, in the Blender simulations, errors occurred at the initiation of a simulation with modelled elements too close to each other. The soil-elements were modelled as the composition of the landslide, and assigned active rigid body physics,

which enables the objects to move and interact with other rigid bodies in the simulation; additionally, the modelled soil-elements were assigned mass based on literature values of a volcanic soil density. Next, the parametric analysis began and the dimensions of the simulated soil-elements were analysed to determine the smallest computationally acceptable size. The size of the simulated soil-elements was determined significant because it directly affects the distribution of elements and simulated impact magnitudes on the building. Next, the modelled geometry at the toe of the landslide was adjusted to remove overhanging cubes which were toppling at the initialisation of the release. A vertical cut was modelled at the toe of the landslide, representative of a real-world cut slope (Figure 2.5b); however, the topography of the hillslope, before the event, was not observed and topographic data, of significant resolution, have not been obtainable due to the site-specific study area.

After cropping the toe of the landslide, run-out simulations were performed, and it was determined adjacent boundaries were needed to restrict lateral displacement of the landslide on the hillslope (Figure 2.5b). The next parameter set in the modelling of the landslide was the surface response for the modelled elements. The modelled soil-elements were assigned a value of 1.0, and the ground plane was assigned the default value of 0.5. The hillslope was initially assigned a surface response value of 1.0; however, was adjusted during the parametric analysis to analyse the effect on the simulated distribution of soil-elements.

Table 2.3: Blender Landslide Properties

Modelling Parameter	Value
Rigid Body Type	Active
Rotation	45°
Dimensions	0.125m ³
Density	1900kg/m ³
Surface Response	1.0

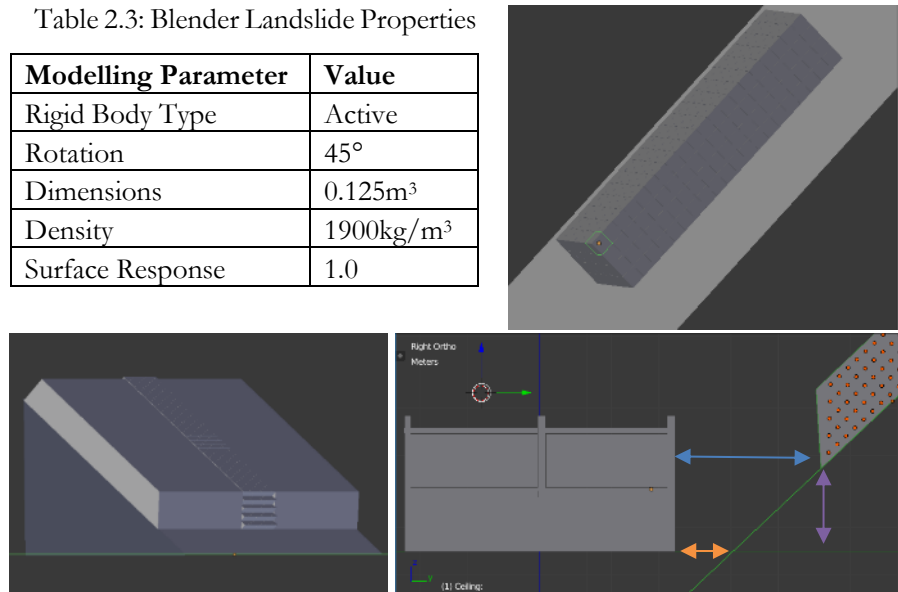


Figure 2.5a – 2.5c: (Top) Preview of modelling a landslide; selected is a single cube and Table 2.3 presents its modelled properties; (Left) Preview of the landslide with boundaries modelled. (Right) By lowering the landslide height (purple), the planar distance between the building and hillslope (orange) increases without changing the planar distance between the building and the landslide (blue); the slope-length is reduced by lowering the landslide height

Initially, the building was modelled as a single element to observe the simulated run-out kinematics, and landslide distribution, with the greatest number of calculations, prioritized on the landslide; the greater number of elements added in a simulation requires a greater division of the simulation steps calculated per second and less accurate simulations of landslide kinematics and the simulated forces of interacting elements. The planar distance, from the modelled landslide to the obstacle modelled in RAMMS, was used to orient the modelled building and landslide in Blender. After, observing the simulated distribution of soil-elements around the modelled building, the landslide model was determined ineffective to simulate flow heights of a relative resemblance to the observed accumulated debris between the building and the hillslope; therefore, the landslide geometry and the location of the landslide model were reconsidered.

An alternative landslide location, area, and depth was modelled in RAMMS using the same procedure described in the subchapter 2.3.1; however the modelled landslide was positioned at a greater planar distance to the modelled obstacle, and a shallower release depth was modelled intending to simulate an accumulation height against the building relatively similar to the height observed during fieldwork. In the initial landslide, simulations resulted in an accumulation height too high, and narrow, at the modelled building in comparison to the observed accumulation of debris between the building and the hillslope.

Furthermore, the new landslide modelled in Blender used the optimal calibrations of soil-element size, and surface response parameters determined during the previous landslide simulations. The initial distance between the building and the hillslope was modelled the same as the previous analysis; however, was determined to be too short of distance to simulate an accumulation geometry, similar to the observed accumulation geometry, between the building and the slope with the previous landslide model; therefore, the distance between the building and the hillslope was increased. The distance between the building and the hillslope was increased by moving the entire hill and landslide, spatially, down, thus reducing the slope length and release height, but increasing the distance between the building and the hillslope without affecting the planar distance between building and the landslide (Figure 2.5c). The planar distance between the building and the landslide, is the same as the planar distance between the landslide and obstacle in the RAMMS analysis; however, the distance between the building and the hillslope was assumed from the observed spatial extent of the walkway on the sides of the building. By decreasing the landslide height, and slope length, the simulated velocity and development of an accumulation zone were affected. The distance between the building and the hillslope was increased to 5.0m and 6.0m, and the surface response of the hillslope was calibrated between 0.0 and 1.0. The optimal calibrations of the distance and surface response parameters were acquired and used in the initial simulations of the modelled building enhanced with the real-world breaking thresholds.

2.3.2.2. Modelling & Discretisation of the Building

The more elements added to a Blender simulation the higher the computational cost; therefore, the structural-resolution of the building directly affects the simulated damage induced. Early into the research, optimistic simulations were performed of a two-story concrete block building surveyed during fieldwork; however, the structural-resolution was inevitably reduced to modelling the concrete blocks, of the observed unaffected walls, with larger slab elements. The processing time was several hours, sometimes days, due to the extensive number of elements in the building model; the number of elements in the building is in addition to the number of simulated landslide elements.

The building, modelled in Blender, was modelled in preparation to use the Bullet Constraint Builder. First, the structural frame of the building was modelled excluding the overlap of beams and columns; this was modelled to simulate the structural frame with, the Bullet Constraint Builder, constraints between elements where they are most likely to separate. Furthermore, when a constraint built between two elements stacked on top of each other is broken the beam will not collapse because the beam is rested on the column (Figure 2.6); therefore, the beams were modelled between columns to fall with gravity when the breaking thresholds of the constraints are exceeded. The columns were modelled as segmented elements which span from the ground to the ceiling, the floor of the second story, and above the

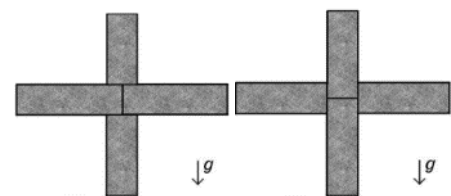


Figure 2.6: Example of how structural frames are modelled in Blender; (left) shows bad example which might not collapse if the constraint is broken; (right) shows beams that will fall with gravity enabled (Kostack, 2015)

ceiling as the structural frame of the second-story. The length of the beams, and discretisation size, directly affect the modelled foundation depth; the smallest discretisation size of the ground floor columns is modelled into the ground for the foundation. After, the infill concrete block walls were modelled. The concrete block courses were modelled between columns, with windows, the same as observed and documented during the collection of data, and the simulation was run to analyse the changes in run-out kinematics due to the increase in elements to the simulation. During this analysis, the building was assigned a passive rigid body type, which allowed the debris to pass through openings such as windows and doorways, and prevented the buildings from collapsing. The passive-building impact analysis was performed to calibrate the surface response and the distance, between the building and hillslope, parameters with the additional elements in the simulation. A distance, between the house and the hillslope, and the surface response of the hillslope were determined, and then the building constraints were modelled with the Bullet Constraint Builder.

The Bullet Constraint Builder requires the elements to be systematically organised to recognize which elements are assigned constraints; therefore, groups were made for the building's beams, columns, and concrete blocks. Next, the building's modelled structural frame and ceiling-slab were discretised by 2.0m. The discretisation divides the columns, beams, and ceiling segments longer than 2.0m into smaller equal segments; the modelled elements are built with constraints between each other, and individual rigid bodies do not show deformation. Therefore, the discretisation is necessary to simulate forces applied along the length of these structural elements. However, a lower discretisation size results in a greater number of elements modelled, affecting the results of the simulation.

Next, the column and beam dimensions, acquired during fieldwork, were used in the calculation of the concrete and reinforcement yield strength. Compressive, tensile, shear, bending, and spring constraints were built with calculated breaking thresholds using the Bullet Constraint Builder (Figure 2.7). The concrete block walls were modelled without a spring constraint; ultimate elastic breaking thresholds for compression, tensile, shear, and bending were estimated from the literature on mortar breaking thresholds (Arash, 2012) and (Still, 2004). The mortar breaking threshold was assigned elastic breaking thresholds because the concrete block walls observed were shearing through the mortar, rather than the concrete blocks, and the strength of mortar is significantly weaker than concrete due to the difference in aggregates used in concrete. After the Bullet Constraint Builder finished applying the constraints to the model, the structure was assessed to identify gaps where constraints were not built, due to modelling errors and overlapping elements, and another analysis of the landslide run-out kinematics, and accumulation distribution, was performed due to the increase in modelled elements from the addition of constraints.



Figure 2.7: Visual representation of generic and spring constraints. The coloured arrows were edited from (Kostack, 2015), to show the six constraint types; Red & Yellow: compression and tensile; Blue & Purple: shear forces; Green & Grey: bending forces

The effect of the number of elements in the simulations became problematic when the analysis of the forces simulated on the building was attempted. The significant increase in elements, with the constraints, applied, ultimately, resulted in the reduction of elements in the building model through the replacement of the modelled concrete blocks, on observed unaffected walls, with larger slab elements. Additionally, a discretisation analysis of the entire building was performed to determine the minimum number of elements which could be modelled

and still produce simulated damage of a relative resemblance to the observed damage. After, determining an optimal discretisation size for the building, the calibration of the mortar breaking thresholds began.

2.3.2.3. Calibration of Mortar Breaking Thresholds & Interpretation of the Simulated Damage

An empirical analysis of the simulated damage was performed aimed at simulating damage resembling the observed damage during fieldwork. Particularly, an observed wall, significantly damaged, yet, not collapsed was intended to be used as an empirical threshold of the mortar shear strength. The initial mortar values in the previous simulations were based on literature values; however, in the previous simulations, the mortar was always damaged more significantly on the ground floor than observed during fieldwork. Therefore, the mortar shear and bending ultimate breaking thresholds were progressively strengthened to observe the changes in simulated damage and accumulation height distribution. The structural frame was analysed, limited to the discretisation size; however, the constraint thresholds were not adjusted because the yield strengths were calculated with the Bullet Constraint Builder, and were derived from the data.

The mortar breaking thresholds were increased, and the forces simulated on the affected façade were analysed, at the moment of failure, to observe the vertical and lateral pressure gradient simulated on the wall. The simulated forces on the affected façade were presented graphically and, then, the applicability, of the software for landslide-induced damage analysis was evaluated. A decision was made to analyse damage induced by single impacts with a known, constant, velocity. Then, the simulated damage results, from the analysis of single impact simulations, were presented as vulnerability curves. The intensity variables were contrasted to determine which variable has the highest transferability. The development of vulnerability curves corresponds to the research specific objective 5; however, the performed analysis with single simulated impacts have not been validated, do not represent an event observed during fieldwork, and were intended to be supplemental for future research using the software.

3. DATA COLLECTION

Data collection activities correspond to the thesis specific objective 1, by incorporating an assessment of satellite image datasets for selection of landslide affected neighbourhoods and development of a damage assessment checklist for fieldwork.

3.1. Site Selection & Developing A Landslide Assessment

Data acquisition sources for the selection of sites and development of an assessment checklist include the Caribbean Handbook on Risk Information Management (CHARIM) GeoNode (Charim.net, 2019), the landslide inventory produced by van Westen and Zhang (2017), © OpenStreetMap Contributors, the Dominica Physical Planning Division (Physicalplanning.gov, 2019), and Google Earth.

3.1.1. Detecting of Landslides and site selection for survey

Van Westen’s et al. (2019) landslide inventory (Figure 3.1) and OpenStreetMap building footprints were used to select neighbourhoods by observing where landslides from the inventory and Google Earth historical imagery overlap with buildings. The towns selected are Elms Hall, Kings Hill, Castle Comfort, Loubiere, Pointe Michel, Pichelin, Soufriere, Berekua, Dubuc, and Fond St. Jean (Figure 3.2); the Physical Planning Department is in Roseau, and it is, also, added to the map. In each town debris flows, debris slides, rock falls, and sediment streams overlap individual buildings or entire neighbourhoods.

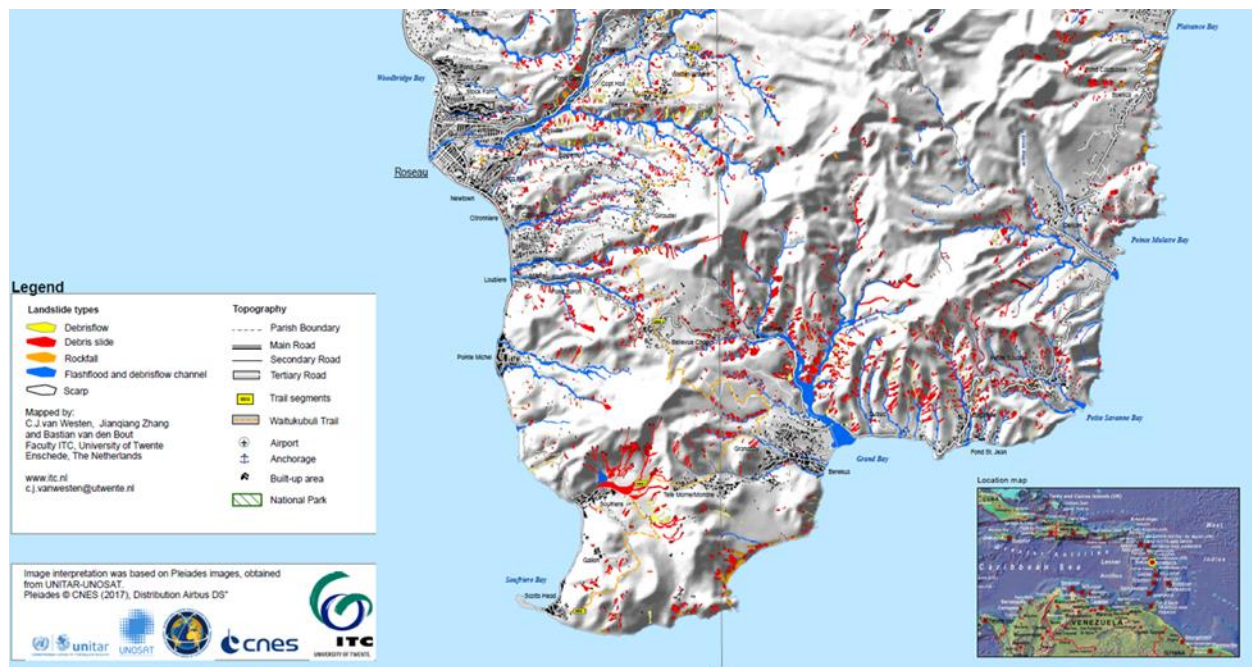


Figure 3.1: Landslide inventory of Dominica’s southern parishes, including debris flows, debris slides, rockfalls, flash floods debrisflow channels, and scarps. Source (van Westen, Zhang & Van den Bout, 2019)

Included in the site selection are buildings observed in Google Earth near landslide scars; several of the scars are visible in later dates of Google Earth historical imagery. In particular, many of the buildings affected by sediment streams in the valleys remain buried in images taken months after, 01/02/2018. Figure 3.2 shows the location of eleven towns overlapping landslides from the inventory. Sediment streams near Pichelin converge and expand across a wider region when reaching the coast between Berekua and Dubuc. In Soufriere, widespread debris slides and flows are observed on the steep slopes and converging at lower elevations. Debris flows and sediment streams, also, profoundly affected Dubuc, Pointe Michel, Loubiere, and Castle Comfort; whereas debris slides predominately affected Elms Hall, Kings Hill, and Fond St. Jean

3.1.2. Building typologies and standard construction materials

The Guide to Dominica’s Housing Standards describes the common building typology as single or two-story reinforced concrete framed homes (Figures 3.3 & 3.4); additionally, Cuny (2019) describes some of the alternative structural types including wood frames and wood framed second-stories on concrete block ground-floors.

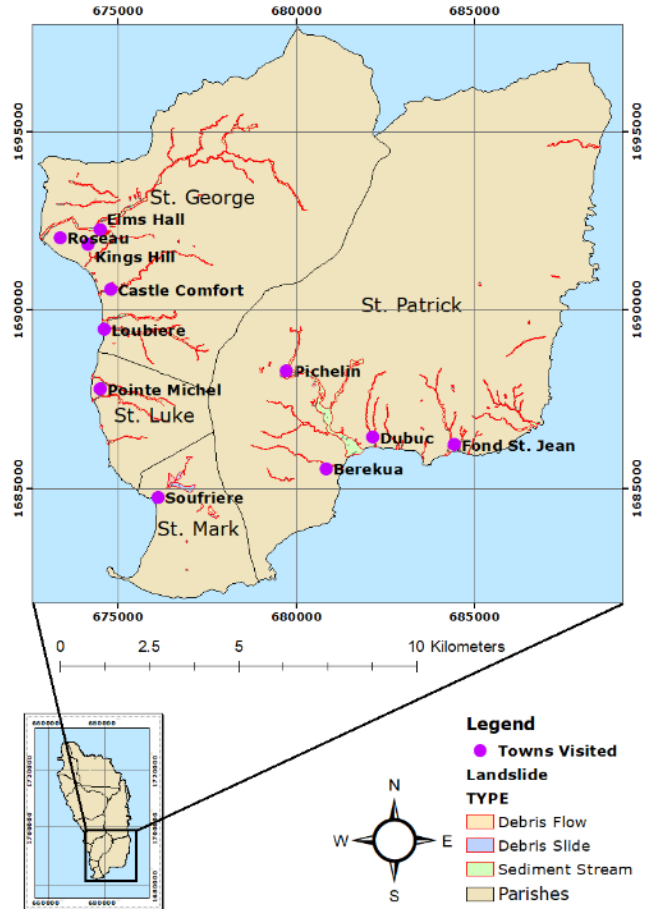


Figure 3.2: Eleven towns with overlapping landslides and building footprints.



Figures 3.3 & 3.4: (Left) Single story concrete block building affected by a debris slide; (Right) single-story building, raised on a reinforced concrete frame, affected by debris flows and a sediment stream.

3.2. Structural Data Collection & Damage Empirical Assessment

The data is organised by site and building numbers; site numbers refer to the order selected during site selection, and the assessment number refers to the order of buildings surveyed during fieldwork. Also included with the site and damage assessments are the Google Earth location plans and maps created during the fieldwork development stage. In the parishes visited, Saint George, Saint Patrick, Saint Luke, and Saint Mark, Hurricane Maria potentially damaged 65%, 73%, 72%, and 62% respectively, of the buildings, as detected in OpenStreetMap cloud-free areas (UNOSAT, 2017). Furthermore, the intensity of the event and the recovery extent is evident from landslides scars and erosion visible in Google Earth historical imagery months after the event.

During fieldwork, a total of 23 sites were visited in the southern parishes, visible in Figure 3.2, which incorporated walk-throughs of the neighbourhood to identify hazards, damaged buildings, and discussion with the locals. From the 23 sites, ten buildings, damaged by landslides, were surveyed; however, here analysis is carried out for Buildings 1 and 2 at Sites 8 and 5 respectively. The supplemental sites are described in Appendix II, and, in addition to presenting the data, the research second specific objective, concerning the collection of data through fieldwork, for impact analysis was completed.

3.2.1. Test site Pichelin and Building 1

Sites 8 & 9 are in Pichelin, and Building 1 is at Site 8 (Figure 3.5). Pichelin is significantly more susceptible to flooding and erosion than other sites visited during fieldwork because of its location at the intersection of two valleys. In addition to Building 1, there was a church and a recreational sports building hit by a debris flow across the sediment stream from Site 8. The sports building's foundation was the only remaining part of its structure; therefore, no survey was performed. The neighbourhood at Site 9 was affected by flooding and wind damage; the excavators use temporary roads constructed on the sediments in the stream beds created by Hurricane Maria. Table 3.1 presents a summary of the survey of Building 1.

It has not been possible to identify the scarp of the debris slide that affected Building 1 by field inspection due to the regrown vegetation; however, the landslide inventory indicates the same slide as developed across the road from the affected house. The regrown vegetation on the slope is dense obstructing access and visibility (Figure 3.6). The lateral geometry of the run-out is concentrated between an unaffected house on the slope and the neighbour's houses



Figure 3.5: Google Earth Historical Image; February 1, 2018; Location plan of Sites 8 & 9 in red circles

surrounding the affected home. The total run-out length has not been discretely identified; however, the debris slide crossed a road to reach Site 8 and Building 1 shielded the buildings successively in the line of a direct hit from the event. The accumulation surrounds the affected house on all sides and the roof of the ground floor.

The owners of Building 1 were available to describe the event; a debris slide, composed of volcanic soil, ferns, and tropical vegetation, from across the road accumulated on the road and damaged the house. The timber frame second-story collapsed from the impact; however, the reinforced concrete frame ground floor was not damaged (Figures 3.6 & 3.7). Additionally, the walls of the ground floor were not damaged; however, there was water inside the building. Furthermore, there were openings and spaces where the walls and frame should touch (Figure 3.7). It is questionable if the house is built in compliance with Dominica's building standards. After debris accumulated at Site 8, vegetation grew from debris and soil accumulated around and on the house. A complete overview of the buildings at Sites 8 & 9 is presented in Figure 3.8.

3.2.2. Test site North-East of Elms Hall (Valley Rd) & Building 2:

Sites 4 & 5 are north-east of Elms Hall and Building 2 is at Site 5 (Figure 3.9). The landslide inventory lists the hazard as a rockfall; however, a debris slide was present in the field. Two-thirds of the building, under construction, was accessible and untouched since the event (Figure 3.10). The ground floor, closest to the hillside, had mud, debris and water inside (Figure 3.11), and the even distribution of soil and water stains beneath the windows indicate flooding continued after the collision. On the north façade, the accumulated debris reaches the roof of the ground floor, approximately 3.0 meters high. The beams and walls were weathered on the second-floor interior, assumed to be the result of no roof. Table 3.2 presents a summary of the survey of Building 2.

A possible debris slide scarp was visible from the back of the house; however, the scarp was not surveyed due to the dense vegetation. The landslide inventory indicates the slide scarp, from the same landslide, further uphill than was visible during the survey of Building 2. Standing from the street; Building 2 had one neighbour on the right and a vacant lot on the left side. Debris was accumulated on the left side of the house, into the vacant lot, around the back of the house, and extended to the neighbouring building. The space between the buildings was 3.5 meters, and debris accumulated ~5.0 meters down the length between buildings.

The debris slide hit the north façade of Building 1, damaging the second floor. Although there was debris visible in the windows of the ground floor (Figure 3.11), there was no significant structural or non-structural damage. Trees and shrubs were pressed against the house in the accumulation, and there were less than a 30.0 centimetres of soil on the ground of the second floor; however, the grass accumulated inside was growing. The debris height accumulated at the house ranged between 2.5 – 3.5 meters, with the highest point in the centre (Figure 3.12). The debris tapered towards the sides of the house where debris could flow around into the vacant lot and space between the neighbouring building. The high point in the centre resulted in the buckling of the second-floor wall which was cracked a connecting corner beam and column (Figure 3.13). Additionally, several cracks propagate through the concrete blocks and mortar. Walking up the toe of the slide; the second-floor wall was visible buckling inward (Figure 3.12). Visible from the inside; a crack extends from the corner of the frame to the bottom right corner of the nearest window (Figure 3.13). The source of the landslide remained undetermined; however, the landslide inventory indicates a further release than what has been visible in the field (Figure 3.14)

Table 3.1: Observed Damage of Building 1

Building Type	Residential
Construction	Reinforced Concrete Frame, Block Walls, Timber Frame
Number of Floors	2
Damage State	Moderate: Significant structural and minor non-structural damage
Hazard Type(s)	Debris flow & Flooding



Figure 3.6 & 3.7: (Top) Building 1 is missing an additional timber framed second-story, and the debris slide mobilised from across the road identified by the red arrow; there is a car parked on the road below building on the hill. (Bottom) Side profile of Building 1; there are cracks visible where the walls do not touch the frame or ceiling slab, and debris accumulated around the buildings

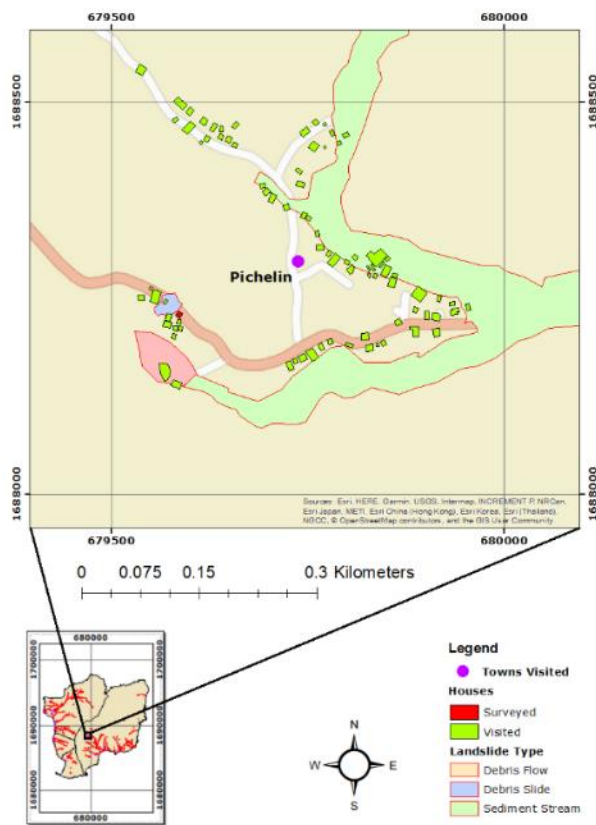


Figure 3.8: Map of Pichelin, Building 1, affected by a debris slide that crossed a road, is highlighted as a red house



Figure 3.9: Google Earth Historical Image; February 1, 2018; Sites 4 & 5 in red circles



Figure 3.10: Debris source indicated by the red arrow; green arrow points to the flooded room in Figure 3.11



Figure 3.11: Flooded room with debris in the windows resulting in an even layer of soil in the room

Table 3.2: Observed Damage of Building 2

Building Type	Residential
Construction	Reinforced Concrete Frame, Block Walls, Timber Beams
Number of Floors	2
Damage State	Moderate: Significant Structural and Non Structural Damage
Hazard Type(s)	Debris Slide & Flooding

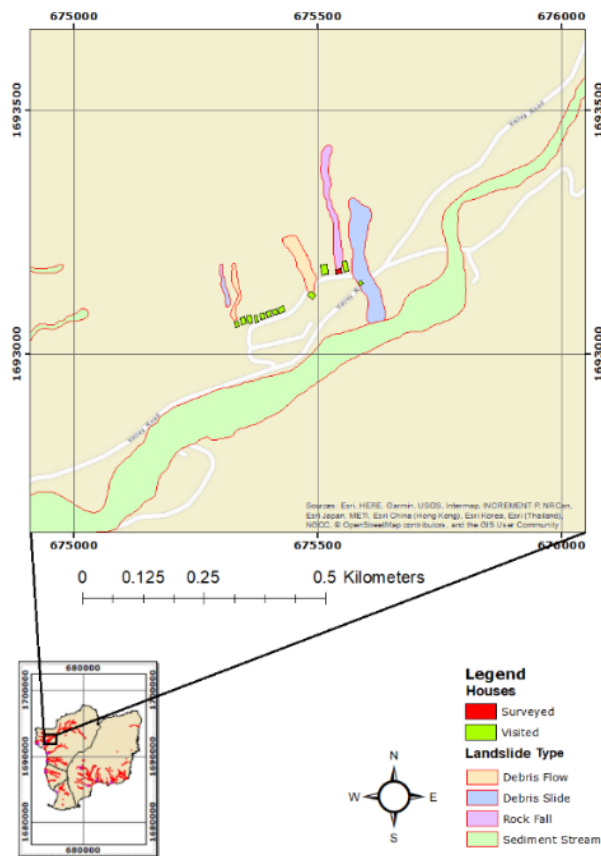


Figure 3.12 & 3.13: (Top) The second-floor of the affected wall on Building 2 was buckling at the red arrow from the accumulated debris; (Bottom) the affected wall and frame was cracked, at the red arrow, due to debris in Figure 3.12

Figure 3.14: Map of North-East Elms Hall and location of Building 2

4. ANALYTICAL SIMULATION OF BUILDING RESPONSE TO LANDSLIDE IMPACTS

The analytical simulations of building response to landslide impacts correspond to the thesis specific objective 3, by incorporating the numerical software RAMMS (RAMMS DEBRISFLOW v.1.7.20, 2018) and specific objective 4 by incorporating the animation software Blender (Blender v.2.79, 2018); including the Blender add-ons Bullet Constraint Builder v.3.30 (Kostack & Walter, 2016), and Impulse v1.0 (Craddock, 2016). The methodology for analytical modelling proceeds as described in the sub-chapter 2.3. Analysis began with the software RAMMS to model max flow heights and velocities in the study area, Building 2, landslide properties such as the release depth, total volume, and planar distance to the building were acquired for modelling in Blender. The Bullet Constraint Builder was applied to connect the building's simulated elements with real-world breaking thresholds, and a parametric analysis was performed to calibrate the size of the simulated soil-elements in the landslide, the distance from the building to the hill, the surface response of the failure plane, and the mortar breaking thresholds of the affected wall. During the parametric analysis of the mortar, the simulated pressure on the affected wall, at the moment of failure, was analysed to observe the simulated vertical and lateral pressure at the moment of failure. Last, a damage analysis was performed simulating single impacts to the building to the modelled building with a constant velocity and assigned volume, rather than a discretised landslide simulation. The max flow height and velocity are derived from the RAMMS analysis and then incorporated into adjusting the height, volume, and velocity of the simulated element impacting the building.

4.1. Landslide Modelling and Flow Simulations using RAMMS

Analysis using RAMMS were performed for Buildings 1 & 2; however, presented here is the analysis of Building 2. The results from the RAMMS analysis of Building 1 are in Appendix III. The RAMMS analysis of Building 2 began with inputting a digital elevation model and a map of the area surveyed during fieldwork. Then, a landslide release location, depth, and friction parameters were applied, and an obstacle was added to deflect flow at the location of Building 2. The parameters were used to model the max flow heights and velocities at the affected building. Then, the RAMMS landslide properties, max flow heights, and velocities were acquired to model the landslide in Blender and calibrate the simulations. The methodology for the RAMMS analysis proceeds as described in the sub-chapter 2.3.1, and is presented below:

4.1.1. RAMMS Topographic Data & Releases Information

A 5.0-meter resolution digital elevation model (DEM) was acquired from the CHARIM GeoNode (CHARIM.net, 2019) and maps were created from Google Earth historical imagery. The DEM and map were then cropped a GIS environment to the spatial extent of Sites 8 and 5, to save processing time. A landslide scarp was not confirmed during the collection of data at Building 2; therefore, the planar distance from the building to the release was estimated to be 4.0 meters. An initial landslide release depth of 2.0 meters was chosen because during fieldwork release depths were measured to be between 2.0 – 4.0 meters in the study area. The release was then assigned a density of 1900 kg/m³, and an internal friction angle of 20°, derived from Zhu (2019), for dry coulomb type friction. Curvature and erosion were disabled in the analysis, and an obstacle

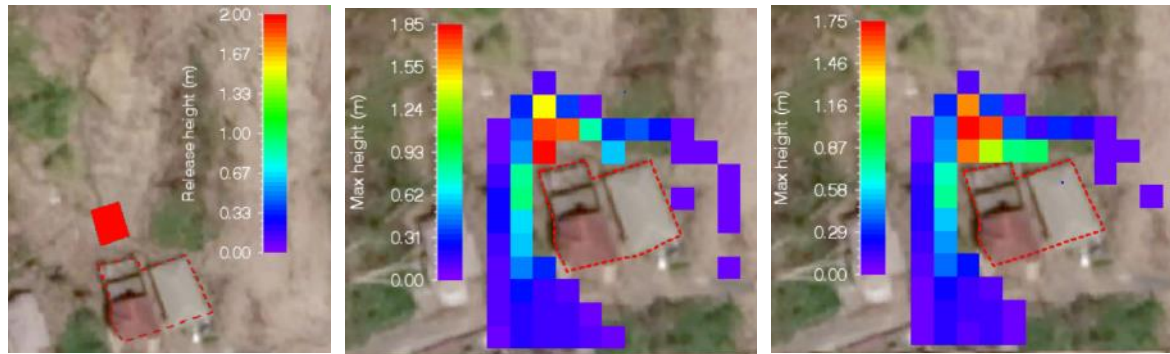
was added in the place of the surveyed building and neighbouring building; the obstacle was added to deflect flow and model max flow heights and velocities at the building.

4.1.1.1. Calibrating the RAMMS Obstacle Geometry

The first RAMMS simulation of Building 2 resulted in debris accumulated for half of Building 2’s affected wall (Figure 4.1 & 4.2). A closer inspection of the obstacle revealed the region, not calculated, was due to the obstacle boundary slightly overlapping a crucial cell of the digital elevation model used for calculating flow direction. The obstacle was redrawn; however, the boundary essentially encloses the entire building and neighbouring building (Figure 4.3). The second simulation resulted in the max flow distribution significantly changing; however the simulated debris height against the affected façade of Building 2 is 1.75 meters; which is less than the observed accumulation of debris at Building 1. Therefore, the release depth was calibrated between 2.0 – 4.0 meters to model a max height against the building close to 3.0 meters, as observed during fieldwork. A release depth of 3.5 meters resulted in 2.0 – 2.5 meters of accumulated debris at the affected façade of the building and was chosen for continuing the analysis in Blender (Figures 4.4 – 4.6); alternative release depths were analysed, and are in Appendix III. Table 4.1 presents the values extracted from the RAMMS analysis for landslide simulation in Blender.

Table 4.1: Release Properties

Mean Slope Angle	(45°);
Projected Area	(75m ²);
Incline Area	(106.1m ²);
Release Volume	(371.23m ³);



Figures 4.1 – 4.3: (Left) Setup of a 2.0-meter release depth and a planar distance of 4.0 meters from the building outlined in a red; (Center) simulation resulted in debris for half of the affected façade; (Right) the adjusted max height distribution after fixing the obstacle boundary models max flow heights 1.2 – 1.6 meters at the affected façade of Building 2.



Figures 4.4– 4.6: (Left) The release depth was adjusted to 3.5 meters; (Center) simulation results in a max debris height of 2.81 meters and 2.0 – 2.5 meters of debris against the building; (Right) The velocity distribution shows a max flow velocity of 7.27 m/s and 4.85 m/s against the affected facade of Building 2.

4.1.2. Simulation of Landslide Mass Interaction with Building and Parametric Calibration Analysis

Blender simulations were performed for Buildings 1 & 2; however, presented here is the analysis of Building 2. The analysis of Building 1 was concluded because a valid way to calibrate the structural response to landslide impacts has not been determined; a back-analysis of the landslide intensity was indeterminable because the deposit was excavated before fieldwork. The modelling of landslide, with the model of Building 2, used the release properties derived from the RAMMS analysis in the previous subchapter. Then the simulated accumulation geometry was assessed, and the surface response of the hill was calibrated to model an accumulation zone with a relative resemblance to the observed accumulation at Building 2 and the RAMMS analysis. The methodology for the Blender simulations proceed as described in the sub-chapter 2.3.2, and is presented below:

4.1.2.1. Blender Landslide Setup

The release properties in Table 4.1, were used to model the landslide's spatial extent, volume, and slope angle. The hillslope was angled to 45° , the same as the model in RAMMS, and assigned a passive rigid body type to remain static throughout the simulation. A surface response value, which has a effect similar to friction, of 1.0 was used for the hillslope in the initial simulation. The landslide was modelled as soil-elements with cubic geometries, and the toe of the landslide was cropped to simulate a cut slope (Figure 4.7). Lateral barriers were not added to the initial simulation to analyse the run-out kinematics without them. A cube shape was chosen to simulate a block release, and simulate layers of soil. The initial model used cubes 1.0 m^3 and 0.125 m^3 in size to model a release depth of 3.5 meters. Tables 4.2 and 4.3 present the modelled landslide properties, the total height and volume of the modelled landslide.

Next, a rectangular element was modelled with the dimensions: 10.0 meters wide, 11.0 meters long, and 5.0 meters high. The element was positioned to simulate the landslide impacting the building. Then, the simulated building was assigned a passive rigid body type, to remain static during the simulations. The distance between the simulated building and the hillslope was assumed to 3.0 meters, which left 1.0 meter for slope length.. The length between the building and the hillslope was determined from observing the width of the walkway on the sides of Building 2 (Figure 4.7).

Table 4.2 & 4.3: Simulated Soil Size & Landslide Properties

Large Soil Size	1.0 m^3	Number of Large Soil-Elements	320
Small Size	0.125 m^3	Number of Small Soil-Elements	400
Total Height	3.5 m	Soil-Element Density	1900 kg/m^3
Total Volume	370 m^3	Soil-Element Surface Response	1.0

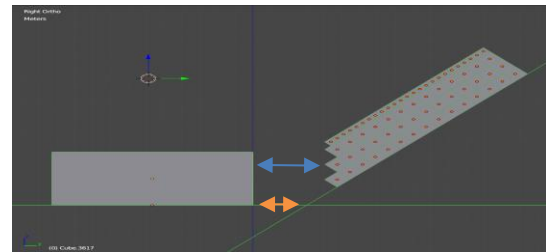
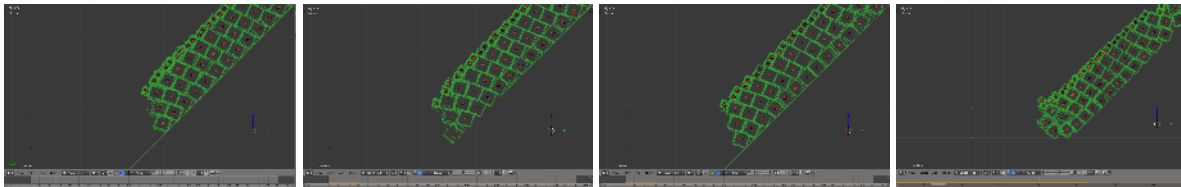


Figure 4.7: Preview of modelled landslide and building element in Blender. The planar distance indicated with the blue arrow between the building and landslide is 4.0 meters; the same distance measured in RAMMS. The distance between the house and the hillslope, indicated with the orange arrow, is 3.0 meters.

4.1.2.2. Surface Response Coefficient

Simulations began with the building modelled as a cube to analyse the simulated landslide run-out kinematics and distribution of soil-elements with the highest processing power; the more elements added to a simulation the greater division of calculations used in the simulation. The surface response of the hillslope was the first parameter adjusted to observe changes in the run-out. The surface response was set to 1.0 on the initial run and reduced three times (Figures 4.8a – 4.8d). Two processing effects were indicated by decreasing the surface response and observing the same frame of each simulation: (i) the landslide increases in velocity and travels further, (ii) the differential displacement between layers reduces; there is differential displacement between the simulated soil-elements because cohesion was not included in the model; furthermore, there is space between the soil-elements, and the upper-layers of soil-elements travel at a greater velocity, initially, at the current slope angle. The differential displacement between the layers is significant because it affects the shape of the landslide when it reaches the building; which affects the magnitude of impact. Additionally, when the upper layer soil-elements fall in front of the landslide, they limit available space for the bottom layers to progress forward, resulting in more of the landslide remaining on the hillslope.



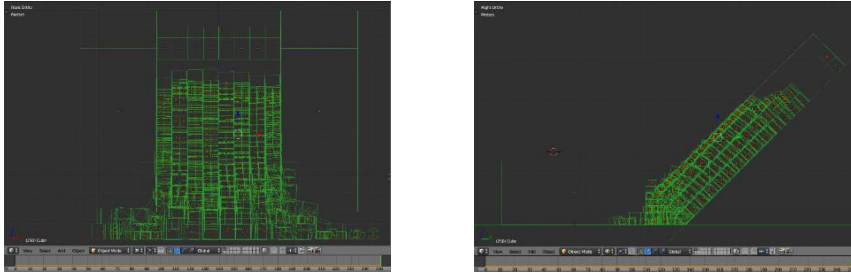
a) Surface Response 1.0 b) Surface Response 0.8 c) Surface Response 0.5 d) Surface Response 0.3

Figures 4.8a – 4.8d: The surface response parameter has an effect similar to friction. By decreasing the surface response of the failure plane, the acceleration of the bottom of the landslide is increased. The modelled elements of the landslide that are not in direct contact with the failure plane, initially, have greater acceleration than the modelled elements on the bottom of the landslide, only for surface response values greater than 0.5, because this is the surface response value assigned to the modelled elements in the landslide. When the surface response is reduced below 0.5 the acceleration along the failure plane is greater than the individual elements of the landslide, and the entire landslide moves, initially, with less displacement between the upper and lower layers of modelled elements. Video available at:

https://www.youtube.com/channel/UCII_8TbvAsG2BZJENUtJcvg:

4.1.2.3. Restriction of Landslide Movement Using Lateral Barriers

Next, barriers were added to the sides of the landslide, to restrict the landslide from displacing laterally (Figure 4.9). The barriers were modelled as passive rigid body types, to remain static during the simulations, with default values for the surface response. However, adding barriers to simulation did not significantly increase the resemblance of the simulated accumulation geometry between the building and hillslope in comparison to the observed accumulated debris during fieldwork (Figure 4.10). The simulated accumulation height against the building is ~2.5 meters, similar to the RAMMS results and collected data; however, there should be several meters of accumulated debris between the building and the new slope (Figure 3.12). From the simulation results, with barriers, it was observed the soil-element size have a significant effect on accumulation geometry. Because the landslide was comprised of mostly soil-elements 1.0 m³ in size, there was less space available for soil-elements to accumulate between the building and the hillslope. Additionally, the large soil-elements modelled were distributed less around the building in comparison to the smaller, 0.125 m³, soil-elements. Therefore, a new analysis was performed using only soil-elements 0.125 m³ in size.



Figures 4.9 & 4.10: (Left) The landslide simulation, with barriers, resulted in more of the landslide model remaining on the hill after the impact; (Right) The building is in front of the accumulated debris, the outline is slightly visible, more so, where simulated soil-elements press against it; however, observing from a right ortho-perspective, it was determined the geometry of the landslide model and distance to the modelled building element was incapable of modelling an accumulation zone with a relative resemblance of the observed accumulation zone. Video available at: https://www.youtube.com/channel/UCII_8TbvAsG2BZJENUtjcvg

4.1.2.4. Effect of Soil-Element Size

A new landslide was modelled using only soil-elements 0.125 m³ in size, and the same landslide geometry as the previous landslide simulations. Tables 4.4 and 4.5 present the simulated landslide properties, and several observations were made using the smaller soil-element size: (i) an increase in the differential displacement between the layers, as seen in Figure 4.8a – 4.8d, (ii) the simulated height of accumulated soil-elements at building was 4.0 meters, and (iii) the simulated accumulation of soil-elements between the building and the hillslope does not resemble the site assessment (Figure 4.11). Due to the significant differences in the simulated landslide accumulation and the observed accumulation of debris, the RAMMS release shape and depth was remodelled. Two adjustments considered were a shallower release, to decrease the accumulation zone height, and a greater distance between the building and the landslide to improve the simulated accumulation geometry.

Table 4.4 & 4.5: Simulated Landslide Properties

Soil Size	0.125 m ³	Number of Soil-Elements	2960
Total Height	3.5 m	Soil-Element Density	1900kg/m ³
Total Volume	370 m ³	Soil-Element Surface Response	1.0

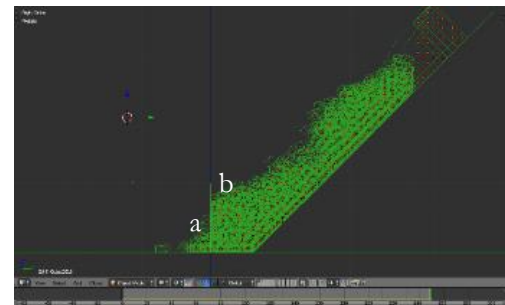


Figure 4.11: The accumulation, after modelling the landslide with a smaller soil-element size, changes in geometry compared to Figure 4.10. The outline of the building is noticeable at the toe of the accumulation, and to the right of the letter (a); the simulation resulted in, relatively, a flatter, and wider, accumulation, between the building and the hillslope compared to Figure 4.10 at the location of the letter (b). Video available at: https://www.youtube.com/channel/UCII_8TbvAsG2BZJENUtjcvg

4.2. Alternative Landslide for Continuing Analysis of Building Response to Landslide Impacts

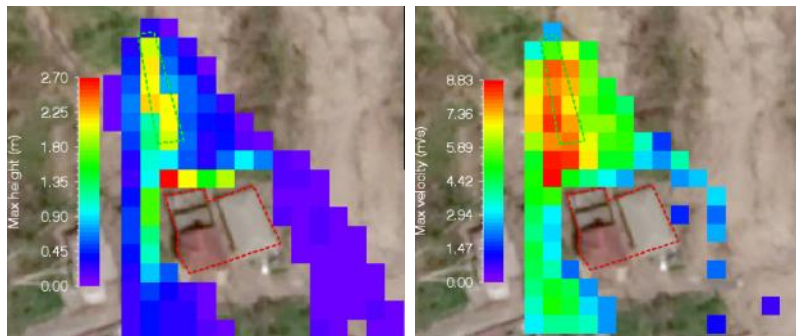
Due to significant differences between the simulated accumulation zone and the observed accumulated debris at Building 2, including debris height against the affect façade of Building 2, and the distribution of debris to the sides of the building, a decision was made to continue the analysis with an alternative landslide model in RAMMS. Presented here are the results from repeating the same procedure as subchapter 4.1, with an alternative landslide geometry and location. The location of the landslide was estimated from erosion scars in Google Earth historical imagery from October 11, 2017. Additionally, three considerations were taken in order to model a max flow height between 2.0 and 3.0 meters, as observed at Building 2, (i) shallow landslides measured during fieldwork were 2.0 – 4.0m; (ii) the landslide shape from the inventory (Figure 3.14); (iii) the computational cost of simulating larger landslides, in combination with the predetermined soil-element size of 0.125 m³. The results from the RAMMS analysis with the alternative landslide are presented below.

4.2.1. RAMMS Results Using Alternative Release Geometry and Location

A 2.5-meter release was chosen for continuing landslide run-out simulations in Blender; the width of the landslide was estimated from the width of the same landslide identified in the landslide inventory, and the length of the landslide was calibrated to simulate a max debris height between 2.0m and 3.0m at the building, the same as observed during fieldwork, using a release depth of 2.5. Additionally, the location and geometry were estimated from the visible erosion, and vegetation, in Google Earth historical imagery. The modelled planar distance from the landslide to the building was 13.0m (Figure 4.12). Table 4.6 presents the release properties of the alternative landslide and Figures 4.12 – 4.13 present the modelled max flow height, and velocity, distributions.

Table 4.6: New Release Properties

Release Volume (m ³)	655.9
Max Velocity (m/s)	8.83
Max Flow Height (m)	2.70
Max Pressure (kPa)	148.19
Mean Slope Angle	(45.5°)
Projected Area	(175m ²)
Inclined Area	(262.4m ²)



Figures 4.12 & 4.13: (Left) The new release area is outlined in green, and the max debris height against the building, outlined in red, is 2.70m; (Right) the max velocity distribution shows velocities between 4.0 – 6.0m/s against the building.

4.2.2. Blender Simulations Using the Alternative Landslide, & Calibration of the Hillslope Surface Response

The setup procedure for simulating the alternative landslide in Blender was the same as the analysis in the subchapter 4.1.2.1; however, due to a significant increase in slope angle in the middle the modelled landslide, the hillslope modelled in Blender was divided into two planes with the average slope angles of the bottom, and upper, halves of the landslide. Tables 4.7 & 4.8 summarise the modelled landslide properties, derived from the RAMMS analysis, used in the Blender models.

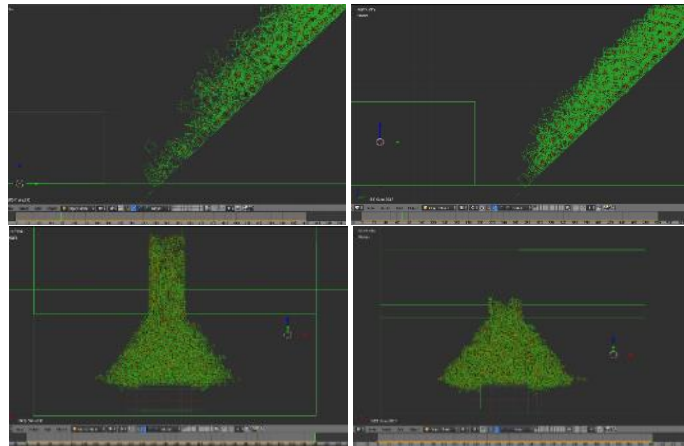
Table 4.7: Simulated RAMMS Landslide Properties

RAMMS Analysis	Value
Down-Hill Average Slope Angle	(43.3°);
Up-Hill Average Slope Angle	(49.4°);
Planar Release Area	(175m ²)
Inclined Release Area	(262.4m ²)
Total Release Volume	(655.9m ³)

Table 4.8: Simulated Blender Landslide Properties

Landslide Model	Value
Soil-element size	(0.152m ³)
Mass	(267.5g)
Total Height	(2.5m)
Total Volume	(435m ³)
Dist. to Slope	(3.0m)
Dist. to Release	(13.0m)

The planar distance from the modelled building and landslide is 13.0m, the same as the RAMMS analysis, and the distance between the building and hillslope is 3.0m, the same as the previous analysis in subchapter 4.1. The calibration of the hillslope surface response was performed the same as the previous analysis in the subchapters 4.1.2.2 & 4.1.2.3. Two observations simulated were: (i) when the hillslope surface response was decreased, the bottom-most layer of soil-elements, initially, move at a greater velocity (Figures 4.14a & 4.14b); (ii) the height and width of the accumulation zone increased when the surface response was reduced (Figures 4.15a – 4.15b). The simulated accumulation at the building, during the surface response calibration, ranged between 2.75m and 4.0m. However, the simulated accumulation geometry, and distance, from the building to the hillslope, was relatively similar to the results presented Figure 4.11; therefore, the modelled distance from the building to the hillslope was determined to be insufficient, and a decision was made to increase the distance between the building and the toe of the hill.



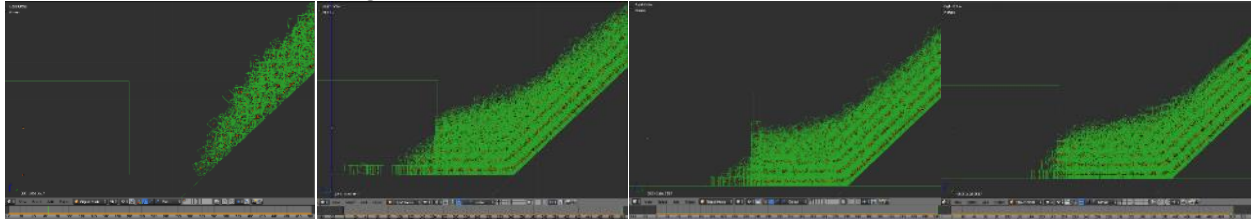
Top Figures 4.14a & 4.14b: (Left 4.14a) Simulated landslide, with a hillslope surface response of 1.0, resulted in more differential displacement between the layers; (Right 4.14b) a surface response of 0.3 results a denser mass at the toe, and more uniform displacement; Bottom Figures 4.15a – 4.15b: (Left 4.15a) Front view of model with surface response of 1.0; the majority of the landslide remaining the slope; (Right 4.15b) a surface response 0.3 resulted in a wider accumulation and a greater accumulation height against the building. Surface response video available at:

https://www.youtube.com/channel/UCII_8TbvAsG2

4.2.2.1. Effect of Increasing the Distance from the Building to the Hillslope

A parametric analysis was performed, assuming different distances of the building to the hillslope, to analyse how the distance of the building to the toe of the hillslope affected the simulated velocity and geometry of the landslide deposits. The release height was decreased, as described in the methodology subchapter 2.3.2 and Figure 2.3, to increase the distance from the building to the hillslope, without changing the planar distance of 13.0m. Furthermore, after the distance from the building to the hillslope was modelled to 4.0m, the surface response of the hillslope was reset to 1.0, and calibrated to observe the change in run-out kinematics and accumulation geometry. The simulations, using a surface response value of 1.0 for the hillslope, resulted in a denser, relatively uniform distribution of soil-elements approaching the building (Figure 4.16a); however, the

simulated total height of accumulated soil-elements against the building was less than 2.0m. Next, the surface response was decreased to 0.5, and the simulated height of accumulated debris at the building increased to ~3.5m. Then, the effects of the parameters, building to hillslope distance and surface response of the hillslope, were considered and it was determined that increasing the distance from the building to the hillslope has a more significant, and favourable in this analysis, effect on the simulated distribution of soil-elements between the building and the hillslope. Therefore; the distance between the building to the hillslope was calibrated between 4.0 – 6.0m, and the results are presented in Figures 4.16b – 4.16d. Essentially, increasing the distance from the building to the hillslope resulted in simulating a wider and longer accumulation zone between the building and the hillslope; additionally, the simulated accumulation of soil-elements against the building ranges 2.5 – 3.5m, the same as observed at Building 2.



Figures 4.16a, 4.16b, 4.16c, 4.16d are presented left to right respectively: A relatively uniform distribution of soil-elements approached the building after the surface response was adjusted to 0.5; (4.21b) the distance modelled between the building and hillslope was adjusted to 4.0m which resulted in a simulated height of ~3.5m against the building. (4.21c) The distance between the building and the hillslope was adjusted to 5.0m, and the simulated accumulation height of soil-elements resulted in ~3.0 meters; (4.21d) at a distance of 6.0 meters the simulated accumulation height of soil-elements against the building reduced to ~2.5 meters. How to adjust distance video available at: https://www.youtube.com/channel/UCII_8TbvAsG2BZJENUtjcvq

The presented simulations in Figures 4.16a – 4.16d were performed altering the distance from the building to the hillslope between 4.0 – 6.0m; additionally, the surface response from 0.0 to 1.0. Figures 4.16c & 4.16d are the simulation results using a surface response value 0.5, for distances of 5.0m and 6.0m respectively. At these distances, and surface response, the simulation results have the greatest resemblance to the observed accumulated debris during fieldwork and the RAMMS results. Both a 5.0m and 6.0m distance resulted in a relatively flat accumulation zone, 2.5 – 3.0m at the building. Therefore, 5.0m and 6.0m distances, between the building and hillslope, were selected for continuing the structural analysis, as well as, a surface response value of 0.5. The complete parametric analysis calibrating surface response for distances 4.0 – 6.0 meters between the building and hillslope is in Appendix IV.

4.2.3. Structural Response and Damage Analysis

The structural response analysis began with replacing the modelled building element, presented in subchapters 4.1 and 4.2, with a building modelled from the measured dimensions and documented attributes. The methodology for modelling the building with constraints, and simulations, proceed as described in the subchapter 2.3.2.2; however, the modelled building, particularly with concrete blocks for walls, increased the total number of elements in the simulation significantly, which affected the simulated landslide run-out kinematics and simulated distribution of soil-elements. Therefore, analytical simulations were performed to calibrate the surface response of the hillslope, again, starting at a value of 0.5, because this value simulated the best results in the previous analysis.

The structural elements modelled include concrete blocks, reinforced concrete beams, columns, and a ceiling-floor slab between the ground floor and second floor. The building was initially modelled as a passive rigid body type because structural constraints had not been added yet; therefore, the building was unstable from its weight and would collapse upon impact from the landslide. Simulating the building as a passive rigid body means the building remained static throughout the simulation; however, the modelled soil-elements can pass through the openings such as windows and doorways, as well as, accumulate against the building and on the second-story floor. Figure 4.17 presents the modelled building with the landslide used in the following analysis.

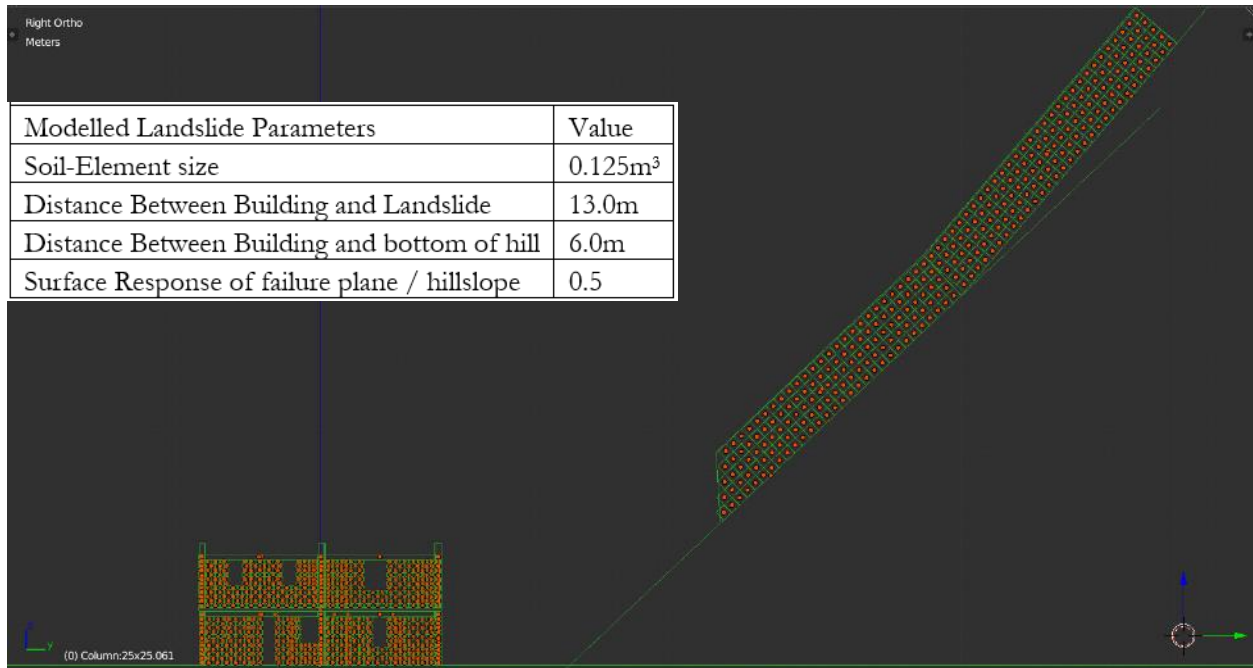
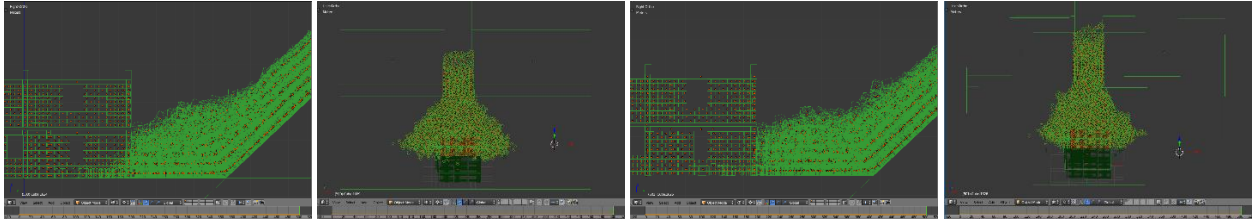


Figure 4.17: Right-ortho-perspective of the modelled Building 2 and landslide; The landslide properties including soil-element size, total volume, and slope angles are the same as presented in Table 4.3; the planar distance of 13.0m between the building and the landslide is the same as the RAMMS analysis presented in Figure 4.12 and the analysis presented in subchapter 4.2.

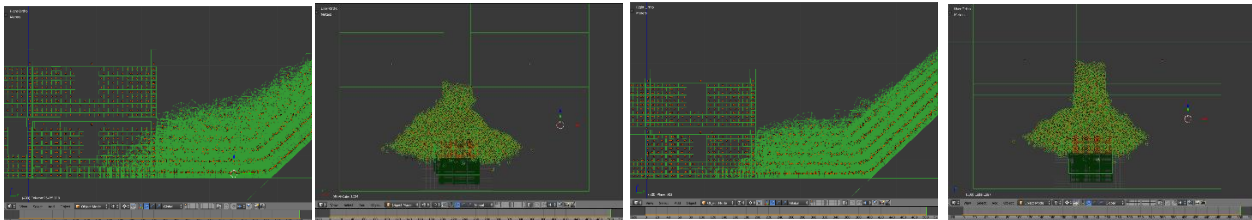
4.2.3.1. Calibration of Surface Response For Distances of 5.0m & 6.0m Between the Building and Hillslope

Presented below are the simulated results for surface response values of 0.5, 0.3, and 0.0, beginning with 0.5, because this value, from the previous simulations, simulated an accumulation geometry of the greatest resemblance to the observed accumulated debris during fieldwork. Figures 4.18a – 4.18d present the simulated soil-elements accumulated against the building and the spatial extent of the landslide between the building and the hillslope. There were two observed differences in the simulation using a 5.0m and 6.0m distance between the building and hillslope; (i) the geometry of the simulated accumulation using 6.0m has a, relatively, greater resemblance to the observed accumulated debris and RAMMS results, including accumulation height at building and a level geometry between the building and the slope; (ii) a 5.0m distance resulted in more soil-elements laterally displaced on the hillslope, because there was a more space, due to the longer slope length, in comparison to using a 6.0m distance between the house and the hillslope.



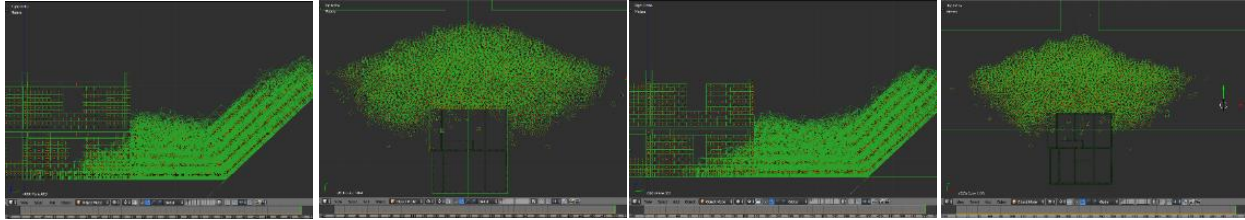
Figures 4.18a, 4.18b, 4.18c, 4.18d are presented from left to right respectively: Figure 4.23a & 4.23b present the simulation results with a 5.0m distance between the house and the hillslope. The simulation resulted in nine soil-elements entering the building, through the windows, on the ground floor. The simulated height of soil-elements against the building was $\sim 2.5\text{m}$ and the middle window of the ground floor was covered, the same as observed during fieldwork. Figure 4.23b presents the front view of the results. Figure 4.23c presents the simulation results with a 6.0m distance between the building and the slope. The geometry was relatively more level between the building and the slope than Figure 4.18a, and the accumulated debris against the building was $\sim 2.5\text{m}$ the same as observed during fieldwork. Figure 4.23d presents the front view using a 6.0m distance and more of the landslide remained on the hillslope. Passive rigid body building video available at: https://www.youtube.com/channel/UCII_8TbvAsG2BZJENUtjcvq

From the simulated results, using a surface response value of 0.5, a 6.0m distance between the building and the hillslope has the greatest resemblance to the observed accumulated debris during fieldwork. The simulated accumulation height of soil-elements against the house was greatest in the centre, tapered towards sides, and soil-elements were distributed on both sides of the building, the same as observed during fieldwork. In the next simulation, the surface response of the hillslope was reduced to 0.3. Figures 4.19a – 4.19d present the simulated results at 5.0m and 6.0m distances between the building to the slope.



Figures 4.19a, 4.19b, 4.19c, 4.19d are presented from left to right respectively: Figure 4.19a & 4.19b present the simulated results with a 5.0m distance between the house and the hillslope. The simulated accumulation of soil-elements against the building was $\sim 2.6\text{m}$, two of the ground floor windows were covered, and 10 soil-elements entered the building through the windows on the ground floor; additionally, a surface response of value 0.3 for the hillslope resulted in less mass on the hillslope; Figures 4.19c & 4.19d present the simulated results with a 6.0m distance between the house and the hillslope. The simulated accumulation of soil-elements against the building was $\sim 2.5\text{m}$, and the tops of the ground floor windows were visible from outside the building; however, the simulated accumulation geometry between the building and hillslope has a relatively higher resemblance than simulation results using a 5.0m distance between the building and the hillslope. Passive rigid body building video available at: https://www.youtube.com/channel/UCII_8TbvAsG2BZJENUtjcvq

From the simulated results, using a surface response of 0.3, a 6.0m distance between the house and the hillslope, again, has the greatest resemblance to the observed accumulated debris against the building in comparison to a 5.0m distance. In the next simulation, the surface response of the hillslope was reduced to 0.0. Figures 4.20a – 4.20d present the simulated results at 5.0m and 6.0m distances between the building to the slope.



Figures 4.20a, 4.20b, 4.20c, 4.20d are presented from left to right respectively: Figure 4.20a & 4.20b present the simulated results with a 5.0m distance between the house and the hillslope and a hillslope surface response value of 0.0. The simulated results significantly improve in resemblance of the debris accumulated against the building and between the building and the hillslope relative to the observed accumulation during fieldwork. The simulated accumulation height against the building, using a 5.0m distance, is ~3.0m and 12 soil-elements enter the building through the ground floor windows. Figures 4.20c & 4.20d present the simulated results with a 6.0m distance between the house and the hillslope. The simulation resulted in an accumulation of soil-elements ~3.0m high against the building, 10 soil-elements entering the building through the ground floor windows, and one soil-element entering the building through the centre window of the second floor. Passive rigid body building video available at: https://www.youtube.com/channel/UCII_8TbvAsG2BZJENUtjcvg

From the simulated results, using surface response values of 0.5, 0.3, and 0.0, a 6.0m distance between the house and the hillslope in every simulation resulted in the greatest resemblance to the observed accumulated debris during fieldwork; specifically, a surface response value of 0.0 resulted in the greatest resemblance. The simulated accumulation height of soil-elements against the house was greatest in the centre, sloping on the sides, and soil-elements were distributed on both sides of the building. Therefore, a 6.0m distance from the building to the hillslope and a surface response value of 0.0 for the hillslope were accepted as the optimal parameters for continuing the structural response analysis.

4.2.3.2. Addition of Structural Constraints

The addition of structural constraints to the simulation proceeds as described in the methodology subchapter 2.3.2.2, and began with removing the passive rigid body settings from building. The Bullet Constraint Builder, calculates real-world breaking thresholds, was utilised on the modelled building’s elements, and enabled active rigid body settings for the building; the active rigid body settings enable the modelled building to be affected and respond to the simulated landslide impacts. Table 4.9 presents the initial pre-processing settings used, and Tables 4.10 – 4.12 present the initial element group settings. The connection type set for the mortar was based on ultimate elastic breaking thresholds, whereas the ceiling slabs, beams and columns were modelled with spring constraints which simulate yield thresholds equal to the strength of the reinforcement.

Table 4.9: Pre-processing Settings

Discretise Size for Structural Frame	2.0m
Foundation Range	0.1m

Table 4.10: Concrete Blocks & Mortar; Connection Type 15

Compressive	Tensile	Shear	Bend	Density
N/mm ²	N/mm ²	N/mm ²	N/mm ²	Kg/m ³
5.0	2.0	0.5	0.5	2400

The mortar compressive strength was based on 1:4 mortar thresholds (Arash, 2012), tensile, shear, and bending thresholds were estimated from cement, sand, water ratios (Still, 2004). The mortar density was estimated from a 1:3 mortar with a 40% water content, and the mortar shear and bending thresholds are calibrated in the following subchapter because the values were not documented during fieldwork.

Table 4.11: Ceiling (Slab);

Member Thickness	Member Width	Bar ϕ	Bar Distance	Bar amount	Stirrup ϕ	Stirrup Distance	Concrete Cover	Strengths Fs/Fc
[mm]	[mm]	[mm]	[mm]	[-]	[mm]	[mm]	[mm]	[N/mm ²]
150	2000	19.1	203.2	20	7.94	203.2	30	413.7/20.7

Table 4.12: Beams/Columns;

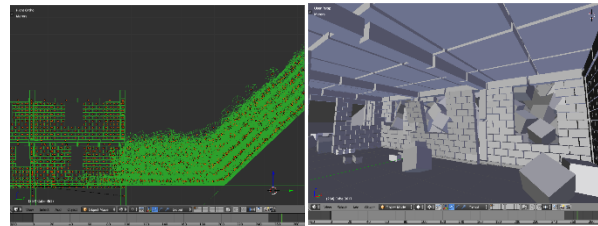
Member Width	Member Height	longitudinal bars, ϕ	longitudinal bar amount	Stirrup ϕ	Stirrup Distance	Concrete Cover	Strengths Fs/Fc
[mm]	[mm]	[mm]	[-]	[mm]	[mm]	[mm]	[N/mm ²]
250	250	12.7	4	9.52	203.2	30	413.7/20.7

Member dimensions were defined according to the observed member section in the study area. The construction materials were based on observations, the Guide to Dominica's Housing Standards (The Ministry of Planning and Economic Development, 2018), and the Caribbean Disaster Mitigation Project (Organization of American States & USAID, 2001)

4.2.3.3. Damage Simulations with Structural Constraints Added

Collectively, the pre-processing, constraint building, and simulation run-time, for this analysis, required four hours, this was significantly longer than the previous analysis, without constraints in the simulation, when simulations would process in 30 – 60 minutes. Additionally, the addition of structural constraints increased the total number of elements in the simulation significantly which affected the simulated landslide run-out kinematics and impact dynamics of the landslide against the building. The simulation, with structural constraints, resulted in wall damaged and several block shearing from contact with the first soil-elements that reached the building (Figure 4.21 & 4.22). The simulated accumulation width between the building and the hillslope was, relatively, similar to simulation without the structural constraints; however, to continue structural response analysis, the forces simulated on the affected façade needed to be analysed, and in order to analyse the forces on the affected wall, the processing time needed to be reduced.

Therefore, the unaffected walls of the building were modelled as larger slabs, with mortar breaking thresholds, to reduce the number of elements in the building model. Then, Simulations were performed discretising the unaffected walls by 2.0m and 10.0m, without discretising the unaffected walls, and removing the unaffected walls. Then, the results were compared



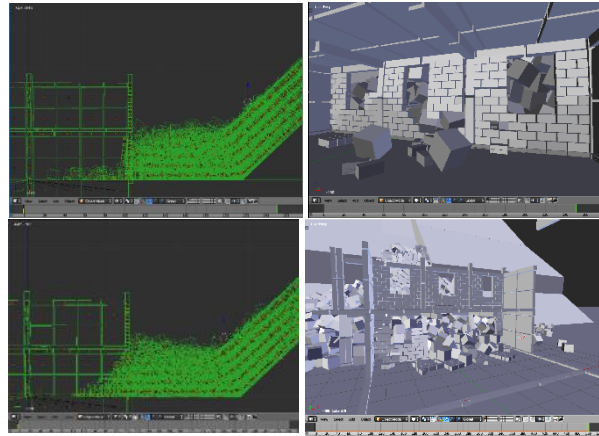
Figures 4.21 – 4.22: The computational cost of adding the constraints has an effect on the geometry of the landslide deposit; as well as, the damage to the building. Video available at: https://www.youtube.com/channel/UCII_8TbvAsG2BZJENUtjcvg

to determine the number of elements in the simulation which would produce a simulated accumulation zone of resemblance to the observed accumulation of debris during fieldwork, and the RAMMS results, at the minimal processing cost; the analysis of the discretisation of unaffected walls is presented below.

- **Damage Using Concrete Slabs, Discretised 2.0m, for the Unaffected Walls**

The observed unaffected concrete block walls during data collection of Building 2 were converted into larger concrete slabs; the walls were converted to continue the structural analysis and at a greater processing speed. The Bullet Constraint Builder's pre-processing discretise tool was used to discretise the unaffected walls with a 2.0-meter limit (Figure 4.23). Then, mortar constraints, with breaking thresholds presented in Table 4.5, were built between the pieces. The simulation processing time, after replacing the block walls with slabs, reduces to 30 minutes.

The simulations performed, with a 2.0m discretisation of the unaffected walled resulted in a simulated accumulation height of ~2.5m against the wall, and a simulated accumulation zone of relative resemblance to the observed accumulated debris; however, it was noticed the landslide had not completely stabilized. The landslide, and building began to stabilise at the end of the simulation; however, the simulation was repeated doubling the simulation run-time. The longer simulation produced an accumulation geometry of a greater resemblance to the observed accumulation during field than the previous simulation run for half the amount of time. Furthermore, as documented during data collection, and in the RAMMS analysis, there was a decrease in the simulated accumulation height close to the hillslope (Figure 4.25). However, the simulated degree of damage to the building was more extensive with several walls collapsing and soil-elements entering the building (Figure 4.26).



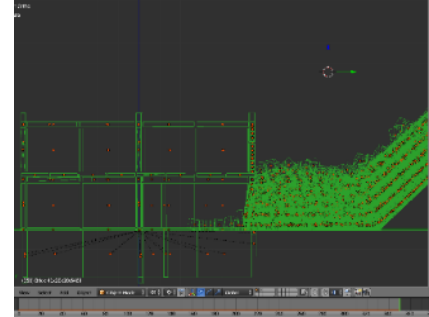
Top Figures 4.23 – 4.24: (Top) Discretising the unaffected walls affects the deposit geometry and damage. Figures 4.25 – 4.26: (Bottom) Increasing the length of the simulation run-time resulted in more damage occurring later in the event. Damage Video available at: https://www.youtube.com/channel/UCII_8TbvAsG2BZJENUtjcvg

Before the simulation of unaffected walls discretised by 10.0m, the distance between the building and the hillslope was modelled at 5.0m, again, using the slabs discretised by 2.0m; the simulation was performed because the results, presented in the subchapter 4.2.3.2, were relatively similar between the two distances, and with the unaffected walls converted into large slabs, thousands of elements were removed from the simulation; therefore, the simulation resulted in different landslide run-outs and distributions. However, the simulations at a 5.0m distance between the building and the hillslope resulted in more extensive damage to the affected wall, and a simulated geometry of accumulated soil-elements had less resemblance to the observed accumulation during fieldwork, in comparison to a 6.0m distance between the building and the hillslope. Therefore, the distance between the building and hillslope remains 6.0m for the remainder of the structural response analysis; the analysis results using a 5.0m distance between the building and the hillslope is in Appendix IV.

- **Damage Using Concrete Slabs, Discretised 10.0m, for the Unaffected Walls**

The simulated damage to the building reduced using a 10.0m discretisation of the unaffected walls; however, the geometry of the simulated accumulation between the building and the hillslope decreased in resemblance, in comparison to the simulation results using a 2.0m discretisation.

Figure 4.27 presents the simulated results using a 10.0m discretisation of the unaffected walls. The simulated accumulation of soil-elements between the building and the hillslope was relatively flat; however, the decrease in height, in the accumulated geometry near the hillslope, was less visible in comparison to Figure 4.25. The simulated geometry of soil-elements against the building was relatively similar to the observed accumulated debris against the building during fieldwork; however, due to the processing time, the unaffected walls were modelled without discretising concrete slabs.

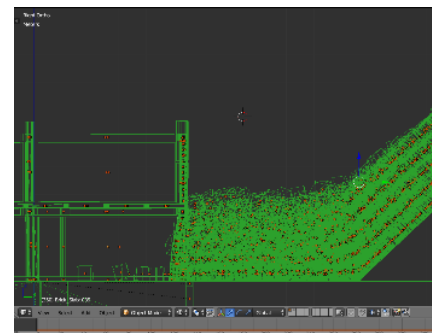


Figures 4.27: Presented is simulation result using a 10.0m discretisation of the unaffected walls; the affected wall was observed shearing less, in comparison to the Figure 4.25.

- **Damage Using Full Concrete Slabs for the Unaffected Walls**

The simulated damage to the building reduced, furthermore, with the unaffected walls modelled as single elements. The geometry of the simulated accumulation of soil-elements between the building and the hillslope had a relative resemblance of the observed accumulated debris during fieldwork, including an accumulation between the building and the hillslope of relative resemblance to the observed accumulation. The windows of the ground floor's affected wall were almost completely covered, and the simulated accumulation at the building slope around the sides.

Figure 4.28 presents the simulation results using full concrete slabs for the unaffected walls and shows the affected wall shearing from the foundation. The simulation results, however, were determined to be too great of a computational cost; therefore, another simulation was performed removing the unaffected walls from the simulation. The results of the analysis are presented below.



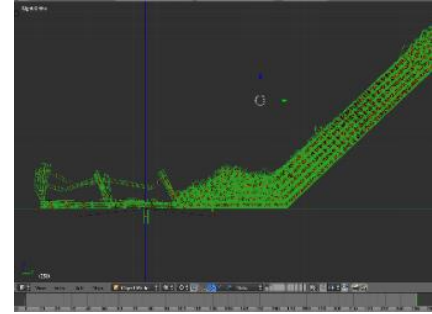
Figures 4.28: Presented is the simulation result using full concrete slabs for the unaffected walls; the affected wall was observed shearing relatively the same amount as Figure 4.27. Damage Video with replaced walls available at:

https://www.youtube.com/channel/UCII_8TbvAsG2BZJENUtjcvjg

- **Damage with the Unaffected Walls Removed**

The simulation, after removing the unaffected walls, resulted in the building collapsing. The slab dividing the ground floor and second-story were displaced laterally and the building buckled. Figure 4.29 presents the simulation results after removing the unaffected walls from the simulation.

The second-story structural frame managed to stay connected and braced; however, the impacted façade and the ground floor have collapsed. However, the landslide does not continue to move over the structure. Due to the results of removing the unaffected walls, and the extensive processing time of the previous analysis, affected wall's concrete blocks were modelled as larger concrete panels designed to break along the window geometry and at connections with beams and columns; the analysis with the affected wall modelled as concrete panels is presented below.

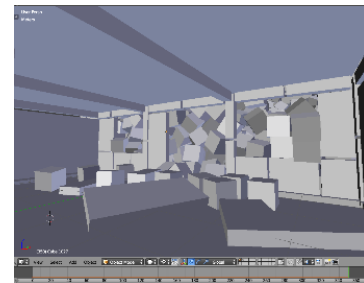
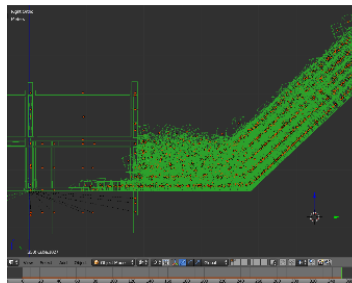


Figures 4.29: Presented is the simulation result after removing the unaffected walls; the structure collapses, however, the landslide displacement does not progress.

- **Damage Using Concrete Panels for the Affected Wall**

The modelled façade of Building 2, impacted by the landslide, was adjusted by modelling the concrete blocks into larger concrete panels designed to break along the geometry of the windows; additionally, the simulated unaffected walls presented here were not discretised. The panels were simulated this way because mortar traditionally shears near openings and corners, and more elements need to be removed from the simulation. Figure 4.30 presents the simulated accumulation of soil-elements against the building and the simulated geometry of the accumulated soil-elements between the building and the hillslope. The geometry was determined to have a greater resemblance to the observed accumulated debris during field work than the previous analysis discretising the unaffected walls.

The simulation results, with concrete panels for the impacted wall, resulted in a simulated accumulation height ~2.75 meters against the building, relatively close to the observed accumulated debris against the building during fieldwork. However, the constraint thresholds of the ground floor panels were exceeded, and soil-elements entered the building (Figures 4.30 & 4.31); two panels broke on the sides of windows, and the centre of the impacted façade collapsed spilling soil-elements into



Figures 4.30 & 4.31: Simulation results after converting the affected wall into larger concrete panels; the centre part of the affected wall received the most damage, and panels were sheared on the sides. Damage Video available at: https://www.youtube.com/channel/UCII_8TbvAsG2BZJENUtjcvg

the building. At the current number of elements in the simulation, the processing time was determined to be acceptable for continuing the analysis and calibration of the mortar constraints.

4.2.3.4. Calibration of Mortar Breaking Threshold

To continue analysis of the forces simulated on the affected wall, the optimal parameters calibrated in the previous analysis were utilised. Table 4.13 summarises the calibrations chosen for the next simulation, and Table 4.14 presents the initial mortar properties. The mortar shear and bending ultimate breaking thresholds needed to be calibrated because they were derived from literature values, rather than observed during data collection, and currently, simulate damaged more extensively than observed. To validate the calibration of the mortar, the simulated damage needs to be within the range of the literature values, and the simulated damage should be, empirically, relatively similar to the damage observed at Building 2. The damage to the second-story of the affected wall, visible in Figure 3.13, shows the mortar shearing from the corner of the wall to the window, and the reinforced concrete frame cracked. The degree of damage observed in the second-story wall is used as an empirical threshold of the mortar's ultimate shear strength. The initial simulation results using the parameters in Table 4.8 is presented in Figure 4.32

Table 4.13: Constant Parameters during Mortar Calibration

Affected-Wall Discretise Limit	2.0 meters
Unaffected-Wall Discretise Limit	None; Full Slab Walls
Ceiling-Floor Discretise Limit	10.0 meters
House-to-Slope Distance	6.0 meters
Slopes Surface Response	0.0
Soil-Element Surface Response	1.0
Soil-Element Dimension	0.125 m ³
Debris slide & Ground-Surface Response	1.0
Column & Beam Breaking Thresholds	Tables 4.6 & 4.7

Table 4.14: Initial Mortar Properties

Compressive	Tensile	Shear	Bend	Density
N/mm ²	N/mm ²	N/mm ²	N/mm ²	Kg/m ³
5.0	2.0	0.5	0.5	2400

The simulated damage, in Figure 4.33, was more extensive than the observed damage during fieldwork. The ground floor during fieldwork was observed to have no significant damage to the reinforced concrete frame or the concrete block infill walls in order to determine if the simulated damage was an effect of the discretisation of the affected wall. The model was analysed using the modelled concrete blocks with the same constraint values.

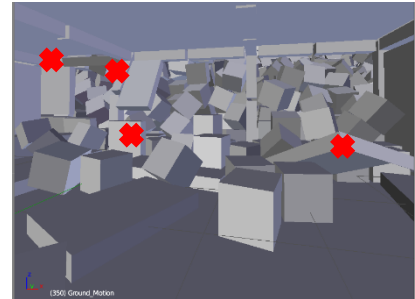


Figure 4.32: The initial run to calibrate the mortar strength results in structural and non-structural damage; red (x)'s show the locations of a collapsed wall, broken beam, buckling wall and column.

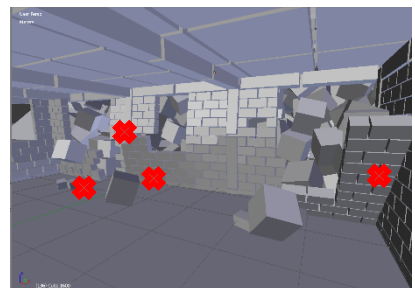
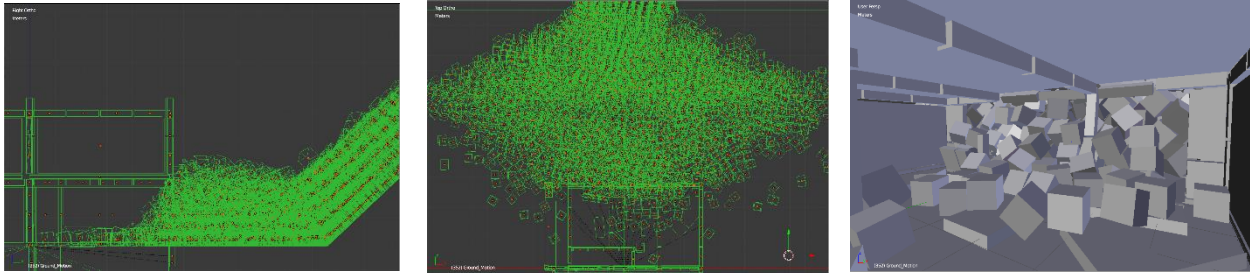


Figure 4.33: Simulation results using the parameters in Table 4.8 and concrete blocks for the affected wall; red (x)'s show the locations of a collapsed wall, a buckling wall, and column

The simulated damage using blocks was similar to the simulated damage with panels (Figure 4.34); however, in both simulations, the damage to the ground floor was more extensive than the observed damage to Building 2 during fieldwork. Therefore the shear and bending breaking thresholds were adjusted to 1.0 N/mm^2 ; although, a value of 0.5 is closer to the literature values of mortar shear breaking thresholds. Figures 4.34 – 4.36 present the simulated results; the affected wall's degree of damage does not decrease after the mortar shear and bending breaking thresholds were increased. The simulated accumulation height of soil-elements against the buildings was ~ 2.75 meters, relatively similar to the observed debris accumulated against the building during fieldwork; however, the affected walls concrete panels collapsed.



Figures 4.34 – 4.36: (Left 4.34) The simulation result after increasing the shear and bending breaking thresholds to 1.0 N/mm^2 modelled an accumulation height of ~ 2.75 meters; (Centre 4.35) the simulated geometry of the deposit was relatively similar to the site assessment; (Right 4.36) however, increasing the shear and bending breaking thresholds do not significantly decrease the degree of damage to the house. Damage video available at: https://www.youtube.com/channel/UCII_8TbvAsG2BZJENUtjcvg

The mortar shear and bending breaking thresholds were not further increased because it would simulate a mortar wall with a greater shear and bending strength than the calculated slab elements; and the slabs have more reinforcement than the block walls, and the shear and bending breaking threshold of the simulated concrete slab should be greater than the mortar wall. Therefore it assumed the simulated degree of damage was significantly the effect of the modelled soil-element size. At the current size, of 0.125m^3 , the soil-elements, simulate a magnitude of the force on the impacted wall significantly greater than the modelled mortar constraints. The initial value of 0.5 N/mm^2 , derived from the literature, was accepted as optimal mortar shear breaking threshold value for continuing the analysis.

4.2.3.5. Visualisation of the Simulated Forces on the Affected Wall

The simulations using 0.5 N/mm^2 for shear and bending breaking thresholds observed in 4.44 and 4.45 resulted in similar type's damage as observed in the field; such as a buckling wall, columns, and minor damage to the structural frame. The difference was the location of damage, which was suspected of being the effect of simulating the soil-elements size. The next simulations used the parameters in Table 4.13 and were analysed at the moment the first constraint in the wall broke, to analyse the shear forces simulated on the affected wall.

After the shear and bending breaking thresholds were modelled back to 0.5 N/mm^2 , the simulation resulted in a greater degree of damage to the affected wall than the previous simulation using the same parameters (Figure 4.37). This was significant because it indicated different degrees of damage could be simulated using the same

setup parameters. The column observed buckling in Figure 4.33 has now collapsed, and the beam was unaffected; however, the total degree of damage to the wall is relatively the same.

The first broken constraints were in the centre of the wall; additionally, one at the foundation, and one between the centre concrete panel and column (Figure 4.38). The constraints analysed on the affected wall are illustrated in Figure 4.39. There are two constraints that broke when initiating the simulation due to the simulated design and weight of the building; these constraints were excluded from the analysis. The vertical and lateral pressure gradients simulated on the affected wall are presented in Figures 4.40 & 4.41. The gradient charts show how much the pressure reduces near the surface of the impact and sides of the building. There was a significant change in pressure between the constraints at 0.42m and 0.82m; which was suspected of being the effect of the soil-element size, and the shape of the simulated accumulation when it impacted the building. After the initial collision the soil-elements, at about 0.42m height, the bottom layers of the landslide recoiled; however, the second increase in pressure, at 1.14 meters was due to the upper layers colliding with the building at a higher velocity. The vertical pressure gradient, then, dropped near the surface, and there was a final increase in pressure at 2.26 meters due to the top-most soil-elements toppling into the building. Additionally, the simulated average pressure gradients presented in Figure 4.41 are within the range of literature values for 1:4 mortar mix-ratios (Ali et al. 2012). Furthermore, because the simulated pressure on the affected wall was greatest at 1.14m, the horizontal gradient of the modelled constraints at 1.14 meters high was observed. The horizontal pressure gradient was significant to observe the change in simulated pressure laterally against the wall due to soil-elements displacing around the sides of the building.

After the forces on the affected wall were analysed, it was, further, suspected the modelled soil-element size resulted in a greater magnitude of force to the ground floor wall than observed during fieldwork; however, the types of simulated damage were relatively similar to observed damage, such as walls and columns buckling, and shearing of the mortar walls. The difference was the location of damage; the simulated damage was extensive on the ground floor, whereas the observed damage was extensive in the second floor of Building 2. Furthermore, the calculated landslide velocity of the impacting soil elements, from the bottom of the hill to the building, was calculated to be ~ 3.33 m/s, which is in the range of the RAMMS analysis presented in subchapter 4.2.1; RAMMS velocities against the building range between 3.0 – 5.5 m/s.

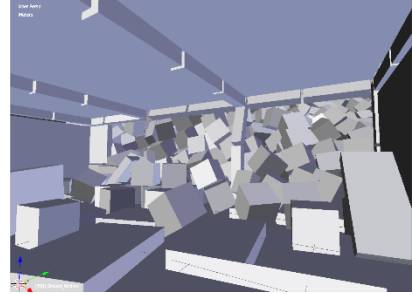


Figure 4.37: With mortar's shear and bending breaking threshold reset to 0.5 N/mm^2 , the simulation results in different elements damaged.

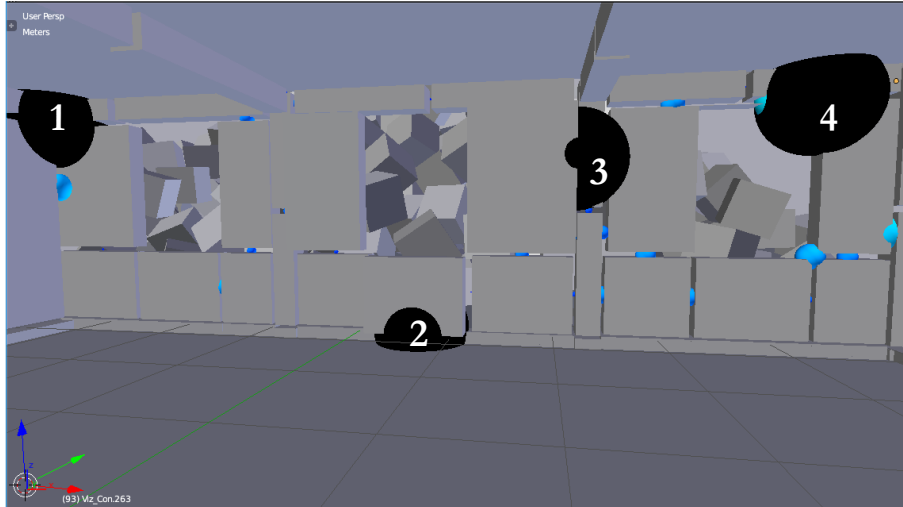


Figure 4.38: Presented is the moment the first constraint breaks from the impact; the constraints, where connecting elements model the breaking thresholds, 1 & 4 break before the impact due to the design of the model, and constraints 2 & 3 shear from the foundation of the building and the column respectively.

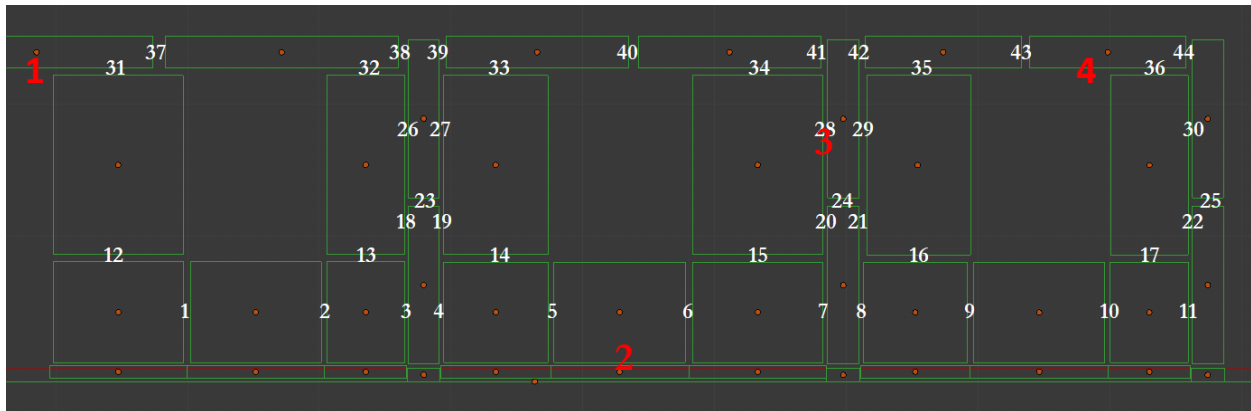


Figure 4.39: Constraint numbers for analysis of pressure gradients are presented in white; broken constraints in Figure 4.38 are presented in red

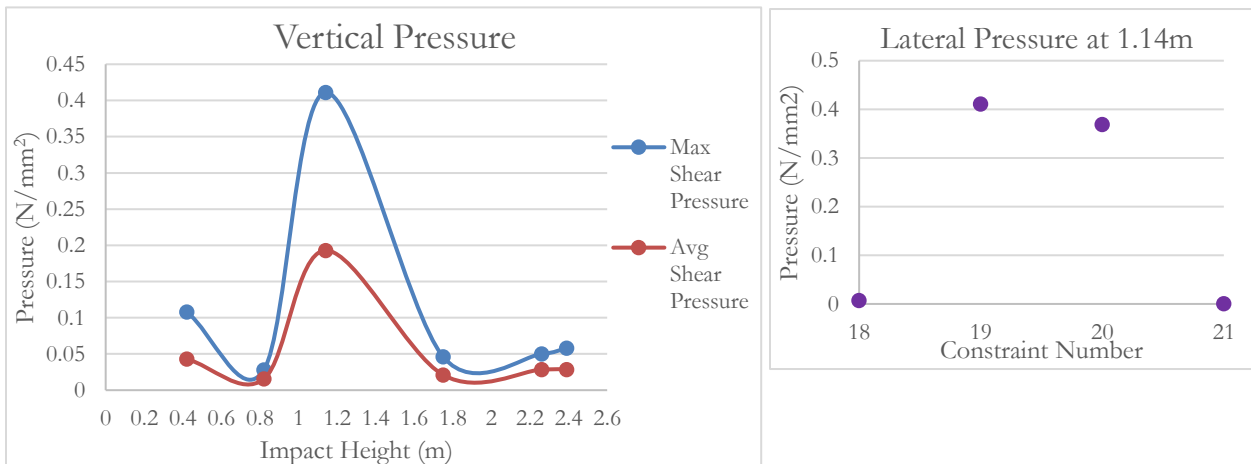


Figure 4.40 & 4.41: (Left) Presented is the vertical pressure gradient of simulated average and max shear forces on the affected wall; (Right) the lateral pressure presented shows the simulated forces on the affected wall at

the height of 1.14 meters. The constraints are between the simulated concrete panels and the columns on the affected wall; the simulated pressure was highest in the centre of the affected façade and reduced near the sides of the building where the simulated debris was displaced around the sides of the building.

4.2.4. Event Simulations with Controlled Impulse Velocity

The results presented in the previous analysis were the final simulations using the alternative landslide release selected in the subchapter 4.2. The following simulations were performed to assess the degree of damage simulated when using a single impacting element, and do not directly correspond to the data collected or release properties previously used. However, the simulations were performed to develop alternative vulnerability curves relating the degree of damage induced to common structural typology from a range of impact intensities. The vulnerability curves presented show the varying degrees of damage induced from specific impact heights, velocities, and volumes.

4.2.4.1. Damage Using a Single Impacting Element and Controlled Velocity

The modelled element for impact analysis was modelled in height between 0.5 – 3.0 meters, and simulated with velocities between 3.0 – 5.0m/s; the width of the element was modelled to 11.0m, equal to the width of the building. Additionally, the impacting element's volume was adjusted in length, to observe changes in damage with a change in the centre of mass. The length was adjusted between 1.0m – 5.0m and the element was modelled with a density of 1900kg/m³, representative of volcanic soil. The classification scheme for the simulated degree of damage was modified from the classification scheme used during fieldwork, presented in the subchapter 2.2.1, to provide more specific classifications. Figures 4.43 - 4.47 present the results of the damage analysis.

0: None

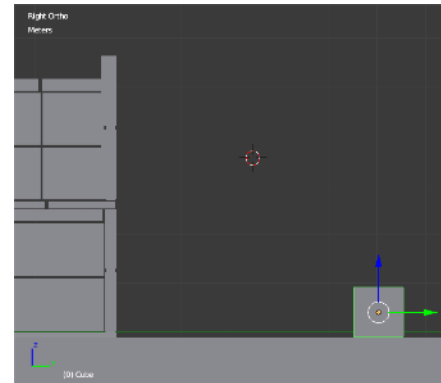
1: Broken masonry wall

2: Multiple masonry walls damaged; flexing columns or beams

3: Broken column, beam, and masonry damage

4: Multiple columns, beams are broken, and non-structural damage;

5: Irreparable structural damage or complete structural collapse



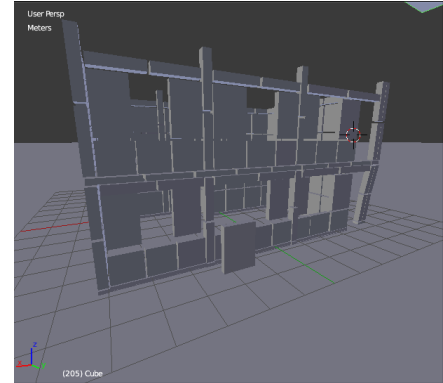


Figure 4.43a -4.43c: Adjusting the height of debris results in significant changes to the degree of damage at 1.0 meter; furthermore, increasing the velocity for debris heights over 1.0 meter significantly changes the degree of damage. (Top) The initial set up with a modelled element 11.0m in width and 1.0m in length and height for impact analysis; (Bottom) the simulated damage for a D2 classification at 4.0m/s. 1.0m video available at: https://www.youtube.com/channel/UCII_8TbvAsG2BZJENUtjcvg

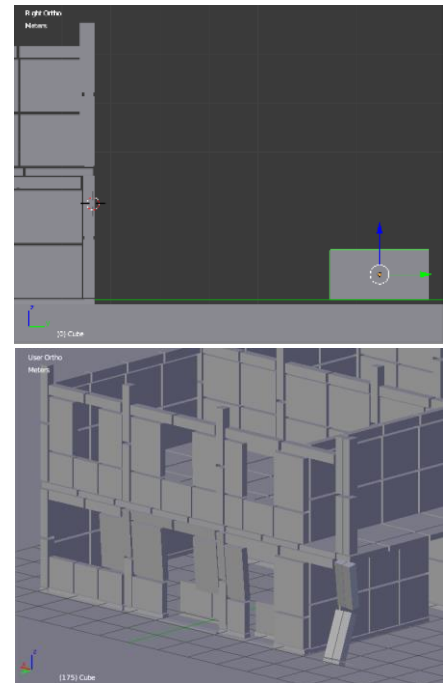
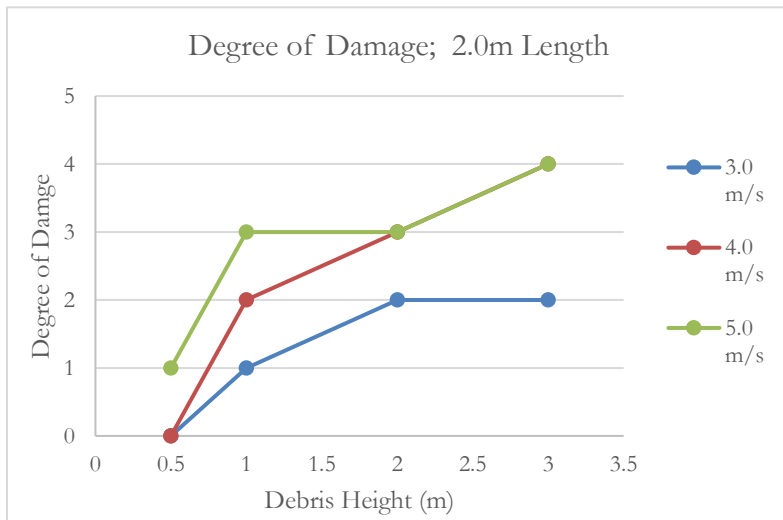


Figure 4.44a – 4.44c: Adjusted length of 2.0 meters, 4.0m/s Results in increased damage in the mortar walls and the columns on the right side of the building. 2.0m video available at: https://www.youtube.com/channel/UCII_8TbvAsG2BZJENUtjcvg

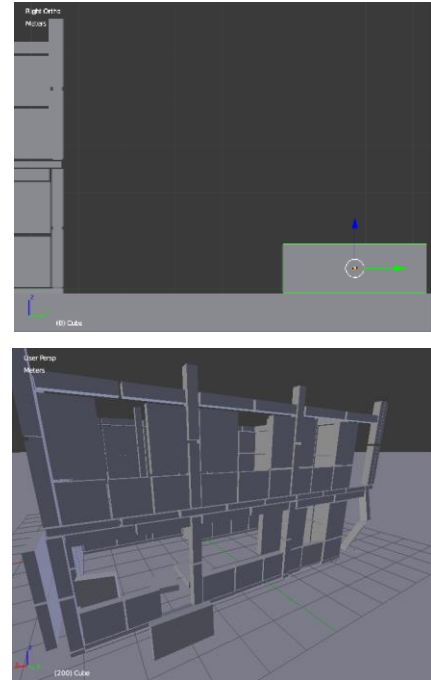


Figure 4.45a – 4.45c: 3.0-meter length results in similar damage for 3.0 – 4.0 m/s; however, the damage was observed in the unaffected walls, and the impact wall was significantly more damage. 3.0m video available at: https://www.youtube.com/channel/UCII_8TbvAsG2BZJENUtjcvg

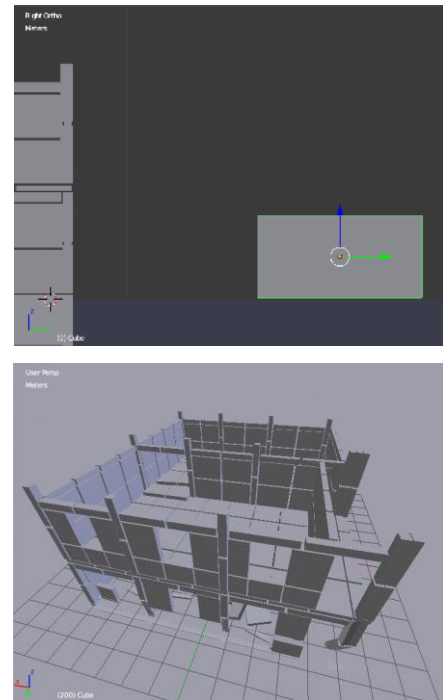
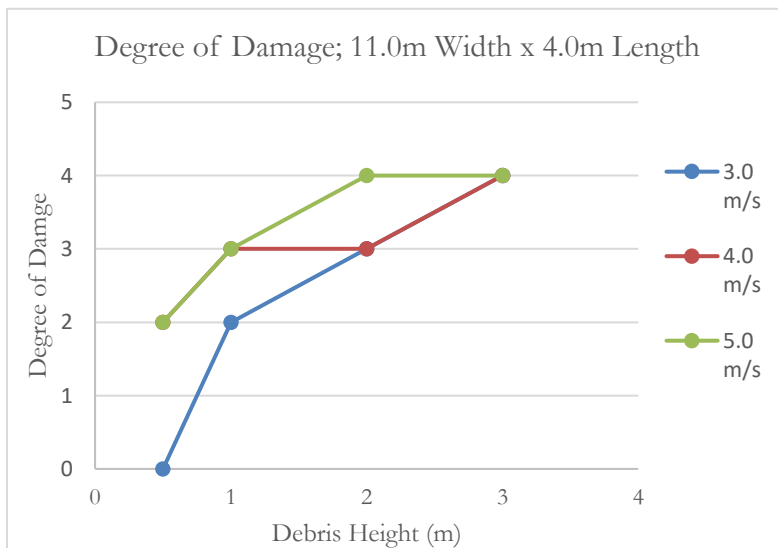


Figure 4.46a – 4.46c: A 4.0-meter length results in D2 damage for all velocities at a debris height of 1.0, and significant damage was observed in the entire buildings. Collapsed floors are observed on the second floor and all of the beams on the impacted wall have sheared from the foundation. 4.0m video available at: https://www.youtube.com/channel/UCII_8TbvAsG2BZJENUtjcvg

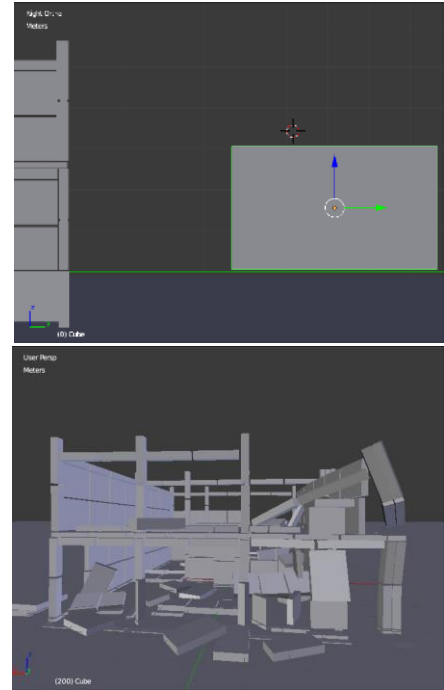
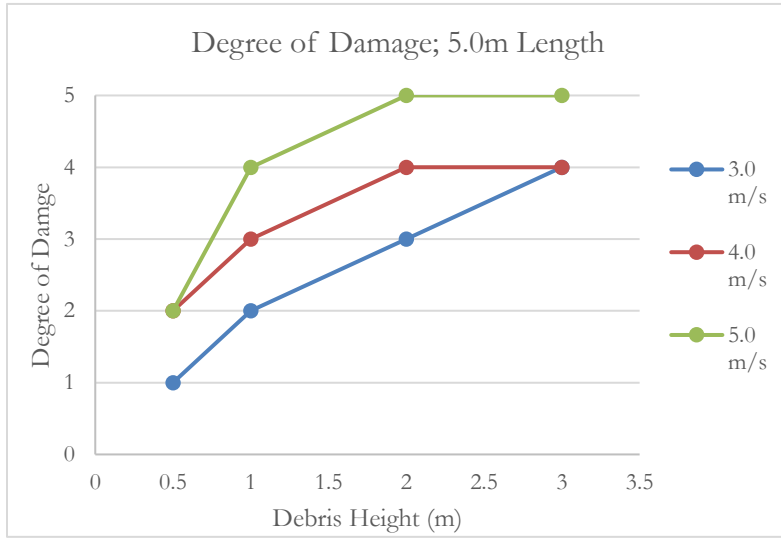


Figure 4.47a – 4.47c: A 5.0-meter length resulted in shallow impacting heights exceeding D1 damage, and 3.0-meter debris height exceeding D4. 5.0m video available at: https://www.youtube.com/channel/UCII_8TbvAsG2BZJENUtjcvg

5. DISCUSSION & CONCLUSIONS

This research aimed at using analytical methods for the development of vulnerability curves, and primarily focused on simulating damage to a common structural typology, of the country Dominica, to landslide impacts. Twenty-three sites were selected by overlapping the post-Hurricane Maria landslide inventory developed by van Westen et al., (2017) and OpenStreetMap building footprints in the parishes St. George, St. Patrick, St. Luke, and St. Mark. Data collection began on September 30, 2018, just over one year since Hurricane Maria, and by then much of the country was recovering in infrastructure and vegetation. In larger cities, such as Roseau, and along important roads connecting towns, debris had been excavated and the 23 sites selected during the fieldwork development stage, presented in the subchapter 3.1, were visited.

From the 23 sites visited, 10 buildings were surveyed with damage induced by debris slides, debris flows, flooding, and high wind-speeds; the analysis presented here focused on Building 2, which was affected by a debris slide, and there is supplemental data for Buildings 1 and 3 – 10 in the data collection chapter and appendixes. During the analyse the structural response of Building 2, the focus of the analysis shifted toward determining which parameters have the most significant effect on the simulations. The simulations began optimistically to simulate the building and the landslide with greatest number of elements, to simulate the highest detail, accuracy, in the building's response to landslide impacts. This resulted in extensive processing time, and, ultimately, the replacement of the modelled concrete block walls with larger structural elements, that were not representative of the measurements acquired during data collection of Building 2; additionally, the modelled soil-elements in the landslide simulations were limited to 0.125m³ in size, which essentially, were small cubic boulders.

Furthermore, the simulated magnitude of the landslide and induced damage to the building model presented in the core of this analysis was partially the effect of the absence of cohesion, vegetation, and water, which makes the simulated events significantly different in comparison to the events observed during fieldwork. In addition to these differences in the simulations and the real-world events, there were numerous uncertainties presented during data collection and analysis, which are further discussed below.

5.1. Effect of Input-Data Quality

The analysis presented in chapter four of this thesis was limited to the data collected during fieldwork. The collected data included information about the type and extent of damage; additionally, the types of hazards that affected the buildings. However, whether the damage was due to initial impacts, secondary impacts, or successive failures in the structure was undetermined. Furthermore, damaged induced by flooding, high wind speeds, or other hazards were difficult to differentiate when spatially close to damage induced by landslides. All of the surveyed buildings had flooding damage; Building 2 had an evenly distributed thick layer of soil and water, possibly the result of water infiltrating through the debris, pressed against the building, after the collision, and entered the building through the windows, slowly bringing soil in with it.

Another drawback due to the date of data collection was the vegetation had significantly regrown over the affected hillslopes and accumulated debris. Furthermore, in several of sites visited during fieldwork, the accumulated debris had been excavated; Buiding 1, at Site 8, for example, in the Google Earth historical images taken on October 11, 2017, one month after Hurricane Maria, debris had already been cleared from the road (Figure 3.5). Additionally, trees at Site 4, observed during the survey of Building 2, were displaced by the debris

slide, however, continue to grow in the accumulation of debris between the building and the hillslope (Figure 3.12). The rapid regrowth of vegetation obstructed access and made distinguishing the spatial extent of the debris slide a challenge. Another example, in Soufriere, the debris flows that occurred across Sites 20 & 21 were had regrown vegetation; however, the sediments from the debris flows at Sites 20 & 21 are visible in historical images on February 1, 2018, whereas most of the other sites have regrown vegetation. On the one hand, in the damage assessment of Building 1 the removal of debris from the road removed a large quantity of the debris slide before data could be collected, which hindered further analysis. On the other hand, the removal of debris from Site 6 was necessary to survey Buildings 6 & 7.

The extent of structural and damage data collected was limited to empirical assessments acquired during fieldwork. The level of detail, in the structural data collected, primarily included the dimensions of the structural frames, infill walls, and construction materials. In regards to the of surveying the damage, another issue presented during data collection was several owners had made repairs the damaged parts of the homes; the cottages hit by a debris flow at Site 21 were completely restored, and the owners of Building 10 had already rebuilt their wall that was damaged. Fortunately, the owners at both locations were able to describe the events and damage to some extent. Inevitably, there were numerous uncertainties throughout the data collection stage of research about the surveyed structures, damage, and hazards; then, the uncertainties were carried into the presented RAMMS and Blender analysis.

The presented RAMMS analysis in the subchapters 4.1.1 & 4.2.1 used a 5.0m resolution DEM made from contours. The DEM was acquired from a ITC member of the CHARIM project; however, the creator of the DEM has been undetermined. The contours file, available on the CHARIM GeoNode, used to create the DEM was relatively smoothed, affecting the quality of the DEM; the smoothed edges decrease the accuracy of ridgelines and slope direction. The effect results in simulated flow diverted from obstacles with less than 5.0m space between them, such as neighbouring buildings.

Additionally, the resolution and georeferencing of the maps used for the RAMMS analysis have drawbacks as well. One issue was presented in the subchapter 4.1 and Figures 4.1 – 4.3, when the obstacle used for the dam, in the RAMMS landslide simulation, restricted the simulated flow to half of the affected façade observed during data collection. Another example, presented during the analysis of Building 1; in Google Earth historical images there appeared to be a scarp from the same debris slide identified in the landslide inventory (Figure 5.1).

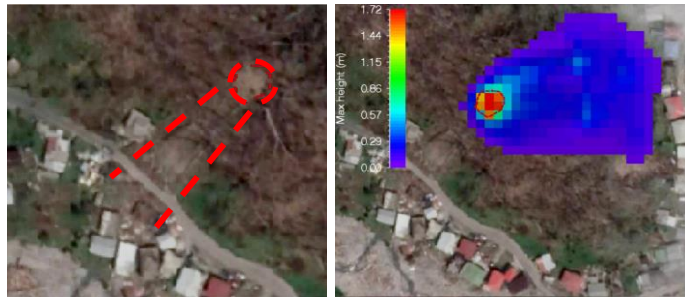


Figure 5.1 & 5.2: (Left) The expected flow direction during analysis of Building 1; (Right) the simulated flow direction

The location was chosen for the release location; however, the run-out analysis resulted in a simulated flow in the opposite direction expected (Figure 5.2). Unfortunately, Google Earth historical imagery was the only option determined available for maps in the analysis. The availability of imagery from an earlier date, than the maps used during this analysis, is limited due to cloud coverage days after Hurricane Maria, and the availability of high-resolution aerial imagery is limited in spatial coverage to the major cities such as Roseau.

5.2. Limitations of the Performed Simulations

The methodology of the RAMMS analysis included assigning a landslide type; the debris slides observed during the data collection of Buildings 1 & 2 resembled block releases; therefore, block releases were chosen for the RAMMS analysis. However, flooding played a significant role in the observed events and was excluded from the RAMMS and Blender analysis. The release soil density used in the analysis is 1900 kg/m^3 ; however, the soil observed during fieldwork was heterogeneous and inconsistent in mixed debris with layers of variously sized sediments distributed from past events. Vegetation, also, plays a significant role in the soil strength and hazard properties. For example, vegetation was observed growing in the accumulation zones developed against Buildings 2 where the debris slide impacted the wall.

Several factors affected the simulated landslide kinematics in the including the geometry, slope angle, and surface response parameters. For example, a simulated debris slide design with a rectangular geometry constructed from cubes 0.125 m^3 in size, resulted in the upper-layers overhanging and toppling at the beginning of the simulation. Two adjustments were made to the geometry to prevent the toppling and simulate a landslide without an overhanging section; a vertical cut and an angled cut was made at the toe of the landslide (Figure 5.3). The simulation using the vertical cut Figure 5.3 resulted in a more uniform displacement between the layers, which is why it was chosen for the analysis, and collectively the geometries presented in Figure 5.3 result in three significantly different shaped landslides when they reach the flat ground surface. From this, it was determined the initial geometry of the landslide, as well as the distance, significantly affects the run-out and impact kinematics. In addition to the geometry of the slide, the simulations without adjacent boundaries resulted in the body of the debris slide spreading laterally (Figures 5.5). A final concern of the Blender landslide analysis was the number of computation steps used in the simulations; as presented in the analysis the higher resolution simulations required extensive processing times, and reducing the number of elements in the simulation decreases the resemblance to a real-world building. There is potential for more updates, and add-ons, such as the Bullet Constraint Builder to improve the landslide models and accuracy of the results.

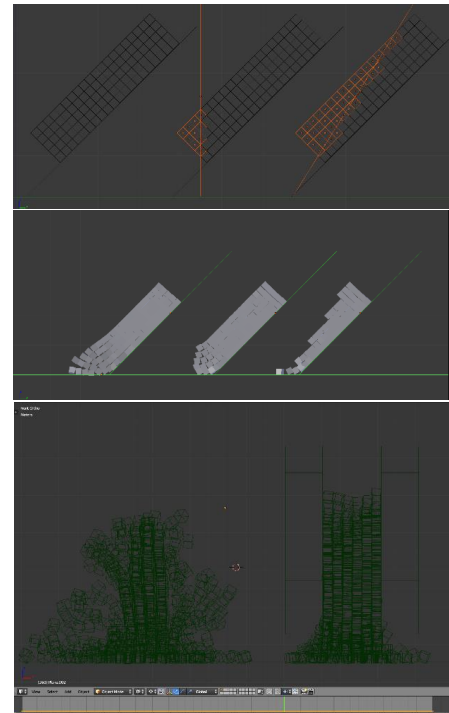


Figure 5.3 – 5.5: (Top) Two options, in orange, to adjust the landslide geometry; a vertical and angled cut; (Mid) resulting in different run-out kinematics and accumulation geometries. (Bot) Effect of adding barriers

5.3. Conclusions on Analysis of Buildings Subject to Simulated Landslide Impacts

The landslide simulation performed in RAMMS were repeated multiple times to position and size a model which resulted in max flow heights between 2.5 – 3.0m as observed during fieldwork; however, to optimise this part of the methodology a more precise release geometry need to be acquired either through data collection before an event or a more strategic surveying methods of estimating landslide volume such as presented by Han (2018). Furthermore, in RAMMS simulations presented there is a high level of uncertainty in the values simulated against the obstacle due to the resolution of the input data, and numerical model used. RAMMS

explicitly states in the RAMMS DEBRISFLOW User Manual that dams, or obstacles, are better simulated to deflect flow laterally, rather than perpendicularly.

In the analysis presented, the simulated soil-element size has one of greatest effects on the simulation results. The soil-element size directly affects the differential displacement between layers, the shape of the slide at a collision, the magnitude of force simulated against the building, and the simulated accumulation density. The geometry of the release and distance to the building, also, greatly affects the simulation results. The results from the simulations, with more elements incorporated, have significant differences in the simulated damage and accumulation geometry; however, the damage was always more extensive than observed in the during the data collection of Buildings 1 & 2. The simulated damage in the subchapter 4.2.3.11, presented the simulated vertical and horizontal pressure gradients on the buildings the moment a simulated constraint on the building was broken. It was determined the size of the soil-elements and the shape of the landslide as it reached the building resulted in high-pressure values up to 0.41m, then a drop in pressure, and another rise at 1.14m, then another drop, and a final increase in pressure at the top of the ground floor wall. The rise at 1.14m was significant because at that height a mortar constraint was broken, and the rise at the top of the ground floor is significant because it was simulated from the upper-most layers of the landslide impacting the wall, which is what was observed in Building 2 during fieldwork. The upper layer of the observed accumulated debris against Building 2 resulted in the second-floor of the impacted wall buckling. The horizontal pressure gradient is significant because it shows the degree of pressure reduction near the edges of the building, in comparison to the centre where debris has less room to move.

The simulated damage to Building 2 presented in the subchapter 4.2 was the result of the simulated landslide and structural parameters. The simulated building was modelled using the data collected during fieldwork, the Guide to Dominica's Housing Standards, and literature values of mortar strengths. The buildings simulated was relatively to scale, for example, the concrete blocks simulated were 40.0 x 20.0 x 20.0 cm³; however, the degree of detail did not exceed simulating concrete blocks, and a reinforced concrete frame. The constraints added to the buildings in the simulations performed were simulated using the Blender add-on Bullet Constraint Builder, which calculates the breaking thresholds based on the geometry of the simulated elements and the user-defined yield strengths. The validation of the performed analysis was based on data collected during the field work for the landslide characteristics, debris deposits and damage, and literature values of mortar engineering properties. However, the simulated damage from the analysis was always more extensive than the observed damage during data collection. It was determined the modelled particle size of the landslide and assigned breaking thresholds of the mortar walls, in particular of the mortar, have the most significant effect in the simulation performed while researching the vulnerability of buildings subject to landslide impacts.

The presented research for building vulnerability to landslide impacts and damage analysis is not ready to be transferred and applied in risk assessments. There needs to be a more systematic method of determining the initial landslide volume; however, there is potential with new add-ons to improve landslide models, or modelling rock falls could reduce the uncertainties presneted with the landslide intensity. The vulnerability curves presented in the subchapter 4.2.4.1, simulated several distinct effects; (i) an impact intensity defined by volume could result in different degrees damage based on the geometry, impact height, and centre of mass, (ii) damage to the second-story was not simulated for modelled heights less than 3.0m; (iii) progressive damage could be simulated when the impacted wall on the ground floor collapsed, (iiii) and at a velocity of 5.0m/s the impacting energy was transferred significantly through the building, damaging walls not directly impacted.

LIST OF REFERENCES

- Adam, J. M., Parisi, F., Sagaseta, J., & Lu, X. (2018). Research and practice on progressive collapse and robustness of building structures in the 21st century. *Engineering Structures*, 173, 122–149. Retrieved from <https://www.sciencedirect.com/science/article/pii/S0141029618306849>
- Ali, Q., Badrashi, Y. I., Ahmad, N., Alam, B., Rehman, S., & Banori, F. A. S. (2012). Experimental investigation on the characterisation of solid clay brick masonry for lateral shear strength evaluation. *International Journal of Earth Sciences and Engineering*, 5(4), 782–791.
- Amatya, S. C. (2014). *Report on Jure Landslide, Mankha VDC, Sindbupalchowk District. Ministry of Irrigation, Government of Nepal*. Retrieved from http://www.sabo-int.org/case/2014_aug_nepal.pdf
- Arash, S. (2012). Mechanical Properties of Masonry Samples for Theoretical Modeling. *15th International Brick and Block Masonry Conference*.
- Bessette-Kirton, E. K., Cerovski-Darriau, C. C., Schulz, W. H., Coe, J. A., Kean, J. W., Godt, J. W., ... Hughes, K. S. (2019). Landslides Triggered by Hurricane Maria: Assessment of an Extreme Event in Puerto Rico.
- Burt, C. C. (2014). Worst Landslides in U.S. History. Retrieved February 19, 2019, from <https://www.wunderground.com/blog/weatherhistorian/worst-landslides-in-us-history.html>
- Central Intelligence Agency, U. S. (1990). *Perry-Castañeda Map Collection: Maps of the Americas*. Retrieved from <https://legacy.lib.utexas.edu/maps/americas.html>
- Ciurean, R. L., Schroter, D., & Glade, T. (2013). Conceptual Frameworks of Vulnerability Assessments for Natural Disasters Reduction. In *Approaches to Disaster Management - Examining the Implications of Hazards, Emergencies and Disasters*. InTech. Retrieved from <http://www.intechopen.com/books/approaches-to-disaster-management-examining-the-implications-of-hazards-emergencies-and-disasters/conceptual-frameworks-of-vulnerability-assessments-for-natural-disasters-reduction>
- Craddock, N. (2016). Impulse Blender Add-On.
- Cuny, F. C. (n.d.). *Vulnerability Analysis of Traditional Housing in Dominica*. Dallas. Retrieved from http://oaktrust.library.tamu.edu/bitstream/handle/1969.1/160060/cuny_intertect_000006_13.pdf?sequence=1
- DeGraff, N. (1999). Natural Hazards and Disasters Landslides in St. Vincent. Retrieved February 19, 2019, from https://www.mona.uwi.edu/uds/Land_St_Vincent.html
- DeGraff, J. V., Brice, R., Castro, S. M., Jibson, R. W., & Rogers, C. (1989). Landslides: Their extent and significance in the Caribbean. In *Landslides: Extent and Economic Significance* (pp. 51–80).
- DeGraff, J. V., Bryce, R., Jibson, R. W., Mora, S., & Rogers, C. (1989). Landslides: Their extent and economic significance in the Caribbean, (January), 51–80.
- Dominica Meteorological Service. (n.d.). Climate Data. Retrieved February 4, 2019, from <http://www.weather.gov.dm/climate-data>
- Foundation, T. B. (2018). Blender. Retrieved from www.blender.org
- Froude, M. J., & Petley, D. N. (2018). Global fatal landslide occurrence from 2004 to 2016. *Natural Hazards and Earth System Sciences*, 18(8), 2161–2181. Retrieved from <https://www.nat-hazards-earth-syst-sci.net/18/2161/2018/>
- Fuchs, S., Heiss, K., & Hübl, J. (2007). *Natural Hazards and Earth System Sciences Towards an empirical vulnerability function for use in debris flow risk assessment. Hazards Earth Syst. Sci* (Vol. 7). Retrieved from www.nat-hazards-earth-syst-sci.net/7/495/2007/
- Garces, A. (2019). *Sausalito Declares Local Emergency After Mudslide*. Retrieved from <https://www.kqed.org/news/11727125/sausalito-declares-local-emergency-after-mudslide>
- Geology All about Dominica's geological make up. (2018). Retrieved February 20, 2019, from <https://www.avirtualdominica.com/project/geology/>
- Government of the Commonwealth of Dominica. (n.d.). Home - Physical Planning Division. Retrieved February 21, 2019, from <http://physicalplanning.gov.dm/>
- Government of the Commonwealth of Dominica. (2017). *Post-Disaster Needs Assessment Hurricane Maria September 18, 2017*. Retrieved from <https://reliefweb.int/report/dominica/post-disaster-needs-assessment-hurricane-maria-september-18-2017>

- Gu, X., Wang, X., Yin, X., Lin, F., & Hou, J. (2014). Collapse simulation of reinforced concrete moment frames considering impact actions among blocks. *Engineering Structures*, 65, 30–41. Retrieved from <https://www.sciencedirect.com/science/article/pii/S0141029614000601>
- Han, J. (2018). *Landslide volume estimation using reconstructed failure surfaces*. ITC University of Twente. Retrieved from https://webapps.itc.utwente.nl/librarywww/papers_2018/msc/aes/han.pdf
- Hodge, W. H. (1943). The Vegetation of Dominica. *Geographical Review*, 33(3), 349. Retrieved from <https://www.jstor.org/stable/209801?origin=crossref>
- Jaboyedoff, M., Michoud, C., Derron, M., Voumard, J., Leibundgut, G., Sudmeier-Rieux, K., ... Leroi, E. (2016). Human-Induced Landslides: Toward the analysis of anthropogenic changes of the slope environment. *Landslides and Engineered Slopes. Experience, Theory and Practice*, 217–232. Retrieved from <http://www.crcnetbase.com/doi/10.1201/b21520-20>
- Jalayer, F., Aronica, G. T., Recupero, A., Carozza, S., & Manfredi, G. (2018). Debris flow damage incurred to buildings: an in situ back analysis. *Journal of Flood Risk Management*, 11, S646–S662. Retrieved from <http://doi.wiley.com/10.1111/jfr3.12238>
- Kostack, K. (2015). *Bullet Constraints Builder Manual*. Retrieved from https://inachuslaurea.files.wordpress.com/2015/11/kk_bullet_constraints-builder1.pdf
- Kostack, K., & Walter, O. (2016). Bullet Constraints Builder add -on, (09), 1–8.
- Longshaw, S., Turner, M. J., Finch, E., & Gawthorpe, R. (2009). *Physics Engine Based Parallelised Discrete Element Model*. Manchester. Retrieved from https://www.researchgate.net/profile/Stephen_Longshaw/publication/269928403_Physics_Engine_Based_Parallelised_Discrete_Element_Model/links/5499632f0cf22a83139613bb/Physics-Engine-Based-Parallelised-Discrete-Element-Model.pdf
- Mavrouli, O., & Corominas, J. (2010). Vulnerability of simple reinforced concrete buildings to damage by rockfalls. *Landslides*, 7, 169–180. Retrieved from <https://link.springer.com/content/pdf/10.1007%2Fs10346-010-0200-5.pdf>
- Mavrouli, O., Fotopoulou, S., Ptilakis, K., Zuccaro, G., Corominas, J., Santo, A., ... Ulrich, T. (2014). Vulnerability assessment for reinforced concrete buildings exposed to landslides. *Bulletin of Engineering Geology and the Environment*, 73(2), 265–289. <https://doi.org/10.1007/s10064-014-0573-0>
- Momsen, J. D., & Niddrie, D. L. (2018). Dominica. Retrieved February 19, 2019, from <https://www.britannica.com/place/Dominica>
- Office of the United Nations Disaster Relief Co-ordinator. (1980). *Natural disasters and vulnerability analysis : report of Expert Group Meeting (9-12 July 1979)*. Retrieved from <https://archive.org/details/naturaldisasters00offi/page/4>
- Ontanillas, J. E. A. I. (2018). *DSWD DROMIC Terminal Report on the Landslide Incident in Naga City, Cebu*.
- Organization of American States, & USAID. (2001). Building Guidelines Drawings. Retrieved February 16, 2019, from <https://www.oas.org/cdmp/document/codedraw/intro.htm>
- Palmisano, F., Vitone, C., & Cotecchia, F. (2016). Methodology for Landslide Damage Assessment. *Procedia Engineering*, 161, 511–515. Retrieved from <https://www.sciencedirect.com/science/article/pii/S1877705816329083>
- Papathoma-Köhle, M., Keiler, M., Totschnig, R., & Glade, T. (2012). Improvement of vulnerability curves using data from extreme events: debris flow event in South Tyrol. *Natural Hazards*, 64(3), 2083–2105. Retrieved from <http://link.springer.com/10.1007/s11069-012-0105-9>
- Pasch, R. J., Penny, A. B., & Berg, R. (2018). *Tropical Cyclone Report | Hurricane Maria*. Retrieved from https://www.nhc.noaa.gov/data/tcr/AL152017_Maria.pdf
- Petley, D. (2012). Global patterns of loss of life from landslides. Retrieved February 19, 2019, from <https://blogs.agu.org/landslideblog/2012/08/16/global-patterns-of-loss-of-life-from-landslides-my-new-paper-in-the-journal-geology/>
- Petley, D. (2018). Fatal landslides in 2017. Retrieved February 19, 2019, from <https://blogs.agu.org/landslideblog/2018/04/08/fatal-landslides-2017/>
- Quan Luna, B., Blahut, J., Westen, C. van, Sterlacchini, S., Van Asch, T. W. J., & Akbas, S. O. (2011). Natural Hazards and Earth System Sciences The application of numerical debris flow modelling for the generation of physical vulnerability curves. *Hazards Earth Syst. Sci*, 11, 2047–2060. Retrieved from www.nat-hazards-earth-syst-sci.net/11/2047/2011/
- RAMMS DEBRISFLOW v.1.7.20. (2018). WSL.

- Remondo, J., Bonachea, J., & Cendrero, A. (2005). A statistical approach to landslide risk modelling at basin scale: from landslide susceptibility to quantitative risk assessment. *Landslides*, 2(4), 321–328. Retrieved from <http://link.springer.com/10.1007/s10346-005-0016-x>
- Roobol, J., & Smith, A. L. (2004). Geological Map of Dominica, West Indies. University of Puerto Rico, Mayaguez.
- Rouse, W. C., Reading, A. J., & Walsh, R. P. D. (1986). Volcanic soil properties in Dominica, West Indies. *Engineering Geology*, 23(1), 1–28. Retrieved from <https://www.sciencedirect.com/science/article/pii/0013795286900141>
- Schellenberg, K., Kishi, N., & Kon-No, H. (2011). Analytical Model for Rockfall Protection Galleries-A Blind Prediction of Test Results and Conclusion. Retrieved from www.scientific.net/AMM.82.722
- Still, G. T. (2004). Strength of cementitious mortars : a literature review with special reference to weak mortars in tension, 1–25.
- The Commonwealth. (n.d.). Member Countries: Dominica. Retrieved January 17, 2019, from <http://thecommonwealth.org/our-member-countries/dominica>
- The Ministry of Planning and Economic Development. (2018). *Guide to Dominica's Housing Standards*. Retrieved from http://physicalplanning.gov.dm/images/guide_to_dominica_houses_standard_may_2018.pdf
- USGS. (n.d.). Natural Hazards FAQ. Retrieved February 2, 2019, from https://www.usgs.gov/faqs/how-many-deaths-result-landslides-each-year?qt-news_science_products=0#qt-news_science_products
- Westen, C. van. (2015). National scale landslide susceptibility assessment for Dominica. *CHARIM Caribbean Handbook on Risk Information Management*, (May). <https://doi.org/10.13140/RG.2.1.4313.2400>
- Westen, C. van. (2016). National Scale Landslide Susceptibility Assessment for Dominica Multi-Hazard Analysis in Central America View project RIED project View project. Retrieved from <https://www.researchgate.net/publication/305115228>
- Westen, C. van, Sijmons, K., & Zhang, J. (2017). *Tropical Cyclone Maria. Inventory of landslides and flooded areas*. Retrieved from https://www.unitar.org/unosat/node/44/2762?utm_source=unosat-unitar&utm_medium=rss&utm_campaign=maps
- Westen, C. van, & Zhang, J. (n.d.). Caribbean Handbook on Risk Management CHARIM. Retrieved February 20, 2019, from <http://www.charim.net/>
- Westen, C. van, & Zhang, J. (2017). *Dominica Landslides and floods triggered by Hurricane Maria (18 September, 2017)*. Enschede.
- Yifru, J. (2015). *National Scale Landslide Hazard Assessment Along the Road corridors of Dominica and Saint Lucia*. University of Twente. Retrieved from https://webapps.itc.utwente.nl/librarywww/papers_2015/msc/aes/yifru.pdf
- Zhu, T. (n.d.). *Some Useful Numbers on the Engineering Properties of Materials (Geologic and Otherwise)*. Retrieved from <http://www.jsg.utexas.edu/tyzhu/files/Some-Useful-Numbers.pdf>

APPENDIX I: SURVEYING ASSESSMENT TEMPLATES

Surveying Assessment for Landslide Induced Damage to Homes											
1. Location	Locality, address, ID, Photo #			12. Ring Beam	Width and depth						
	Owners				size of reinforcement						
2. Surroundings	Functionality, Number of Occupants	residential public other:	auxiliary business	13. Steps	Number of risers						
	Structures around the building				Number of landings						
	Vegetation around the building				height of risers						
	Protection around the building				width of tread						
3. Structural Typology	Easily Identifiable landmarks / features			14. Structural Damage	waist thickness						
	Construction material type	wood reinforced other:	concrete mix		size, arrangmt. Of reinforcement						
	Number of floors	Basement Attic	Ground Floor Additional Floors:		Second Floor	depth size of footing	low grade				
4. Hazards and Damage	Number of Openings	Doors:	Windows:	Other:	Height , material, meth to handrail						
	Hazard inducing damage	wind mix other:	flooding	landslide	means of support						
	Surrounding damage	Structures other:	vegetation	protection	Column damaged / total	Basement Attic/Roof	Ground Floor Additional Floors: Second Floor				
	Number of floors damaged	Basement Attic/Roof	Ground Floor Additional Floors:	Second Floor	Bears damaged / beams	Basement Attic/Roof	Ground Floor Additional Floors: Second Floor				
	Number of rooms w/ debris inside	Basement Attic/Roof	Ground Floor Additional Floors:	Second Floor	Load Bearing Walls / other	Basement Attic/Roof	Ground Floor Additional Floors: Second Floor				
5. Foundation and Retaining walls	Number of Openings Damaged	Doors:	Windows:	Other:	Use of Ground Floor						
	Depth			15. Intensity Indicators	Relative Debris Height	Outside	Inside				
		thickness			Debris Composition	Soil Trees	Rock Other: Shrubs				
	width			16. Landslide Characteristics	Soil type						
		material			Rock type / quality						
	reinforcement size	Wall	Footing		17. Impact Location (Landslide)	Organics					
reinforcement spacing		Wall	Footing			Hill side location	Toe Head	Foot	Main body	Minor Scarp	Major Scarp
method of tying footings/wall/floor				Exent of Hill side		Bellow		Above			
height of retaining wall				Flank Location		Left	Middle			Right	
6. Floor slab on grade	Height of slab above ground			Exent of Flank	Left	Right					
	thickness of slab										
	reinforcement in slab										
7. Columns	support of slab at point of details										
	thickness of blinding										
	damp-proofing material										
8. Beams	thickness of hardcore										
	method of tying slab to wall										
	Size of columns										
9. Roof Members	depth of pads, including thickness										
	size of spacing of reinforcement										
	depth of beam & slab thickness										
	size & arrangmt o reinforcement										
10. Roof Members	cantilever section										
	spacing of ties										
	Size										
	Spacing										
	Size of tie beams										
	roofing materials										
11. Suspended Slabs	method of tying roof to walls										
	length of eaves										
11. Suspended Slabs	ceiling material and support										
	Slab thickness										
	position of beams in slab										
11. Suspended Slabs	Arrangmt. / size reinforcement										

Elms Hall & Kings Hill:

Sites 1-3 are in the towns Elms Hall & Kings Hill, and Building 10 is at Site 1. The landslide inventory shows three debris flows and two debris slides at Site 1, however, evidence of multiple slides is difficult to identify because of regrown vegetation. The landslide scarp of Assessment 10 is observable at Site 1, however, inaccessible. The absence of vegetation at Site 2 is the result of excavation, and the house at Site 3 received no damage according to the owner. Table summarises damage to Building 10.

Table: Summary of Building 10



Building Type	Residential
Construction	Reinforced Concrete Frame, Block Walls, Timber Rafters
Number of Floors	1
Damage State	Moderate: Significant Structural and Non Structural Damage
Hazard Type(s)	Debris Slide & Flooding

Figure: Google Earth Historical Image; February 1, 2018. Location plan of Sites 1-3.

Erosion from the debris slide in Building 10 is visible from the driveway of the house; however, it is inaccessible. Debris and water flooded the house leaving stains on the walls 53cm high. One façade of the house is under reconstruction after collapsing, and the neighbouring houses are unaffected.



Figure: (Left) Debris slide erosion visible from the driveway (Right) Flooding stains along the walls

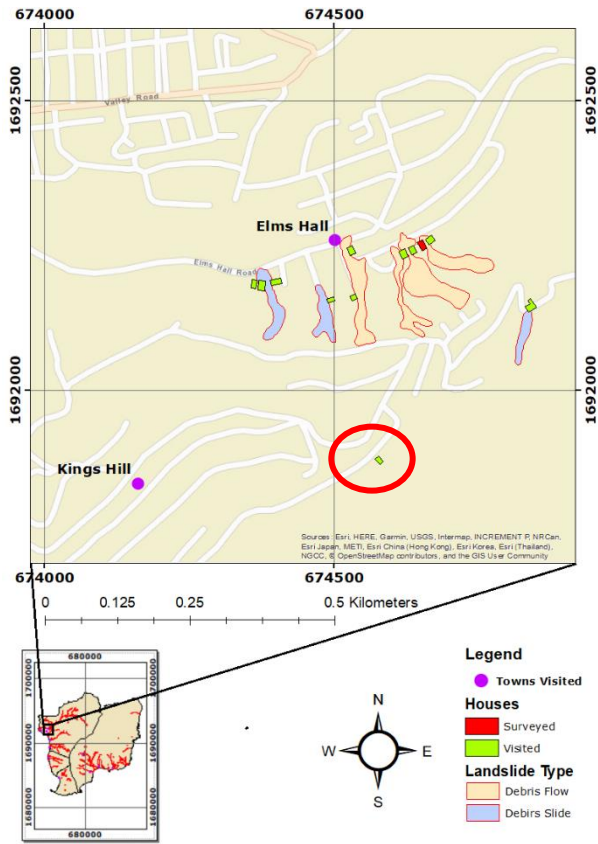


Figure: Map of Kings Hill and Elms Hall. Site 2 identified from Google Earth (red circle)



Figure: Building 10 being constructed to look the as it did before Hurricane Maria

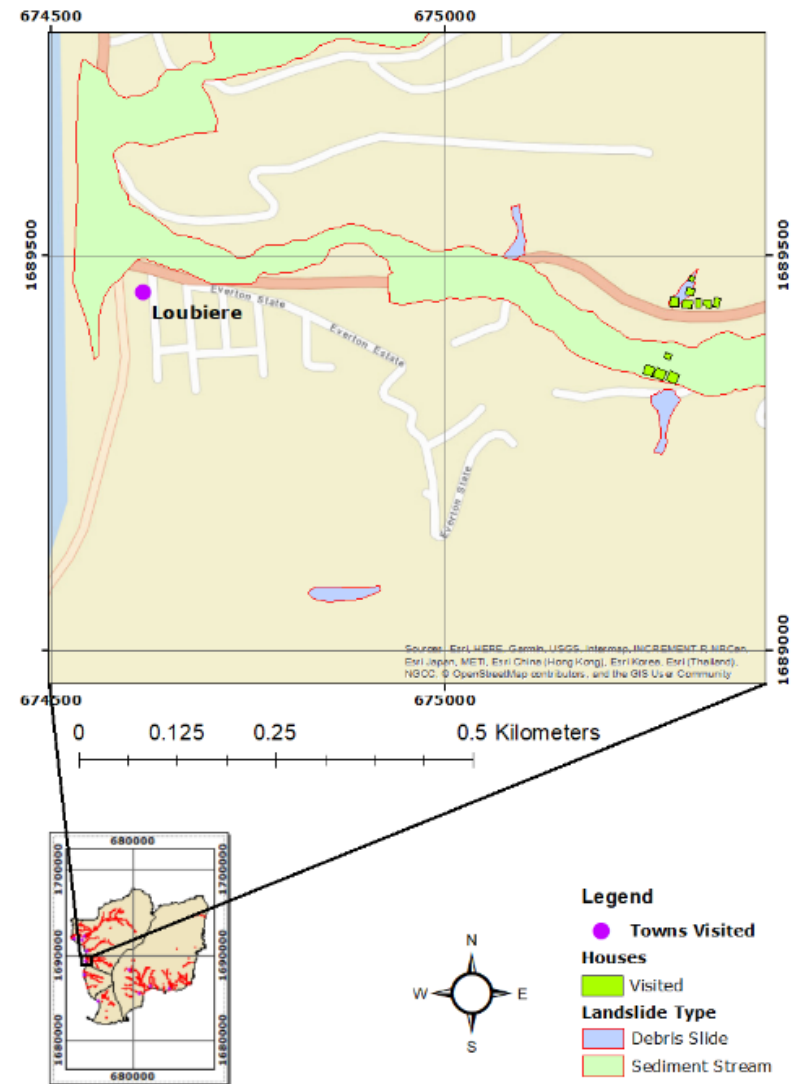
APPENDIX II: SITE ASSESSMENTS 7, 10, 11, 13-15

Loubiere:

Assessment 7, east of Loubiere, and a neighbourhood across the street flooded. The locals recall the sediment stream and flooding causing damage to some houses; however, no homes directly hit by landslides. The landslide inventory has two debris slides identified at Site 7, and across the street. Vegetation is regrown, and evidence of erosion or debris slides is hard to find. Several of the homeowners at Site 7 are not available, and access behind the homes is limited.



Google Earth Historical Image; February 1, 2018. Location plan of Sites 7



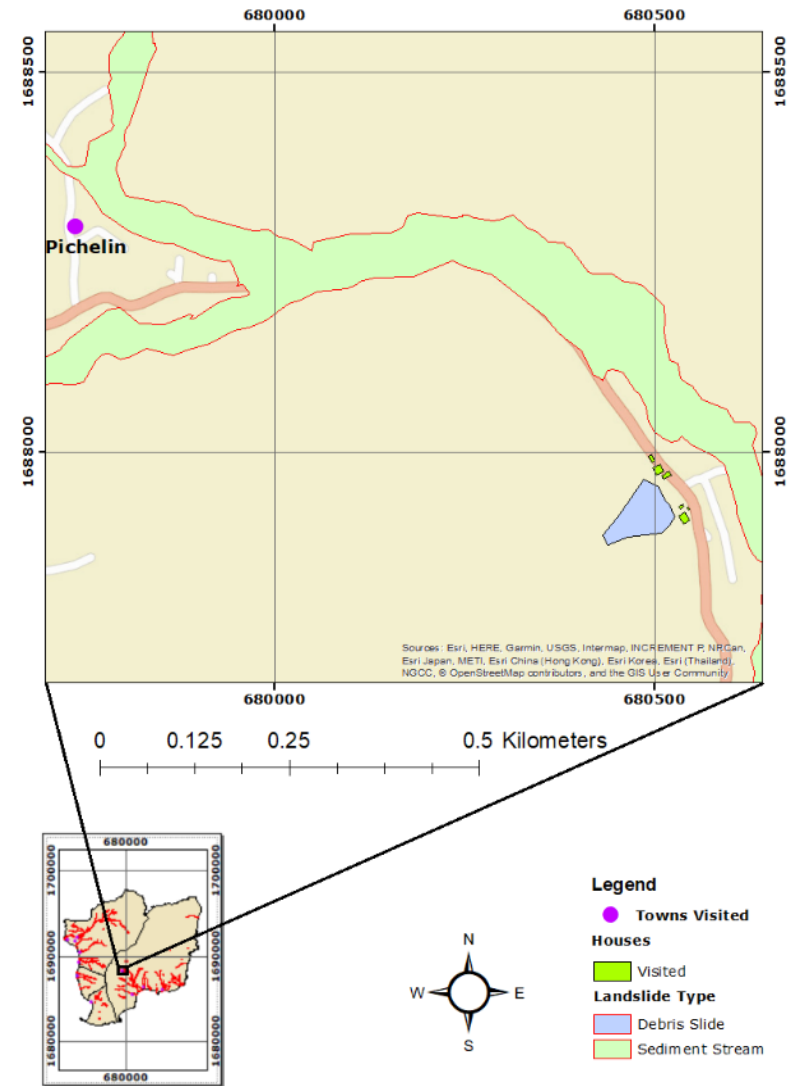
Map of Loubiere and two neighbourhoods visited

East of Pichelin:

Site 10 is east of Pichelin. There is no evidence of houses affected by landslides. The homeowners explain the debris slides behind their homes did not reach their backyards. Across the highway from Site 10, there is a school and neighbourhood affected from flooding, wind and the sediment stream flowing parallel.



Google Earth Historical Image; February 1, 2018. Location plan of Site 10



Map of East Pichelin and Site 10

Castle Comfort:

Site 6 at Castle Comfort shows only signs of flooding. Assessments 5-7 are at another site found during fieldwork upstream east of Site 6. Debris slides, eroded sediments, and flooding accumulated around the houses of Assessments 5-7. The landscape before Hurricane Maria is almost indistinguishable from the current. OpenStreetMap, and discussion with the locals helped determine how the event took place damaging the homes. Before Hurricane Maria, a bridge crossed River Canari upstream of the houses, and retaining walls ran parallel to the river and road. Further upstream, trees dammed the river triggering an intense overflow and flooding. The debris slides and flooding became a whirlpool surrounding Building 5 & 6. Larger sizes and quantities of sediment pushed between and against Houses 6 & 7 following the path of the road as the water level increased; eventually collapsing the retaining walls along the road. Tables present a summary of Assessments 5-7.



Figure 3.13: Google Earth Historical Image; February 1, 2018

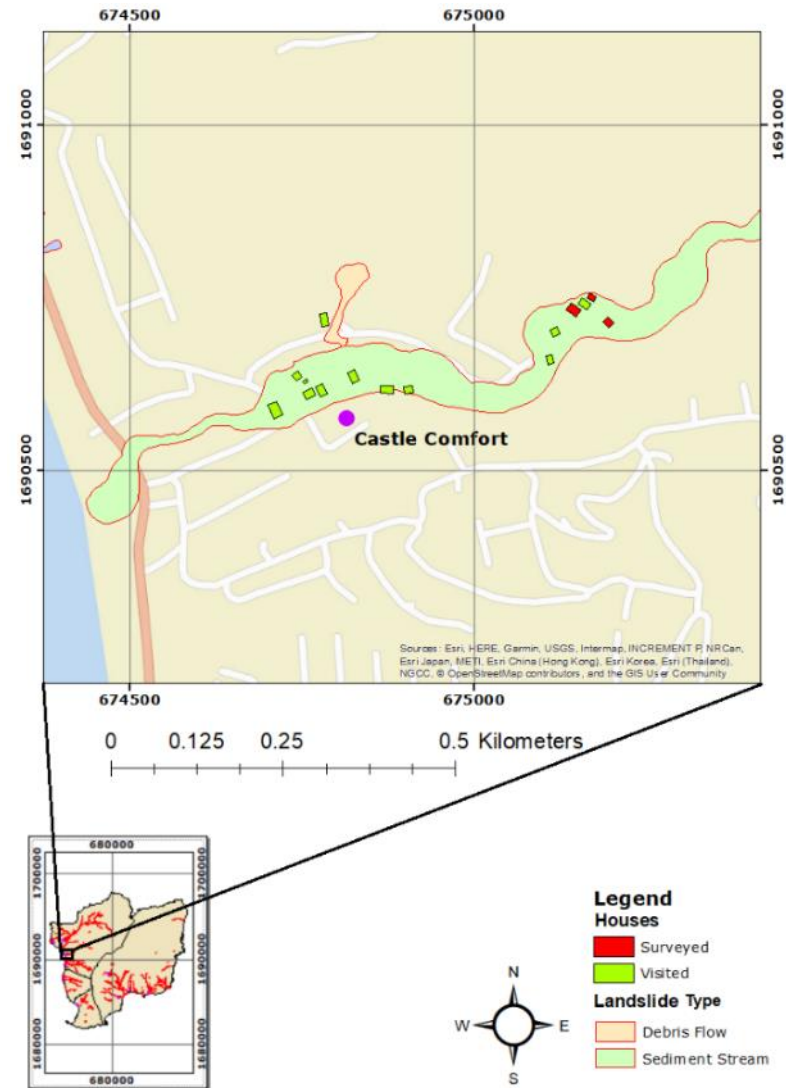


Figure 3.14: Map of Castle Comfort;



Figures: (Above) Plan view of Buildings 5-7. Bridge destroyed at dashed line crossing River Canari.



(Top-Right) Street view; Debris collapsed the retaining walls along the road, and vines hang from the damaged balcony of House 5.



(Bot-Right) Two meter tall retaining walls along the river being excavated

Table 3.3: Summary of Assessment 5

Assessment Number	5
Building Type	Residential
Construction	Reinforced Concrete Frame, Block Walls, Pile Foundation
Number of Floors	2
Damage State	Minor: Significant non-structural damage, minor structural damage
Hazard Type(s)	Debris flow & Flooding

The reinforced concrete frame of the house in Assessment 5 is exposed on the ground floor. Large spruce trees, and boulders half a meter in diameter are scattered and tangled in the frame. There is only minor structural damage to the columns and beams; such as chips in the concrete. The rebar in Figure 3.18 is deformed in the direction of flow from sediment and water pressure greater than the bending strength of the reinforcement. In Figure 3.16 the water level and sediments damaged the balcony. The reinforced column, concrete slab, and decorative railing, now tangled in vegetation, have minor structural and non-structural damaged. The retaining wall (Figure 3.19), and neighbouring houses, shielded the house from a direct impact.

Figures 3.18 & 3.19: (Top) Standing on the stairs looking under House 5. (Bot) Standing from the road, the reinforced concrete retaining wall collapsed in front of House 5.



Table 3.4: Summary of Assessment 6

Assessment Number	6
Building Type	Residential
Construction	Reinforced Concrete Frame, Block Walls, Timber Frame
Number of Floors	2.5
Damage State	Severe/Collapse: Irreparable Structural damage and partial collapse
Hazard Type(s)	Debris flow & Flooding

Assessment 6 is furthest upstream and closest to the river. After the river dammed, sediments accumulated along the north-east façade of the house (Figure 3.20). The sediments reached the top of the ground floor collapsing a timber framed second floor and attic. The remains were either buried or carried away. The weight of sediments and water collapsed the roof of the ground floor (Figure 3.21). Sediments are distributed in every room to the ceiling, except near the back door where sediments continue to flow out the house. The house is in the process of being excavated from debris. Unearthed sections of the home show no significant cracks or breaks other than the collapsed roof; possible due to a gradual increase in pressure rather than a sudden high intensity impact on the house.

Figure 3.20 & 3.21: (Top) Standing from the river bed on excavated ground. (Bot) Standing on the upstream side of



Table 3.5: Summary of Assessment 7

Assessment Number	7
Building Type	Residential
Construction	Reinforced Concrete Frame, Block Walls, Timber Frame
Number of Floors	2
Damage State	Severe/Collapse: Irreparable Structural damage and partial collapse
Hazard Type(s)	Debris flow & Flooding

The damage in Assessment 7 is similar to Assessment 6. An additional timber framed floor collapsed and floated away. The roof of the house is not collapsed; however covered in debris and vegetation. The house is filled with an evenly distributed amount of debris (Figure 3.22). Additionally, less debris excavated around the house limits accessibility. The retaining wall between the house and road is either buried or destroyed. Larger boulders surrounding Assessment 7 and the road, are accumulated around damaged columns of the neighbour (Figure 3.23). Other than the house being partially buried, the exposed frame and walls of the ground floor have no significant damage. The ceiling damage in Figure 3.22 is not noticeable from the roof.

Figures 3.22 & 3.23: (Top) Crouched in the doorway of House 7 looking into the largest room. (Bot) Standing from the neighbour's porch, between Houses 5 & 6.

Soufria



Sites 16-21 are at Soufriere (Figure 3.28), Assessment 8 is at Site 21, and Assessment 9 is at Site 20. There is no evidence of landslide-induced damage at Sites 16 & 19. A debris flow damaged outside stairs leading to the second floor of a house at Site 17; however no further assessment is acquired. Debris accumulated around a home at Site 18, but a wall surrounding the property diverts the flow protecting the house. A debrisflow affected Sites 20 & 21 (Figure 3.29), both sites are part of a botanical garden. The house in Assessment 8 is one of the twin cottages, both affected, and the house in Assessment 9 is a storage building. Debris slides accumulate from multiple directions at these sites, merging into an extensive debris flow. Tables 3.7 & 3.8 presents a summary of Assessment 8 & 9.



Figure 3.28: Google Earth Historical Image; February 1, 2018
Location plan of Sites 16-21

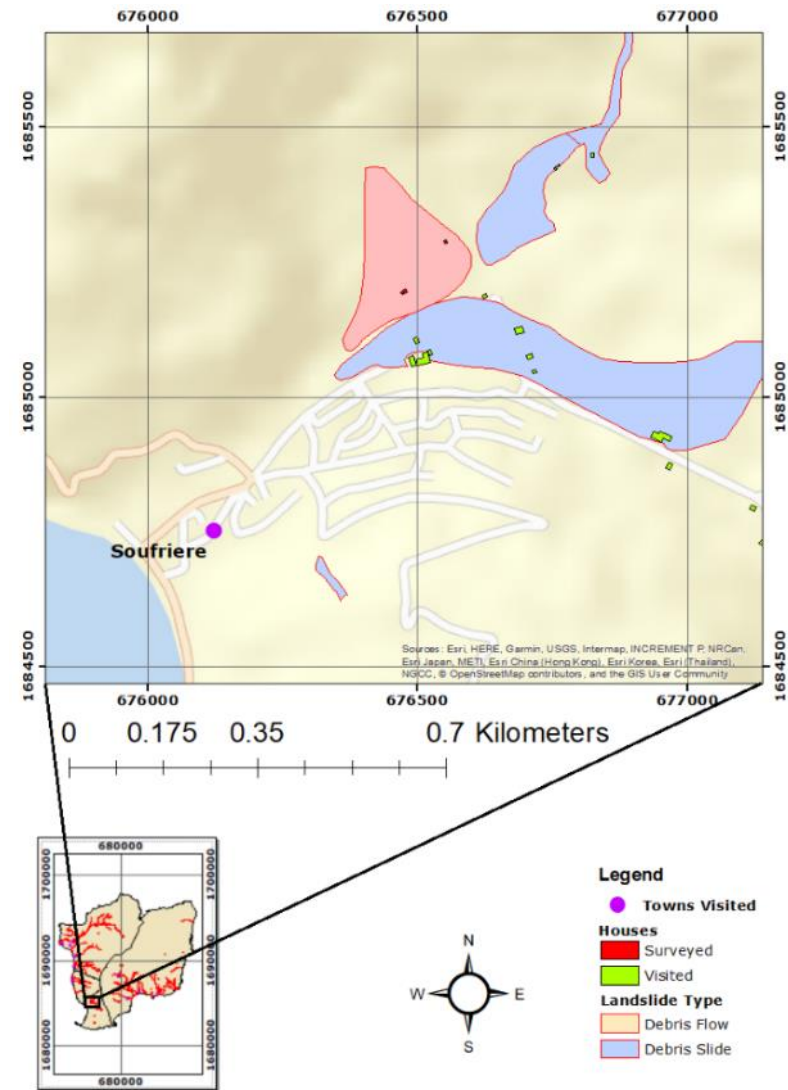


Figure 3.29: Map of Soufriere, houses visted, and surveyed

Table 3.7: Summary of Assessment 8

Assessment Number	8
Building Type	Rentals
Construction	Reinforced Concrete Frame, Block Walls, Timber Rafters
Number of Floors	1
Damage State	Light: Non-structural damage
Hazard Type(s)	Debris flow & Flooding

The owners of the botanical garden repaired the cottages after Hurricane Maria and excavated debris from the front of the cottages (Figure 3.32). Accumulated debris surrounds one side of the cottages, and the owners converted part of the accumulation in the back into a garden. Vegetation on the property is regrown and debris scars, visible in Google Earth, are difficult to distinguish in the field. The cottages are mirror images of each other and built on a single pad foundation. The owners described debris 170cm high accumulated behind the cottages and breaking the windows. In the middle of the cottages, debris 95cm high reached the bottom of the windows.

Table 3.8: Summary of House 9's Assessment

Assessment Number	9
Building Type	Rentals
Construction	Reinforced Concrete Frame, Block Walls, Timber Rafters
Number of Floors	1
Damage State	Light: Non-structural damage
Hazard Type(s)	Debris flow & Flooding

Assessment 9 is a storage facility at the back of the botanical garden and built with a reinforced concrete frame (Figure 3.33). One room, with the roof, is inaccessible and the largest open room, with no roof, is filled with timber. Accumulated debris from the event surrounds the sides and back of the house. The beams of the house are weathered and cracked with chips of concrete missing. The debris behind the house is less than a meter high; possibly the result of a shallow debris flow and mostly water. There is no evidence to suggest the debris flow caused damage to the frame; however,

there is a large opening at on the north façade of the house where debris accumulated on top of timber.



Figure 3.32 & 3.33: (Left) Assessment 8, at Site 21, has been excavated in the front but accumulated debris is left over on the right side; indicated by red arrow (Right) Assessment 9 is a storage facility, the boarded window is part of an inaccessible room

Point Michel:

Assessment 3 is at Site 22 in Point Michel (Figure 3.34). Flooding, trees, and debris damaged the house. No landslide was identified, however, the house was assessed early into fieldwork as a supplemental house to analyse. Assessment 3 is a house the furthest upstream in a line of homes parallel sediment stream, and shielded the neighbours. Another damaged house on the opposite side of the stream, and also furthest up-stream, shows similar signs of shielding the other houses. (Figure 3.35). Table 3.9 presents a summary of Assessment 3.



Figure 3.34: Google Earth Historical Image; February 1, 2018. Location plan of Site 22

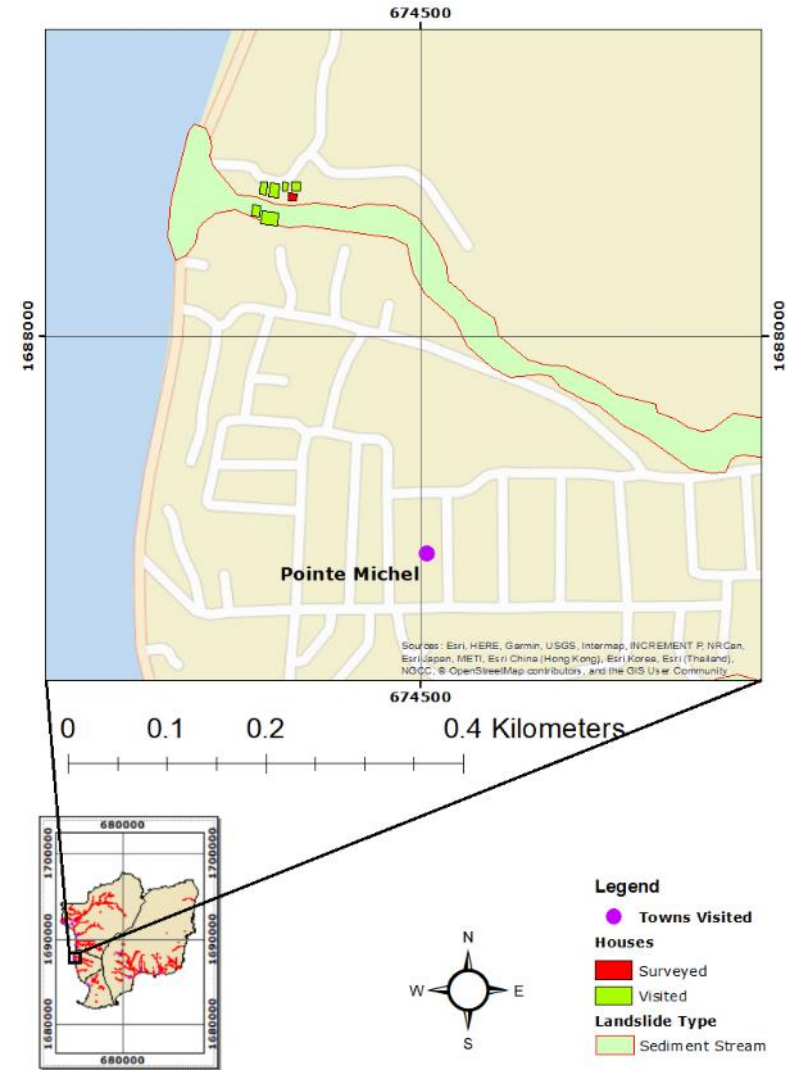


Figure 3.35: Map of Point Michel, houses visited, and surveyed

Table 3.9: Summary of House 3 Assessment

Assessment Number	3
Building Type	Residential
Construction	Reinforced Concrete Frame, Block Walls, Timber Frame
Number of Floors	1
Damage State	Severe: Significant structural and non-structural damage, will require demolition.
Hazard Type(s)	Flooding, Trees, Debris

The upstream façade (east wall) of the house in Assessment 3 collapsed from the pressure of flooding, trees, and debris. The owners of the yellow house across the sediment stream recall the water level reaching the balcony of their home (Figure 3.36). There are columns and reinforcement on the roof of the house damaged; however, there is no evidence of an additional collapsed floor. The wall parallel to the stream bed is partially cracked through the column at the SE corner. The damage is irreparable and will require demolition. Destroyed furniture is mixed with the accumulated trees and debris in every room (Figure 3.37).

Figures 3.36 & 3.37: (Top) Collapsed wall of Assessment 3 and neighbour's damaged balcony from water level indicated with red arrow; (Bot) standing in the opening of Assessment 3, trees meters long extend to the back of the house.



Fond St. Jean:

Assessment 4 is at Site 23 in the town Fond St. Jean (Figure 3.38). A debris slide damaged the house in Assessment 4; however, on the landslide inventory the hazard listed is a sediment stream (Figure 3.39). The owner of the house recalls a similar slide occurring from the previous hurricane, and students from another university came to survey. Table 3.10 presents a summary of Assessment 4.



Figure 3.38: Google Earth Historical Image; February 1, 2018. Sites 23 is at the top.

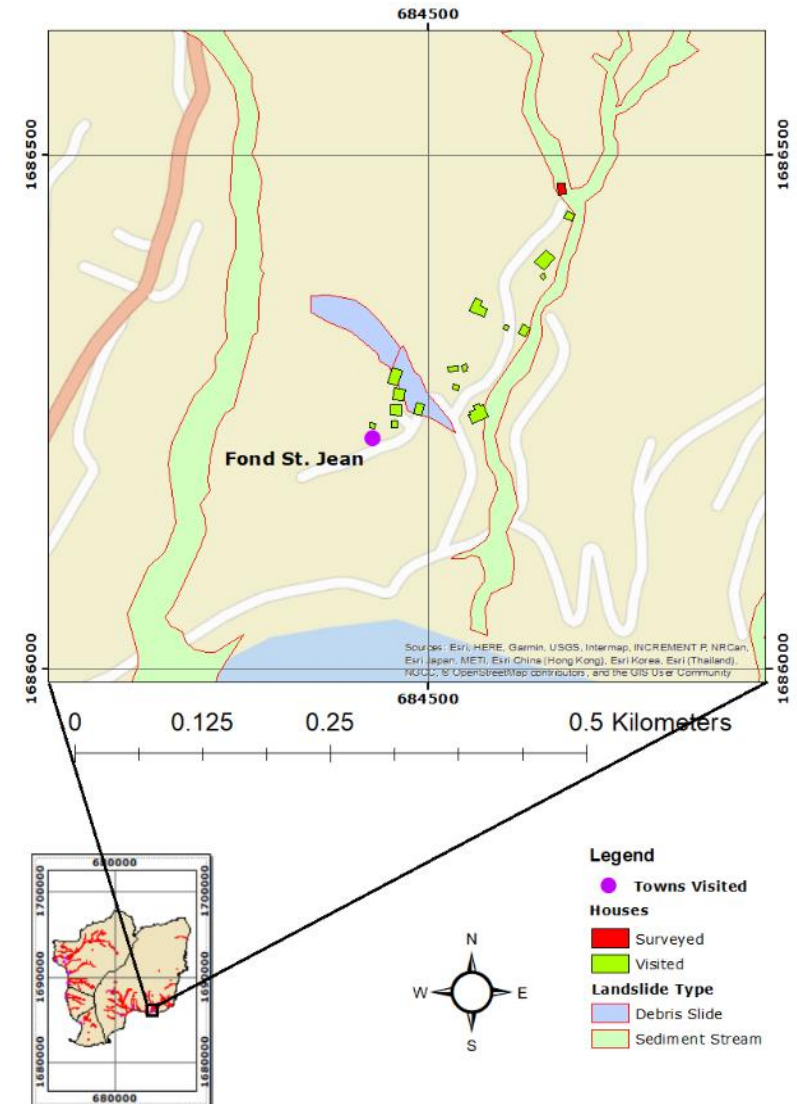


Figure 3.39: Map of Fond St. Jean, houses visited, and surveyed

Table 3.10: Summary of House 4 Assessment

Assessment Number	4
Building Type	Residential
Construction	Reinforced Concrete Frame, Block Walls
Number of Floors	1
Damage State	Minor: Non-structural damage
Hazard Type(s)	Debris slide



The owners of the house in Assessment 4 described the event; a debris slide occurred on the adjacent slope (Figure 3.40), accumulating around the house and on to the roof. Before Hurricane Maria, the owner constructed retaining walls between the stream and the house, also, boarded the windows facing the hill. A hurricane, prior Hurricane Maria, triggered a similar slide and broke the windows of the house. Debris spilled into the rooms, therefore, the owner boarded the windows before Hurricane Maria. The debris slide is composed from a pyroclastic weathered ash deposit (Figure 3.41). The lateral extent wraps approximately 30 meters around the house, and has a slope length 20 meters from the house to the vegetation on top.

Figures 3.40 & 3.41: (Top) Excavated slope at Assessment 4 after debris slide. (Bot) Weathered ash soil of varying sediment sizes at Assessment 4.



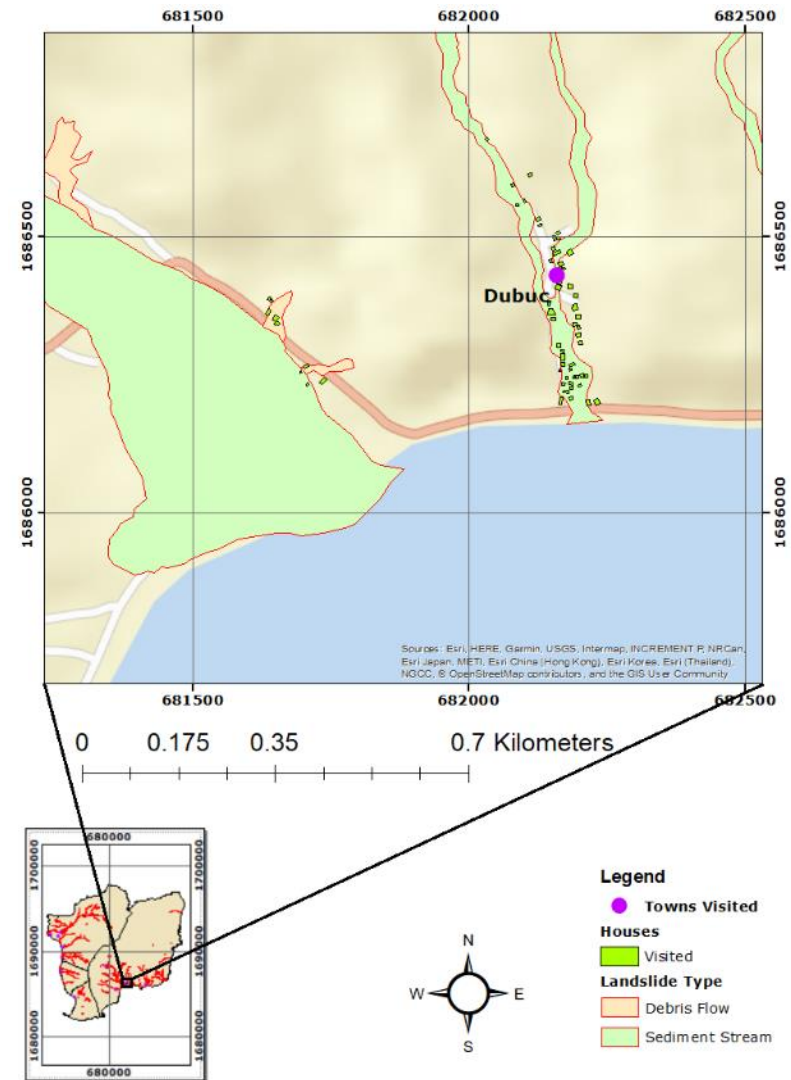
Dubuc:

Site 11 is off the highway on the way to Site 12 and Dubuc. Site 11 has evidence of a debris flow. However, the debris does not reach the house, and no damage is identifiable. High wind speeds and flooding damaged the homes at Site 12. Sediments and trees are damming the channel at Site 12, and two homeowners continue to live in Dubuc.



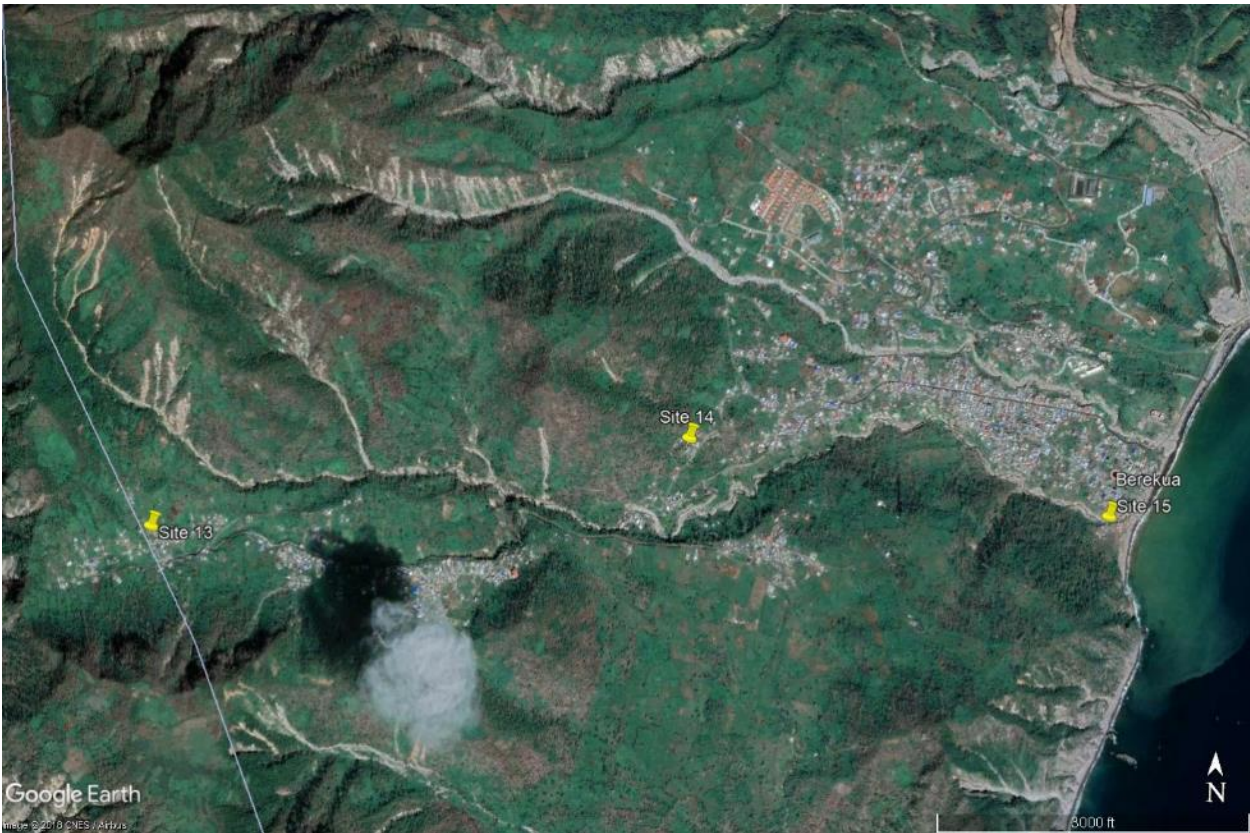
Google Earth Historical Image; February 1, 2018. Location plan of Sites 11 & 12

Map of Dubuc and the houses visited along the way



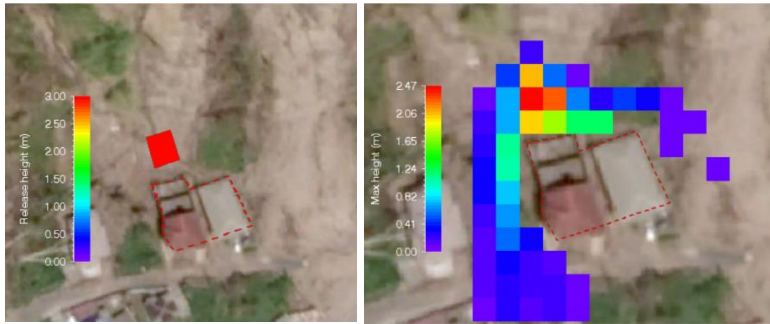
Berekua:

Sites 13-15 spread across Berekua. Landslide scars and debris flows are visible in Google Earth Historical Imagery; however, landslide induced damage is challenging to identify. The locals at Site 13 describe the damage caused by high wind speeds, flooding, and ground shaking. No route found to Site 14, and Site 15 is inaccessible without permission from the homeowners. Along the beach near Site 15, there is timber accumulated from Hurricane Maria.

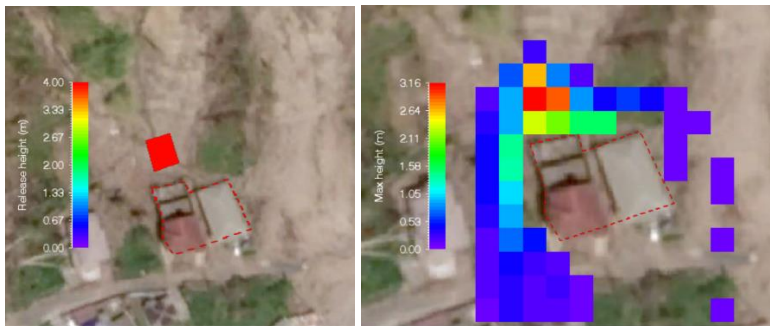


Google Earth Historical Image; February 1, 2018. Location plan of Sites 13-15

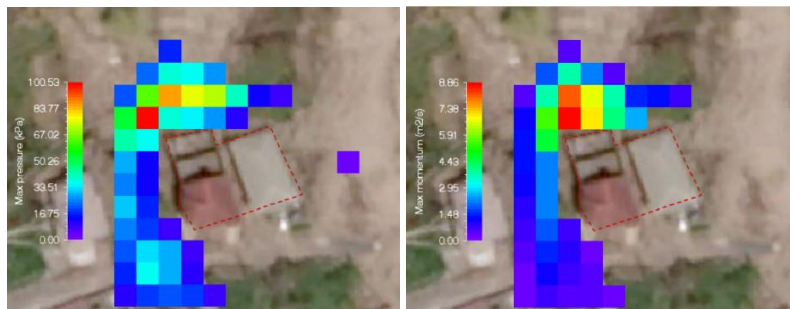
APPENDIX III: RAMMS ANALYSIS ALTERNATIVES



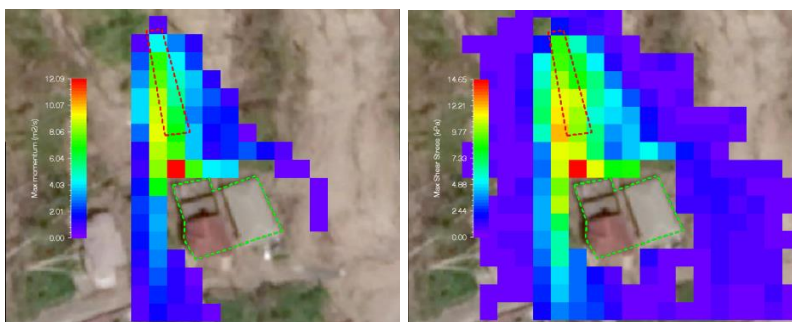
Release Height 3m and max height distribution



Release Height 4m and max height distribution



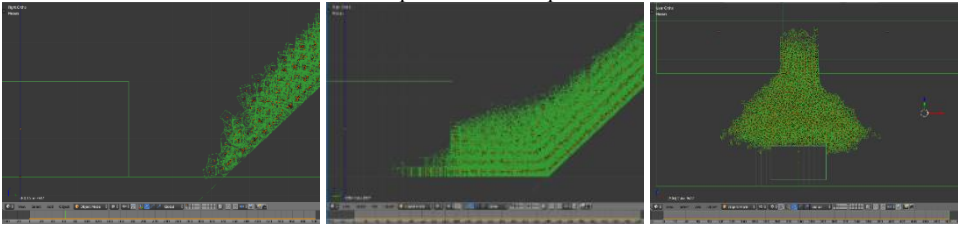
Release Height 3.5m; max pressure and max momentum



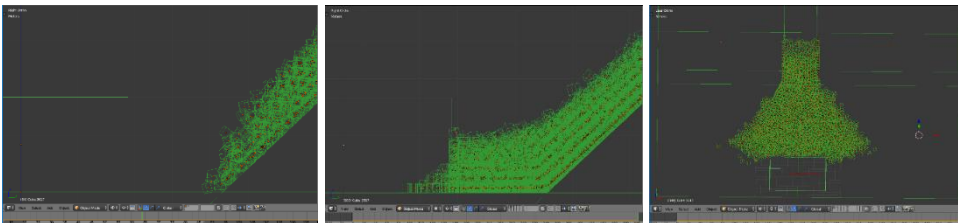
Release height 2.5; max momentum and shear stress distribution

APPENDIX IV: BLENDER RUN-OUT ANALYSIS ALTERNATIVES

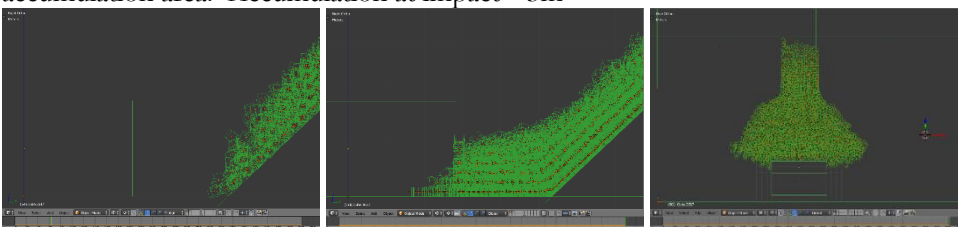
The distance from the house to slope 5.0m; the planar distance 13.0m.



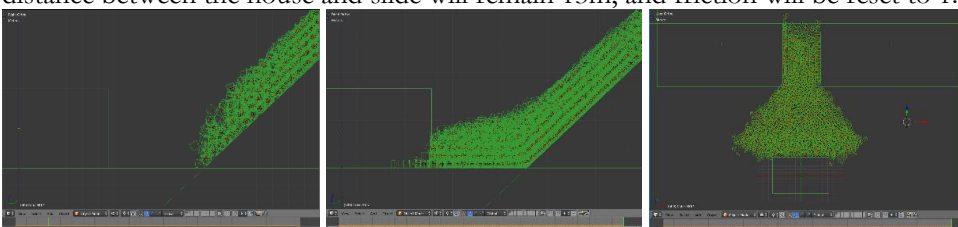
Friction set to 1.0; the accumulation zone is concentrated behind the house with minimal debris wrapping around the sides. Increasing the distance from the house to the slope results in a geometry of higher resemblance to the field assessment behind the house.



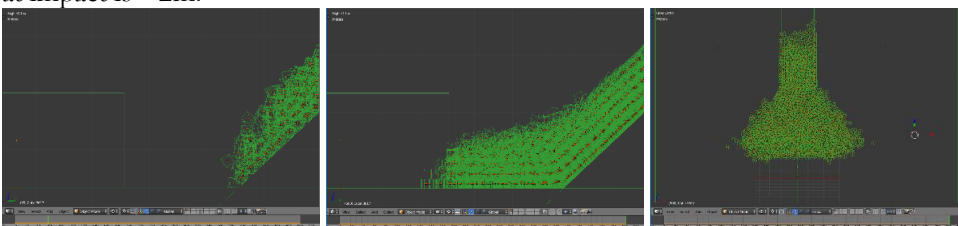
Friction set to 0.5 results a flatter accumulation zone behind the hose with minimal change to the accumulation area. Accumulation at impact $\sim 3\text{m}$



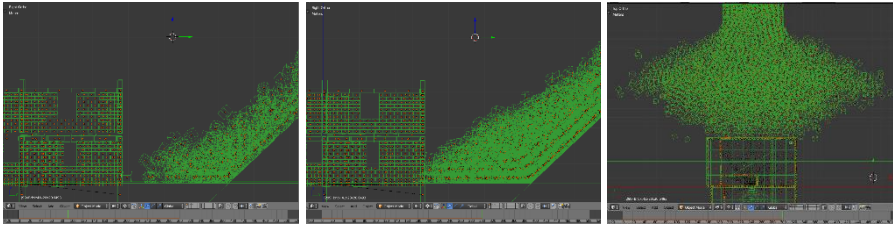
Friction set 0.3 does not improve the geometry of the accumulation zone. The Accumulation at impact is reduced to $\sim 2.5\text{m}$ and appears more sloped. The accumulation zone on the ground is more concentrated in the back of the house. The distance will be adjusted between the house and slope to 6m, the planar distance between the house and slide will remain 13m, and friction will be reset to 1.0



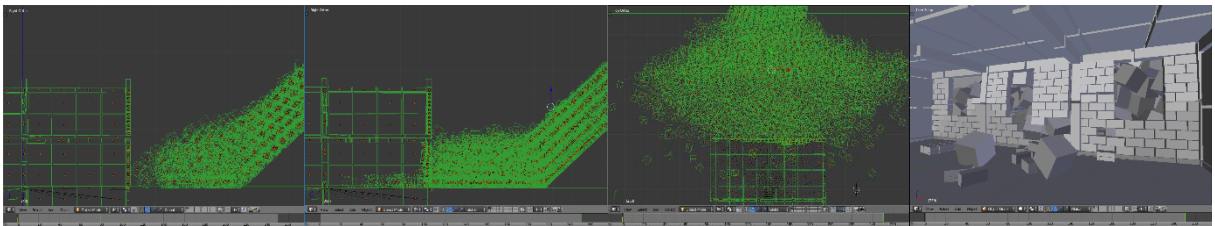
Friction set to 1.0, the slide has a relatively flat accumulation zone behind the house. However, the height at impact is $\sim 2\text{m}$.



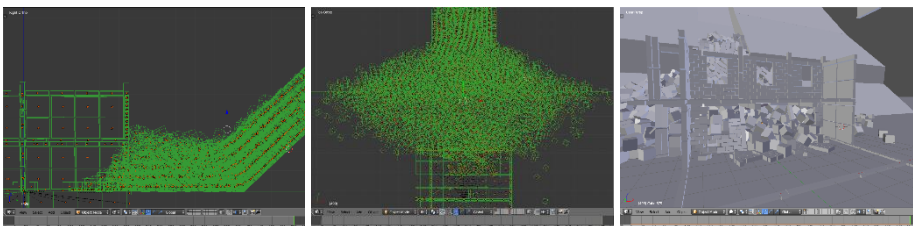
Friction set to 0.5 the accumulation zone at impact is relatively flat with a height of $\sim 2\text{m}$
The simulation settings of five and six meters between the house and slope are chosen for further analysis with the house modelled



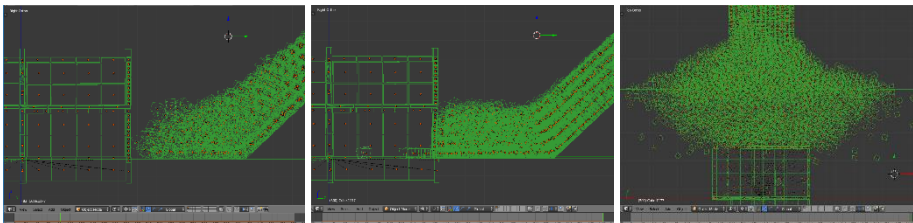
The first soil element to reach the building knocked a brick out of the wall (Shear = 0.5 N/mm²), and the geometry of the slide is slightly different due at the moment of impact in comparison to the passive body model because the computer has to run more calculations. Therefore, the resolution of the house will be reduced by converting the bricks on the side, interior, and front wall into slabs (unbreakable elements) with mortar strength constraints where touching columns and beams. Additionally the ground foundation rigid bodies added to the simulation in the preprocessing steps, add 0.1 meter of foundation and lowered the ground plane below the XY plane which increases the distance from the building to the slope.



The simulation ran for a total of 250 frames; however, the slide was significantly slowing down. Several bricks were immediately sheared from the wall, and more continued; the columns are flexed. The debris height is ~2.5 meters.



Distance 6.0 meters Friction 0.0; Increased the total frames to 500, and reset the simulation. New results show the house ground floor wall breaking more than the first simulation. Windows are partly visible, and debris height is ~2.75 meters. It is possible some of the initial blocks knocked out from the wall by single cubes are due to the cube dimensions. Results could vary with a more gradual accumulation of smaller cubes.



Building 1

The debris slides during data collection were almost indistinguishable from the topography due to regrown vegetation. Therefore, Google Earth historical images aided with determining the release location for analysis. After selecting the location, the release type is set to block release with a density of 1900 kg/m³. The dry-coulomb type friction value (μ) is 0.36, and the remaining simulation parameters set to default. After running the simulation; Figure 4.1 presents the max height distribution, and Table summarises the results. The spatial extent of the run-out is slightly larger than observed during data collection. A second simulation with a smaller release area (Figure 4.2) results in a distribution closer to the field observations. Table 4.2 summarises the results of the second simulation. Next, a “dam” added to the RAMMS simulation takes the place of House 1 for estimating the impact pressures (Figure 4.3-4.6); Tables 4.3 & 4.4 summarise the results from adding a dam to simulations 2 & 3.

Table 4.1:

Release Volume (m ³)	640.48
Max Velocity (m/s)	3.18
Max Flow Height (m)	1.89
Max Pressure (kPa)	19.19
Mean Slope Angle (°)	20.06

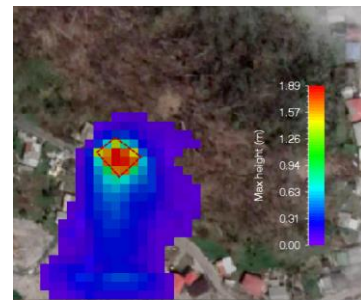


Figure 4.1: (Right) Simulation 1 shows a distribution with a greater spatial extent than observed during data collection

Table 4.2: Results from Simulation 2

Release Volume (m ³)	161.11
Max Velocity (m/s)	3.51
Max Flow Height (m)	1.52
Max Pressure (kPa)	23.37
Mean Slope Angle (°)	21.19

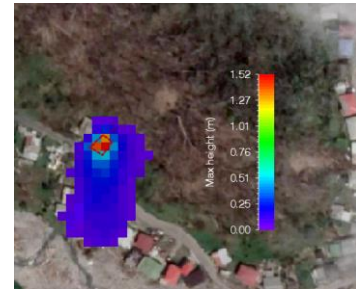


Figure 4.2: (Right) Simulation 2 shows a distribution close to the empirical assessment

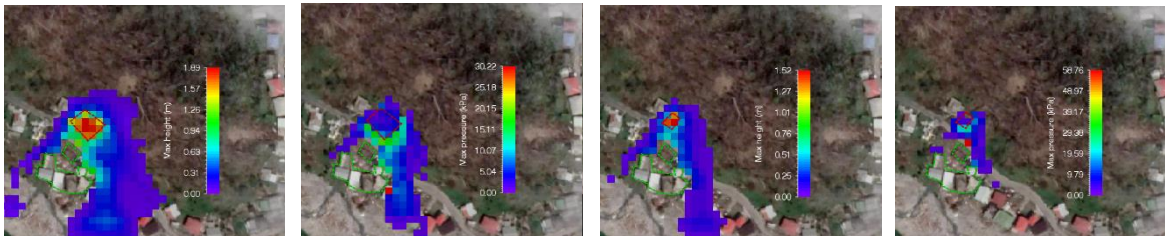


Figure 4.3 & 4.4: (Left) Simulation 2, with dam included, debris slides down the road to neighbours. (Right) Simulation 2’s max pressure distribution with a dam included.

Figure 4.5 & 4.6: (Left) Simulation 3 with dam included; debris divides affecting debris height. (Right) Simulation 3’s max pressure distribution with a dam included.

Table 4.3: Simulation 2 results with dam

Release Volume (m ³)	640.49
Max Velocity (m/s)	3.99
Max Flow Height (m)	1.89
Max Pressure (kPa)	30.21

Table 4.4: Simulation 3 results with dam

Release Volume (m ³)	161.11
Max Velocity (m/s)	5.56
Max Flow Height (m)	1.52
Max Pressure (kPa)	58.76

Tables 4.10 – 4.14: Max Shear Stress Values of Affected Wall

Number	Height	Max Shear Pressure	Number	Height	Max Shear Pressure	Number	Height	Max Shear Pressure
-	(Meters)	(N / mm ²)	-	(Meters)	(N / mm ²)	-	(Meters)	(N / mm ²)
1	0.42	0.032	12	0.82	0.018	23	1.26	0.082
2	0.42	0.036	13	0.82	0.012	24	1.26	0.064
3	0.42	0.058	14	0.82	0.028	25	1.26	0.007
4	0.42	0.072	15	0.82	0.018	26	1.75	0.018
5	0.42	0.031	16	0.82	0.013	27	1.75	0.046
6	0.42	0.016	17	0.82	0.004	28	1.75	Broken
7	0.42	0.108	18	1.14	0.007	29	1.75	0.016
8	0.42	0.047	19	1.14	0.411	30	1.75	0.004
9	0.42	0.03	20	1.14	0.369	31	2.26	Null
10	0.42	0.028	21	1.14	0.001	32	2.26	0.027
11	0.42	0.014	22	1.14	0.177	33	2.26	0.033

Number	Height	Max Shear Pressure
-	(Meters)	(N / mm ²)
34	2.26	0.015
35	2.26	0.050
36	2.26	0.009
37	2.39	0.037
38	2.39	Null
39	2.39	0.058
40	2.39	0.013
41	2.39	0.012
42	2.39	0.020
43	2.39	0.026
44	2.39	0.035

Table 4.16: Soil-Model Properties

Density	1900 kg/m ³
Width	11.0 meters
Length	1.0 meter

Degree of Damage Classification

- D0: None
- D1: Broken masonry wall
- D2: Multiple masonry walls damaged; flexing columns or beams
- D3: Broken column, beam, and non-structural damage
- D4: Multiple columns, beams broken, and non-structural damage;
- D5: Irreparable structural damage or complete structural collapse

Table 4.17: Height 0.5 Meters; Weight 10,450 kg

Velocity (m/s)	Degree of Damage
3.0	D0
4.0	D0
5.0	D1

Table 4.18: Height 1.0 meters; Weight 20,900

Velocity (m/s)	Degree of Damage
3.0	D0
4.0	D2
5.0	D3

Table 4.19: Height 2.0 meters; Weight 41,800

Velocity (m/s)	Degree of Damage
3.0	D2
4.0	D3
5.0	D3

Table 4.20: Height 3.0 meters; Weight 62,700

Velocity (m/s)	Degree of Damage
3.0	D2
4.0	D4
5.0	D4

Effect of Adjusting Centre of Mass with Length and Height

Table 4.21: Soil-Model Properties

Density	1900 kg/m ³
Width	11.0 meters
Length	2.0 meter

Table 4.22: Height 0.5 Meters; Weight 20,900 kg

Velocity (m/s)	Degree of Damage
3.0	D0
4.0	D0
5.0	D1

Table 4.23: Height 1.0 meters; Weight 41,800kg

Velocity (m/s)	Degree of Damage
3.0	D1
4.0	D2
5.0	D3

Table 4.24: Height 2.0 meters; Weight 83,600 kg

Velocity (m/s)	Degree of Damage
3.0	D2
4.0	D3
5.0	D3

Table 4.25: Height 3.0 meters; Weight 125,400kg

Velocity (m/s)	Degree of Damage
3.0	D2
4.0	D4
5.0	D4

Table 4.26: Soil-Model Properties

Density	1900 kg/m ³
Width	11.0 meters
Length	3.0 meter

Table 4.27: Height 0.5 Meters; Weight 31,350 kg

Velocity (m/s)	Degree of Damage
3.0	D0
4.0	D0
5.0	D2

Table 4.28: Height 1.0 meters; Weight 62,700 kg

Velocity (m/s)	Degree of Damage
3.0	D2
4.0	D2
5.0	D3

Table 4.29: Height 2.0 meters; Weight 125,400 kg

Velocity (m/s)	Degree of Damage
3.0	D3
4.0	D3
5.0	D3

Table 4.30: Height 3.0 meters; Weight 188,100 kg

Velocity (m/s)	Degree of Damage
3.0	D4
4.0	D4
5.0	D4

First time a transverse wall breaks

Table 4.31: Soil-Model Properties

Density	1900 kg/m ³
Width	11.0 meters
Length	4.0 meter

Table 4.32: Height 0.5 Meters; Weight 41,800 kg

Velocity (m/s)	Degree of Damage
3.0	D0
4.0	D2
5.0	D2

Table 4.33: Height 1.0 meters; Weight 83,600 kg

Velocity (m/s)	Degree of Damage
3.0	D2
4.0	D3
5.0	D3

Table 4.34: Height 2.0 meters; Weight 167,200 kg

Velocity (m/s)	Degree of Damage
3.0	D3
4.0	D3
5.0	D4

Table 4.35: Height 3.0 meters; Weight 250,800 kg

Velocity (m/s)	Degree of Damage
3.0	D4
4.0	D4
5.0	D4

Table 4.36: Soil-Model Properties

Density	1900 kg/m ³
Width	11.0 meters
Length	5.0 meter

Table 4.37: Height 0.5 Meters; Weight 52,250 kg

Velocity (m/s)	Degree of Damage
3.0	D1
4.0	D2
5.0	D2

Table 4.38: Height 1.0 meters; Weight 104,500

Velocity (m/s)	Degree of Damage
3.0	D2
4.0	D3
5.0	D4

Table 4.39: Height 2.0 meters; Weight 209,000 kg

Velocity (m/s)	Degree of Damage
3.0	D3
4.0	D4
5.0	D5

Table 4.40: Height 3.0 meters; Weight 313,500

Velocity (m/s)	Degree of Damage
3.0	D4
4.0	D4
5.0	D5